



Wayside Charging and Hydrogen Hybrid Bus

Extending the Range of Electric Shuttle Buses

SEPTEMBER 2012

FTA Report No. 0028
Federal Transit Administration

PREPARED BY

Center for Energy, Transportation and the Environment
University of Tennessee at Chattanooga



U.S. Department of Transportation
Federal Transit Administration

COVER PHOTO

Courtesy of Center for Energy, Transportation and the Environment

DISCLAIMER

This document is disseminated under the sponsorship of the U.S. Department of Transportation in the interest of information exchange. The United States Government assumes no liability for its contents or use thereof. The United States Government does not endorse products or manufacturers. Trade or manufacturers' names appear herein solely because they are considered essential to the objective of this report.

Wayside Charging and Hydrogen Hybrid Bus

Extending the Range
of Electric Shuttle Buses

SEPTEMBER 2012

FTA Report No. 0028

PREPARED BY

J. Ronald Bailey and Mark E. Hairr
Center for Energy, Transportation and the Environment
University of Tennessee at Chattanooga

SPONSORED BY

Federal Transit Administration
Office of Research, Demonstration and Innovation
U.S. Department of Transportation
1200 New Jersey Avenue, SE
Washington, DC 20590

AVAILABLE ONLINE

<http://www.fta.dot.gov/research>

Metric Conversion Table

SYMBOL	WHEN YOU KNOW	MULTIPLY BY	TO FIND	SYMBOL
LENGTH				
in	inches	25.4	millimeters	mm
ft	feet	0.305	meters	m
yd	yards	0.914	meters	m
mi	miles	1.61	kilometers	km
VOLUME				
fl oz	fluid ounces	29.57	milliliters	mL
gal	gallons	3.785	liters	L
ft ³	cubic feet	0.028	cubic meters	m ³
yd ³	cubic yards	0.765	cubic meters	m ³
NOTE: volumes greater than 1000 L shall be shown in m ³				
MASS				
oz	ounces	28.35	grams	g
lb	pounds	0.454	kilograms	kg
T	short tons (2000 lb)	0.907	megagrams (or "metric ton")	Mg (or "t")
TEMPERATURE (exact degrees)				
°F	Fahrenheit	5 (F-32)/9 or (F-32)/1.8	Celsius	°C

REPORT DOCUMENTATION PAGE		<i>Form Approved OMB No. 0704-0188</i>	
<p>Public reporting burden for this collection of information is estimated to average 1 hour per response, including the time for reviewing instructions, searching existing data sources, gathering and maintaining the data needed, and completing and reviewing the collection of information. Send comments regarding this burden estimate or any other aspect of this collection of information, including suggestions for reducing this burden, to Washington Headquarters Services, Directorate for Information Operations and Reports, 1215 Jefferson Davis Highway, Suite 1204, Arlington, VA 22202-4302, and to the Office of Management and Budget, Paperwork Reduction Project (0704-0188), Washington, DC 20503.</p>			
1. AGENCY USE ONLY	2. REPORT DATE	3. REPORT TYPE AND DATES COVERED	
	September 30, 2012	Final Report, October 1, 2008—September 30, 2012	
4. TITLE AND SUBTITLE		5. FUNDING NUMBERS	
Wayside Charging and Hydrogen Hybrid Bus: Extending the Range of Electric Shuttle Buses			
6. AUTHOR(S) J. Ronald Bailey, Ph.D., P.E., and Mark E. Hairr			
7. PERFORMING ORGANIZATION NAME(S) AND ADDRESSE(ES) Center for Energy, Transportation and the Environment University of Tennessee at Chattanooga 615 McCallie Avenue 214 EMCS Building, Department 2522 Chattanooga, Tennessee 37403-2598		8. PERFORMING ORGANIZATION REPORT NUMBER FTA Report No. 0028	
9. SPONSORING/MONITORING AGENCY NAME(S) AND ADDRESS(ES) U.S. Department of Transportation Federal Transit Administration Office of Research, Demonstration and Innovation East Building 1200 New Jersey Avenue, SE Washington, DC 20590		10. SPONSORING/MONITORING AGENCY REPORT NUMBER FTA Report No. 0028	
11. SUPPLEMENTARY NOTES [http://www.fta.dot.gov/research]			
12A. DISTRIBUTION/AVAILABILITY STATEMENT Available from: National Technical Information Service (NTIS), Springfield, VA 22161. Phone 703.605.6000, Fax 703.605.6900, email [orders@ntis.gov]		12B. DISTRIBUTION CODE TRI-20	
13. ABSTRACT This report documents the results completed by the Center for Energy, Transportation and the Environment (CETE) at the University of Tennessee at Chattanooga (UTC) under Federal Transit Administration Cooperative Agreement TN-26-7034. This research has addressed the limited range of electric shuttle buses by two different methods: first, by wayside charging using inductive power transfer, and second, by adding a small (10 kW) on-board generator set powered by an internal combustion engine (ICE) fueled by hydrogen. Wayside charging reduced fuel costs to less than \$0.10 per mile while eliminating tailpipe emissions that would have been produced by a similar diesel bus. The hydrogen hybrid bus eliminated emission of CO ₂ , but the cost was found to be prohibitive because of the relatively poor thermodynamic efficiency of the ICE and the high cost of hydrogen. Better results were obtained when the ICE was fueled with compressed natural gas (CNG), which resulted in a range in excess of 170 miles at a lower fuel cost per mile than a comparable diesel-fueled hybrid bus.			
14. SUBJECT TERMS Public transportation, electric buses, wayside charging, inductive power transfer, hydrogen, range extension		15. NUMBER OF PAGES 80	
16. PRICE CODE			
17. SECURITY CLASSIFICATION OF REPORT Unclassified	18. SECURITY CLASSIFICATION OF THIS PAGE Unclassified	19. SECURITY CLASSIFICATION OF ABSTRACT Unclassified	20. LIMITATION OF ABSTRACT

TABLE OF CONTENTS

1	Executive Summary
4	Section 1: Wayside Charging
4	Background
4	Statement of the Problem
5	Advanced Vehicle Test Facility
6	Overview of Wireless Charging By Inductive Power Transfer
7	Organization
7	Roles of the Partners
7	Preliminary Testing
9	Sensitivity to Misalignment and Air Gap Between the Coils
11	Systems Integration
15	Site Preparation
17	Tuning the System
18	Experimental Results
18	Test Protocol
19	Baseline Testing
20	Range with Wireless Charging
21	Charging the Batteries
24	Operating Cost Estimates
26	Measurement of Efficiency
26	Magnetic Flux Emissions
30	Environmental Considerations
30	Compliance with Clean Air Act
30	Reduction in Green House Gases
31	Summary of Wayside Charging Results
31	Lessons Learned About Wireless Charging
32	Section 2: Hydrogen Hybrid Bus Demonstration
32	Background
33	Organization
34	Battery Selection
37	Improvement in Range from LiFePO ₄ Batteries
40	Development of Battery Charging Profile
44	Auxiliary Power Unit (APU) Considerations
45	Engine Modifications
46	Fuel and Ignition
47	Fuel Delivery Apparatus
48	Dual Fuel Feature
48	Test Results with CNG
49	Test Results with Hydrogen
52	Lessons Learned About Use of an APU to Improve Range

53	Section 3: Technical Support
53	Lessons Learned About Technical Support
55	Section 4: Acquire and Install Hydrogen Electrolyzer
57	Lessons Learned about the Hydrogen Electrolyzer
60	Section 5: Outreach
60	Description of EViSim
61	Functionality
62	Promising Applications
62	Implementation
63	Design and Features
66	Route Creation
66	Analysis
67	REFERENCES

LIST OF FIGURES

4	Figure 1-1:	Statement of the Problem
5	Figure 1-2:	Test Track at Advanced Vehicle Test Facility
5	Figure 1-3:	Research Building at Advanced Vehicle Test Facility
6	Figure 1-4:	Bus Being Tested at Advanced Vehicle Test Facility Track in Chattanooga
6	Figure 1-5:	Wireless Charging System Using Inductive Power Transfer
7	Figure 1-6:	Partnership Formed for Wireless Charging using Inductive Power Transfer
8	Figure 1-7:	Power Electronics Components
8	Figure 1-8:	Stationary Coils, Pick-Up Coils, and Rectifiers
9	Figure 1-9:	Laboratory Setup for Component Testing at Advanced Vehicle Test Facility
9	Figure 1-10:	Power Transfer as Function of Air Gap
10	Figure 1-11:	Power Transfer as Function of Misalignment with 0.5" (1.27cm) Air Gap
10	Figure 1-12:	Power Transfer as Function of Misalignment with 2" (5.08cm) Air Gap
11	Figure 1-13:	Rectifiers and Heat Exchanger Installation
11	Figure 1-14:	Battery Management System Control Board behind the Driver's Seat
12	Figure 1-15:	Communication Equipment Installed on Bus
12	Figure 1-16:	Mechanism for Lowering Pickup Coils
13	Figure 1-17:	EVAmerica Assembly Area in Ringgold, Georgia
13	Figure 1-18:	Electric Shuttle Bus with Wireless Charging
13	Figure 1-19:	View of Coils under Bus and Alignment Scheme
14	Figure 1-20:	Electronic Components of Guidance System
14	Figure 1-21:	Display Used to Guide Horizontal Alignment
14	Figure 1-22:	Bus Entering Wireless Charging Area
15	Figure 1-23:	Switch Gear, Voltage Transducer, and Data Acquisition System
16	Figure 1-24:	Labview Screen for Monitoring AC Power
16	Figure 1-25:	Track Supply
17	Figure 1-26:	Simplified RLC Model for Primary Side of IPT Circuit
18	Figure 1-27:	Capacitor Boxes Used to Tune Circuit
18	Figure 1-28:	Downtown Chattanooga Shuttle Route
19	Figure 1-29:	Range Envelope for Existing CARTA Shuttles with PbA Batteries
19	Figure 1-30:	Water Barrels Equivalent to 22 Passengers
20	Figure 1-31:	Baseline Range with Ni-Cd Batteries
20	Figure 1-32:	SOC as a Function of Distance
21	Figure 1-33:	Battery Voltage as a Function of Distance
21	Figure 1-34:	DC Amp Hours Consumed and Replaced over 24-Hour Day

22	Figure 1-35: AC Power for Day of Wireless Charging Covering 39 Trips (117 Miles)
23	Figure 1-36: Power Consumed by Overnight Charging
23	Figure 1-37: Range Envelope with Wireless Charging
25	Figure 1-38: Comparison of Fuel Costs
25	Figure 1-39: Cost Comparison of Diesel Fuel with Electricity
27	Figure 1-40: Dr. John Boys Measuring EMF
28	Figure 1-41: Comparison of Observed Level of Flux with ICNIRP Recommendations
29	Figure 1-42: Poster on Safety for Wireless Charging
30	Figure 1-43: Comparison of CO ₂ Emissions for Diesel and Electric Shuttle Buses
32	Figure 2-1: Fuel Cell Hybrid Bus Built by Ebus and tested at UT Austin
33	Figure 2-2: Hybrid Ebus with a 20 kW Gas Turbine as a Range Extender
33	Figure 2-3: Partnership for Development of Hydrogen Hybrid Bus Demonstration
34	Figure 2-4: Design Review Meeting
34	Figure 2-5: Comparison of Capacity Rating with Level of Maturity for Various Batteries
35	Figure 2-6: Cost Projections with Increased Volume for Li-Ion Batteries
37	Figure 2-7: LiFePO ₄ Batteries Mounted in Battery Box at EVAmerica
37	Figure 2-8: Cell Temperature vs. Distance
38	Figure 2-9: Pack Voltage after Each Trip (~ 3 miles)
38	Figure 2-10: High and Low Cell Voltage vs. Distance
39	Figure 2-11: Trip Amp Hours vs. Distance
39	Figure 2-12: Remaining Amp Hours vs. Distance
40	Figure 2-13: Improvement in Range with LiFePO ₄ Batteries
41	Figure 2-14: ABC-150 Used to Develop Charge Profile for LiFePO ₄ Batteries
41	Figure 2-15: Current during Charging
42	Figure 2-16: Voltage during Charging
42	Figure 2-17: Highest Cell Voltage during Charging at 100 Amps
42	Figure 2-18: Cumulative Amp Hours during Charging
43	Figure 2-19: Cell Temperature (Highest) during Charging
44	Figure 2-20: 10 kW Polar Power APU
45	Figure 2-21: H2/CNG APU Installed in Modified Bus
46	Figure 2-22: Various Hydrogen Fuel and Ignition System Components and Sensors
47	Figure 2-23: Dual Engine Management Diagram
47	Figure 2-24: Hydrogen Delivery Manifold
48	Figure 2-25: Engine Management Panel
48	Figure 2-26: Improvement in Range with 4.95 kW APU Fueled by CNG

49	Figure 2-27: CNG Used by APU in Driving 177 Miles
50	Figure 2-28: Firing Diagram
51	Figure 2-29: Range Improvement with 2.5 kW APU Fueled by Hydrogen
51	Figure 2-30: Hydrogen Used by APU while Driving 117 Miles
55	Figure 4-1: Components of Hydrogen Fueling Station
55	Figure 4-2: Water Deionizer
56	Figure 4-3: PEM Fuel Cell Electrolyzer Supplied by Proton Energy Systems
56	Figure 4-4: Hydrogen Compressor
57	Figure 4-5: Hydrogen Storage Tanks and Dispensing System
58	Figure 4-6: Fueling Bus with Hydrogen
59	Figure 4-7: Hydrogen Tube Trailer
61	Figure 5-1: Screen Shot of Simulator
64	Figure 5-2: Two-Dimensional Overhead Map
64	Figure 5-3: Three-Dimensional Fly-Behind View
65	Figure 5-4: Energy Level and Speed Gauges
65	Figure 5-5: Energy Level History (Time vs. Energy Level)
65	Figure 5-6: Elevation Profile of Route (Distance vs. Elevation)
66	Figure 5-7: Central Status Display
66	Figure 5-8: Customized Driving Route Creation

LIST OF TABLES

26	Table 1-1:	Voltage and Current during Wireless Charging
27	Table 1-2:	EMF Measurements Outside Bus
28	Table 1-3:	EMF Measurements Inside Bus
31	Table 1-4:	Summary of Wayside Charging Results
35	Table 2-1:	Battery Considerations
36	Table 2-2:	Battery Manufacturers

ACKNOWLEDGMENTS

This project was conducted under Federal Transit Administration (FTA) Cooperative Agreement TN-26-7034. Special recognition and appreciation is extended to the Chattanooga Enterprise Center staff and board and the Chattanooga Area Regional Transportation Authority (CARTA), both of which contributed greatly in the completion of this research program. EVAmerica, Embedded Power Controls, Conductix Wampfler, and the University of Auckland, New Zealand, have also contributed to the success of this program.

The project team also wishes to thank Mr. Henry Nejako, FTA Program Management Officer; Patrick Centolanzi, FTA Transportation Program Engineer; Lisa Colbert, FTA Project Manager; and numerous UTC students, faculty, and staff who assisted with many aspects of the projects completed under this work program.

ABSTRACT

The research completed under Federal Transit Administration Cooperative Agreement TN-26-7034 has focused on demonstration of ways to improve the range of electric buses. Methods include wireless charging, installation of better batteries, and use of an auxiliary power unit fueled by compressed natural gas or hydrogen. Results show that the range can be increased to more than 100 miles by any one of these three methods. However, wireless charging using inductive power transfer appears to be the best choice for immediate deployment when the range requirement exceeds 100 miles between overnight chargings. The improved batteries, in combination with wireless charging, should enable use of larger electric buses operating over longer, more difficult routes than previously possible.

EXECUTIVE SUMMARY

The Center for Energy, Transportation and the Environment (CETE) at the University of Tennessee at Chattanooga (UTC) in partnership with the Chattanooga Area Regional Transportation Authority (CARTA) conducted research and outreach tasks aimed at increasing the range of electric shuttle buses. The objectives for this work program are to:

- Demonstrate the use of wireless charging using inductive power transfer (IPT) to increase the range of electric shuttle buses
- Demonstrate the use of advanced batteries and an auxiliary power unit (APU) powered by an internal combustion engine (ICE) running on hydrogen to increase the range of an electric shuttle bus
- Provide assistance to the City of Sevierville to improve operation of its fleet of hybrid electric shuttle buses
- Provide assistance to Emory University to improve operation of its fleet of electric shuttle buses
- Complete procurement and installation of a hydrogen fueling station needed to provide fuel for the APU
- Conduct an outreach program to share lessons learned with stakeholders in public transit

In the first research project, the range of an electric shuttle bus was increased from less than 50 miles on batteries alone to more than 120 miles by wireless charging during the period when passengers are normally boarding the bus. CETE in partnership with CARTA demonstrated wireless charging for electric shuttle buses using IPT technology provided by Conductix Wampfler, AG. This short “opportunity” charge of 3 minutes duration at 60 kilowatts provides enough traction energy to power the bus for approximately 3 miles, thereby eliminating the normal range constraint that, until now, has required battery swapping during the day to cover the required daily route of 100 miles. Overall efficiency from the grid to the vehicle was found to be more than 90%, resulting in an energy cost per mile of less than \$0.10 while producing zero tailpipe emissions. Measurements of electromagnetic field strength at the edge of the coils near street level and at all locations inside the bus were found to be well below draft international standards for exposure.

In the second research project, the range of a battery-centric electric shuttle was increased from less than 50 miles to more than 120 miles by a combination of improved batteries and the addition of an on-board generator powered by a hydrogen-fueled ICE. Because of recent interest in CNG as a fuel for transportation, the ICE controls were made to be switchable between hydrogen and CNG, which produced an increase in range to more than 170 miles when running on CNG with a fuel cost significantly less than hydrogen. However, it should be noted that replacing the original Ni-Cd batteries with LiFePO₄ batteries alone increased the range from less than 50 miles to more than 100 miles. Since

this exceeded the daily range required by CARTA, the added complication and cost of having to establish hydrogen or CNG fueling capability and maintain a unique hybrid bus resulted in a decision by CARTA to remove the generator and deploy the shuttle with the new batteries alone. Perhaps more significantly, this research demonstrated that these new batteries, in combination with wayside charging, have the potential to greatly expand the opportunity for electric buses by making it possible for larger electric buses to travel over longer routes than previously possible.

CETE in partnership with the City of Sevierville evaluated operational problems with its fleet of hybrid electric shuttle buses and reached a mutual agreement that a dedicated technician was needed to maintain these buses. This was accomplished by transferring funds to enable Sevierville to hire a technician.

At Emory University, CETE discovered that the performance of its fleet of electric shuttle buses had deteriorated to such an extent that the operational range had been reduced to less than 25 miles with fully-charged batteries. It was determined that the batteries were in severe need of reconditioning and that the battery chargers being used were the proximate cause of the problem. CETE developed a specification for a new battery charger and was prepared to transfer funds to Emory University to procure this charger when it decided to abandon its fleet of electric shuttles in favor of converting its fleet of diesel buses to run on bio-diesel produced from cooking oil used in the campus food service. With assistance from FTA through Cooperative Agreement TN-26-7035, Emory University's fleet of five electric shuttle buses was transferred to CARTA. One of these buses was equipped with wireless charging equipment and used to demonstrate wayside charging as described above. A second was converted into a hydrogen hybrid bus as part of the second research project described above. A third was put into regular service after an extensive effort to recondition the batteries, which were abused at Emory by use of incorrect charging equipment. The other two are being held in reserve for possible deployment by CARTA. The transfer of these five buses to CARTA made it possible to avoid the cost of purchasing new buses for the wireless charging and hydrogen hybrid bus research projects described previously.

The hydrogen fueling station that was started under FTA Cooperative Agreement TN-26-7032, East Tennessee Hydrogen Initiative, was completed and commissioned in December 2009. It is now capable of producing 2 kg per day and storing 10 kg of hydrogen at 6,000 psi.

The outreach task included publication of a number of peer reviewed journal articles; presentations at regional, national, and international professional society technical meetings; and frequent demonstrations at the Advanced Vehicle Test Facility (AVTF) and elsewhere to showcase wayside charging and hydrogen as a fuel for transportation. The director of CETE has also served as Editor-in-Chief

of the *World Electric Vehicle Journal* and is currently serving as a member and chair of the bus subcommittee of an international taskforce that is charged by the Society of Automotive Engineers (SAE) with drafting a standard for wireless charging of vehicles.

The demonstration of wireless charging has opened up new opportunities for deployment of electric buses with larger buses over routes, which was heretofore impossible for electric buses. The demonstration of an inexpensive APU as a means of building a battery-centric bus could open up opportunities for deployment, especially where transit operators already use hydrogen or CNG. Technical support for the City of Sevierville enabled it to continue successful operation of its fleet of hybrid electric buses. Work with Emory University enabled the transfer of five electric buses to CARTA, saving money on this project by forgoing the expense of purchasing new buses while also giving CARTA some lightly-used buses that could be deployed immediately. Lessons learned have been published and presented at national and international conferences.

SECTION
1

Wayside Charging

Background

The Chattanooga Area Regional Transportation Authority (CARTA) has been operating a fleet of electric shuttle buses since May 1, 1992. The decision to convert to electric buses was driven by a community effort to improve the air quality in Chattanooga and to comply with all provisions of the Clean Air Act. Anyone visiting Chattanooga today who has not visited lately would have difficulty recognizing it because of the remarkable improvements in air quality that not only have put Chattanooga into a state of attainment with all U.S. Environmental Protection Agency (EPA) air quality regulations but also has allowed for continued economic development, such as the new Volkswagen assembly plant that is now in full production in Chattanooga, partly because of the strong community commitment to the environment. CARTA now carries approximately one million passengers each year on its electric shuttles. To remove the CARTA shuttles from Chattanooga today would be as unthinkable as removing the cable cars from San Francisco.

Over the years, CARTA experimented with virtually every new product that promised to extend the range of electric buses. This included various combinations of new battery chemistries, more efficient drive systems, and gas turbines running on diesel fuel or propane as range extenders that could recharge the batteries during operations.

Statement of the Problem

After almost 20 years of continuous operation of electric shuttles, the problem for CARTA is shown in Figure I-1.

Figure 1-1
Statement of Problem



- Shuttle runs every thirty minutes from 6:30 AM until 11:00 PM
- Downtown Route is approximately 3 miles
- Range requirement is ~100 miles
- Limitations
 - Downtown Routes Only
 - Not enough Power to climb hills on UTC campus
 - Not enough Range
 - Batteries Swapped at Mid-Day for Downtown Route
 - Other Routes Out of the Question for Electric Shuttle
 - Fleet is beyond original design life
 - Newest Shuttle is over fifteen years old
 - Manufacturer is no longer in business

Advanced Vehicle Test Facility

This demonstration project was conducted at the Advanced Vehicle Test Facility (AVTF), which consists of a 1-mile banked asphalt test track and a 9,400-square-foot research building located on 52 acres approximately 6 miles from the University of Tennessee campus in Chattanooga. An aerial photograph of the test track is shown in Figure I-2. The research building at the AVTF is shown in Figure I-3. A photograph of a bus being tested at the AVTF track is shown in Figure I-4.

Figure 1-2

Test Track at AVTF



Figure 1-3

*Research Building
at AVTF*



Figure 1-4

*Bus Being Tested
at AVTF*

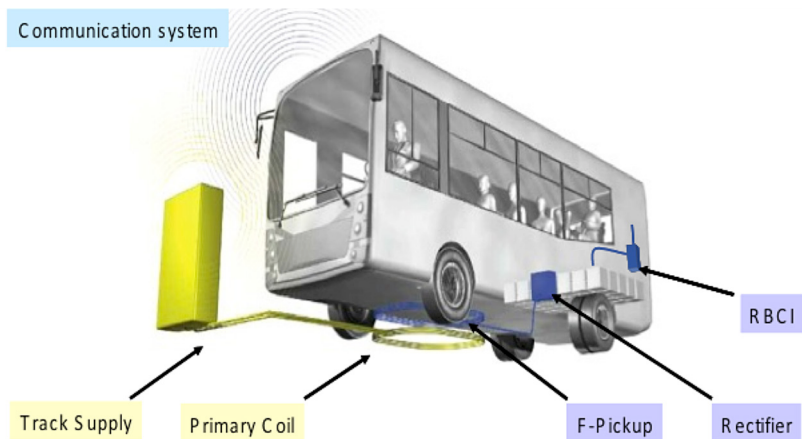


Overview of Wireless Charging by Inductive Power Transfer

Wireless charging by inductive power transfer (IPT) is accomplished by providing power to a stationary (primary coil) buried in the pavement, which induces a current in a pickup coil mounted on the bottom of the vehicle. The major systems components are shown in Figure 1-5.

Figure 1-5

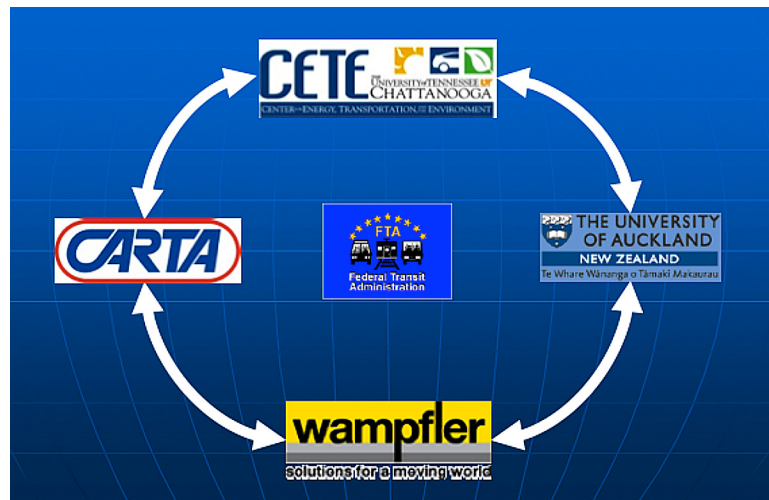
Wireless Charging System using Inductive Power Transfer



Organization

A multidisciplinary team was assembled to conduct this research project. The project partnership is represented graphically in Figure 1-6.

Figure 1-6
Partnership Formed
for Wireless Charging
using Inductive
Power Transfer



Roles of the Partners

Roles of the partners in the project were the following:

- FTA provided funding under FTA Cooperative Agreement TN-26-7034.
- CARTA provided experience and expertise in transit operations and equipment.
- EVAmerica provided systems integration and fabrication capability.
- Embedded Power Controls provided power electronics expertise.
- Conductix Wampfler, AG provided technical assistance and all of the inductive power transfer equipment.
- University of Auckland, New Zealand, provided expertise in wireless charging.
- Center for Energy, Transportation and the Environment (CETE) provided overall project management.

Preliminary Testing

All of the components for the wireless charging system were tested in the laboratory before installing them on the bus. Some of the components are shown in Figure 1-7.

Figure 1-7

Power Electronics Components



The equipment shown in Figure I-7 includes the battery management system circuit board, the inductors, and the communications module with wireless modem. The switch board on the right was used to simulate the controls that would be installed on the bus to allow the operator to initiate charging. Most of these components were designed and built by Embedded Power Control to specifications provided by Conductix Wampfler, AG.

The two stationary coils that are encased in concrete are shown in Figure I-8, which also shows two yellow pick-up coils (one standing on edge) and the rectifiers (with cover removed) in the background. The overall stationary setup that was used for preliminary testing is shown in Figure I-9.

Figure 1-8

*Stationary Coils,
Pick-Up Coils (yellow)
and Rectifiers
(covers off)*

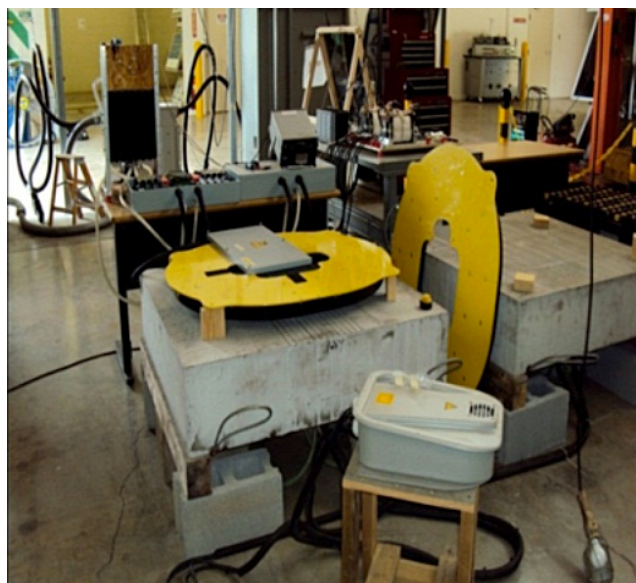
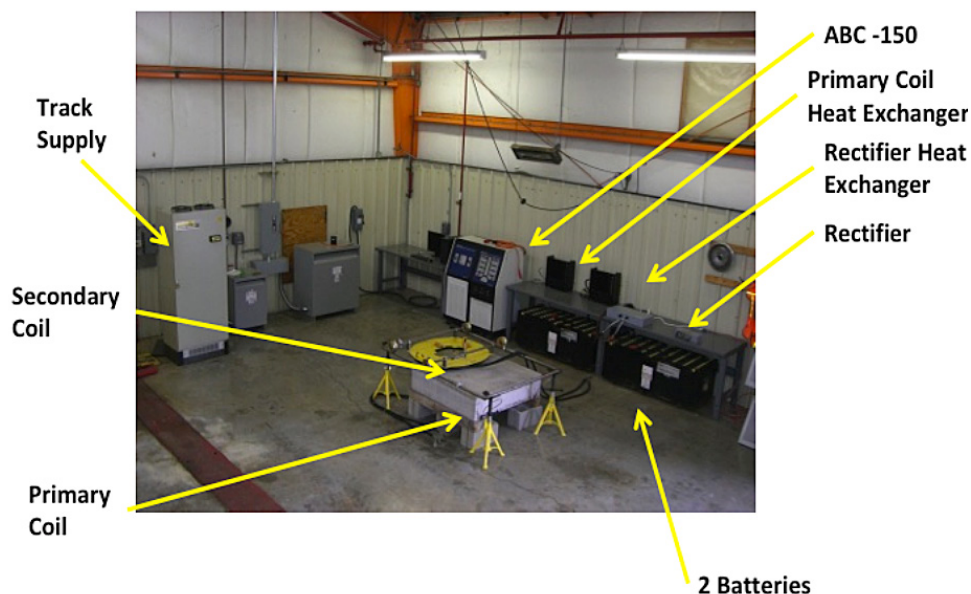


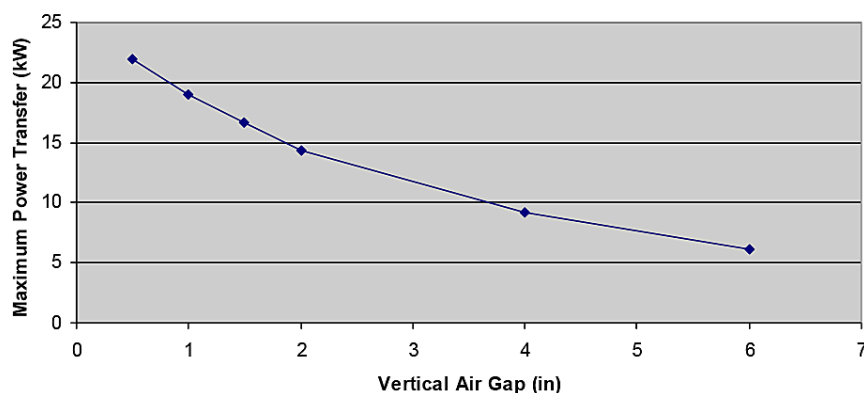
Figure 1-9
Laboratory Setup for Component Testing at Advanced Vehicle Test Facility



Sensitivity to Misalignment and Air Gap between IPT Coils

With near-perfect horizontal alignment between the two coils, the rate of power transfer as a function of vertical air gap is shown in Figure 1-10. As expected, the power transfer rate decreases with air gap, dropping to less than 10kW when the gap reaches 4 inches (10.1 cm). The maximum power transfer rate of 22 kW occurred when the two coils were at the centered position. Increasing the misalignment resulted in a decrease in the power transfer rate, falling to 16 kW in the area of misalignment enclosed by 3 inches (7.62 cm) in the X direction (aligned with the major axis of the coil) and about 2.5 inches (6.35 cm) in the Y direction. As expected, the power transfer rate decreased rapidly as the misalignment increased. This led to the conclusion that it would not be possible to achieve a satisfactory rate of power transfer without either lowering the bus or installing a positioning mechanism under the bus that would lower the coils.

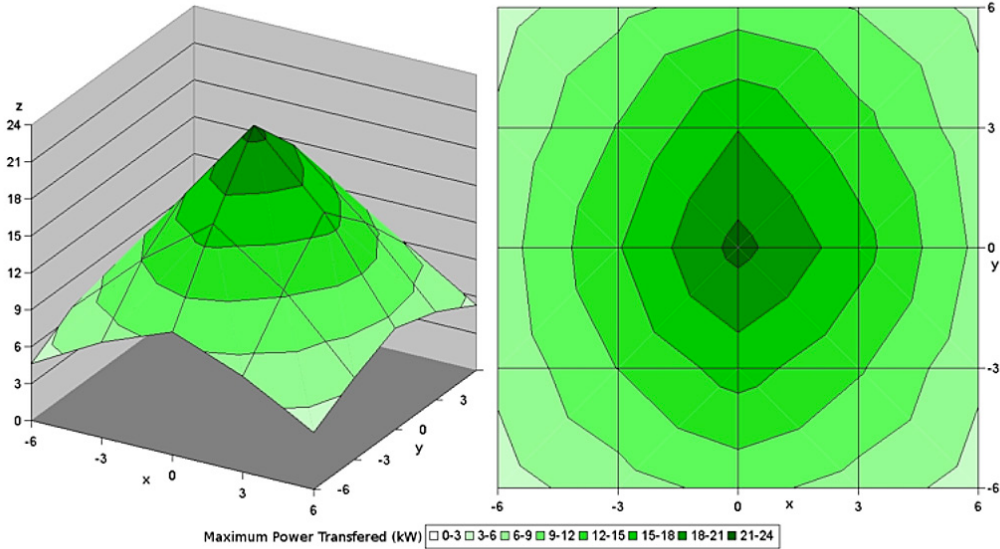
Figure 1-10
Power Transfer as Function of Air Gap



Tests were also conducted to determine the sensitivity of power transfer at various air gaps when the coil is misaligned. Power transfer rates were collected at 0.5 inch (1.27 cm) intervals between a 0.5 inch (1.27 cm) air gap and 4 inches (10.1 cm). Results for testing with a 0.5 inch (1.27 cm) air gap are shown in Figure 1-11.

Figure 1-11

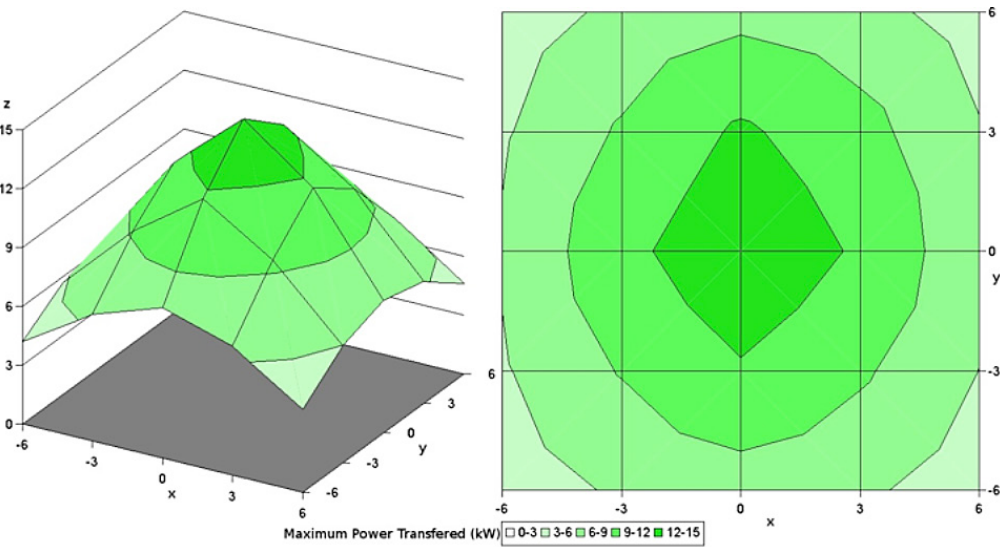
*Power Transfer
as Function of
Misalignment with 0.5”
(1.27cm) Air Gap*



With larger separation between the primary and secondary coils, the rate of power transfer was reduced as expected, but the larger air gap also reduced the gradient for horizontal misalignment. Typical results are shown in Figure 1-12 for an air gap of 2 in. (5.08 cm). This characteristic may enable larger air gaps for future generations of IPT equipment, especially if interoperability between and among equipment from multiple suppliers becomes important.

Figure 1-12

*Power Transfer
as Function of
Misalignment with 2”
(5.08 cm) Air Gap*



Systems Integration

After component testing, duplicates of all the power electronics equipment shown in Figure 1-6 and Figure 1-7 were installed on the bus by EVAmerica.

The rectifiers and heat exchanger were placed in an open compartment on the side of the bus, as shown in Figure 1-13. The output of each coil is connected to an associated rectifier module. The rectifier modules are configured in parallel for charging the batteries. The battery pack consists of 100 amp-hour, Ni-Cd, 6 voltage modules. Modules of 0.25 are connected in series to form a string. Two pairs of parallel strings make up the 100-cell traction battery with a total nominal capacity of 200 A-hrs. The battery management system control board was installed inside the bus behind the operator's seat, as shown in Figure 1-14.

Figure 1-13

Rectifiers and Heat Exchanger Installation



Figure 1-14

Battery Management System Control Board behind Driver's Seat



The communications equipment shown in Figure 1-15 was installed in the passenger compartment directly behind the operator and includes an on-board wireless modem and an antenna for communications with the stationary Track Supply.

Figure 1-15

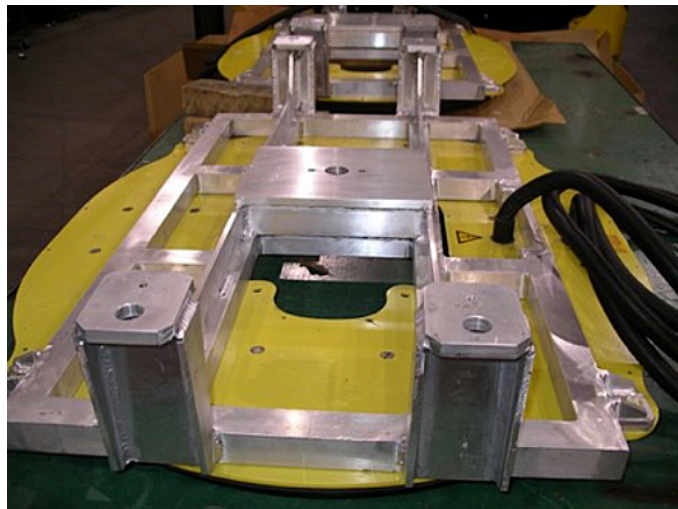
Communication Equipment Installed on Bus



To achieve the optimum air gap for charging, two pneumatically-actuated mechanisms were designed and built by EVAmerica to lower the pickup coils into place. Figure 1-16 shows the pickup coils (yellow) and pneumatic mechanism ready for installation at the EVAmerica vehicle manufacturing plant in Ringgold, Georgia. The frame for the mechanism was made of aluminum to avoid interference with the electromagnetic field generated when charging

Figure 1-16

Mechanisms for Lowering Pickup Coils



All of the power electronics equipment shown in Figures I-10 through I-13 was installed on the bus and integrated with on-board systems by EVAmerica at their plant in Ringgold, as shown in Figure I-17. The fully integrated bus shown in Figure I-18 was delivered by EVAmerica to UTC in May 2011.

Figure 1-17

EVAmerica
Assembly Area in
Ringgold, Georgia

**Figure 1-18**

*Electric Shuttle Bus
with Wireless Charging*



UTC students designed and installed a guidance system outlined in Figure 1-19 to assist the operator in positioning the bus for charging. Components of the guidance system are shown in Figure 1-20. These are off-the-shelf commercial components commonly used in recreational vehicles. The camera was mounted inside the bus near the center of the windshield. The display was mounted on the dashboard as shown in Figure 1-21.

Figure 1-19

*View of Coils under
Bus (left) and
Alignment Scheme
(right)*

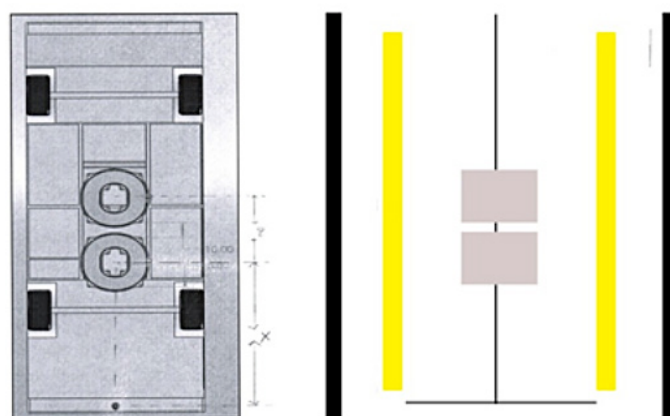
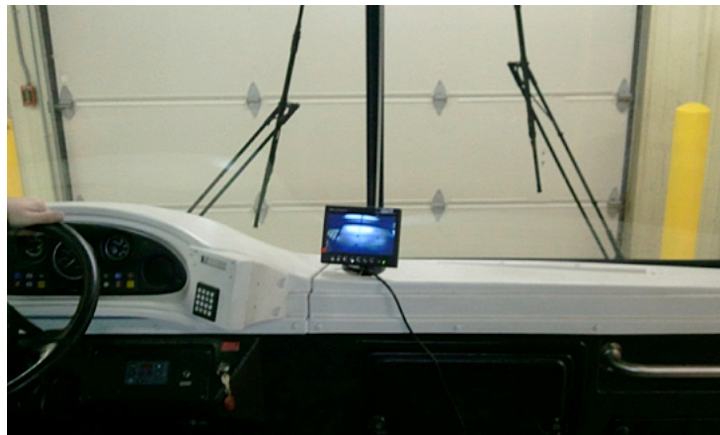


Figure 1-20

Electronic Components of Guidance System

**Figure 1-21**

Display Used to Guide Horizontal Alignment



The white lane markers are used by the operator to get the bus started toward alignment, as indicated in the photograph in Figure 1-22, which shows the bus entering the charging area. Secondary guidance for final alignment is accomplished by a camera mounted inside the windshield aimed at the yellow line down the center of the charging area. When the bus is properly positioned, the vertical yellow line representing the centerline of the charging pad and a horizontal line representing the correct stopping point will be aligned with cross hairs on the camera display, indicating to the operator that the bus is in the correct position for charging.

Figure 1-22

Bus Entering Wireless Charging Area



Site Preparation

In parallel with the design and integration work being done by EVAmerica, UTC installed all the stationary equipment on the grid side of the air gap at the AVTF. Beginning at the power grid, pull-down switches were installed to provide connection to a 100 KVA, 480V, 3-phase circuit. A second switch was installed to allow power to be directed toward the inductive power transfer system or the direct chargers, which were each equipped with individual disconnect switches that are necessary to comply with national and local electric codes.

Voltage transducers and current transformers were installed inside the main power switch to monitor grid voltage and current. These signals were fed through a data acquisition board into a PC that was equipped with Labview for data collection and analysis. Power from the grid was monitored by a voltage transformer. The photograph in Figure I-23 shows the switch gear in the background, the data acquisition board in the upper left, the voltage transformer in the lower center, and the Labview data acquisition system in the lower left. The Labview screen for monitoring AC voltage and current is shown in Figure I-24. The Track Supply shown in Figure I-25 provides up to 60 kW of power at 20 kHz.

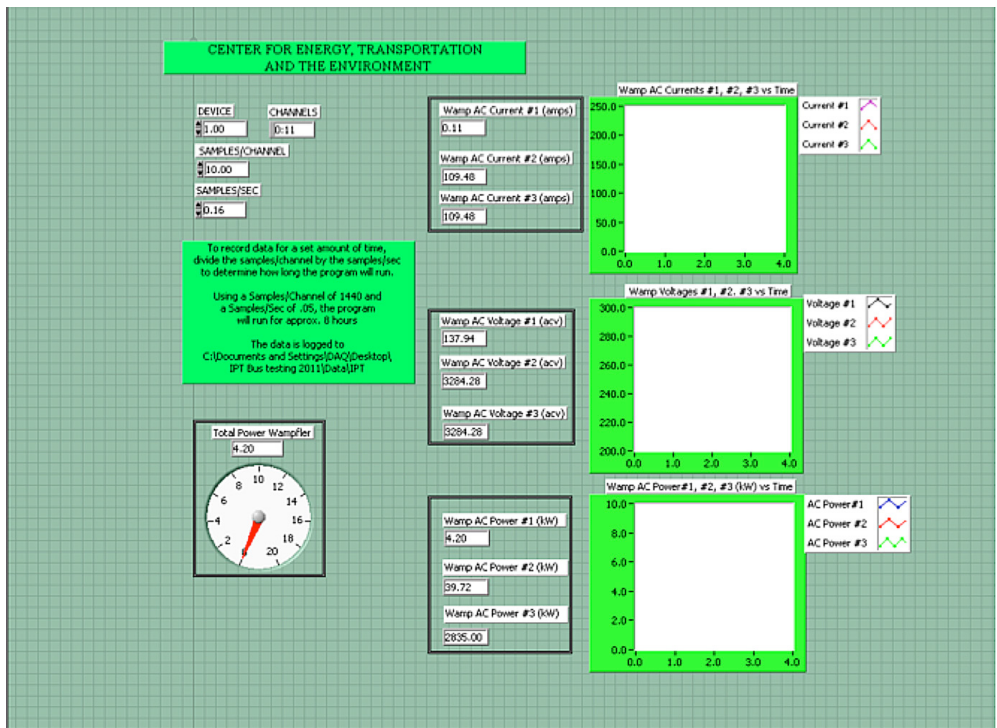
Figure 1-23

Switch Gear, Voltage Transformer, and Data Acquisition System



Figure 1-24

Labview Screen for Monitoring AC Power

**Figure 1-25**

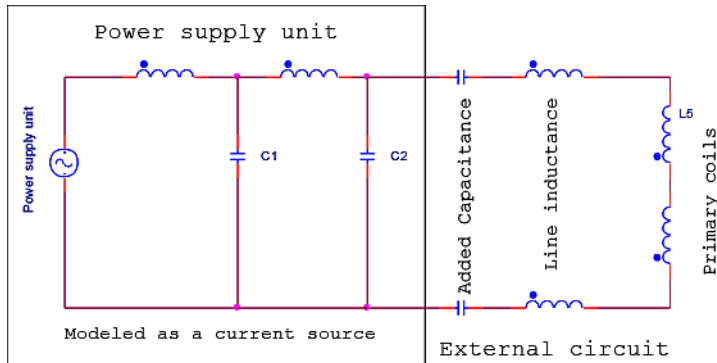
Track Supply



Tuning the System

A simplified circuit diagram for the system is shown in Figure I-26.

Figure 1-26
Simplified RLC Model
for Primary Side
of IPT Circuit



The resonant frequency for this circuit is given by

$$\text{Resonant frequency} = \frac{1}{2\pi\sqrt{LC}}$$

The values of inductance and capacitance that will result in resonance at a given frequency could be derived from the above formula, and is given as

$$L = \frac{1}{4\pi^2 f r^2 C} \quad \text{or} \quad C = \frac{1}{4\pi^2 f r^2 L}$$

Since inductance is fixed as determined by the design of the IPT coils and the length and diameter of the Litz wires that connect the circuit, tuning is accomplished by insertion of capacitors to compensate for the inductance of the Litz cables. In this case, two capacitors were installed in series with the other components to tune the resonant frequency. Note that only finite values of capacitance can be used, so perfect tuning cannot be achieved without also changing the length of the Litz cables, which was not necessary for this installation.

Figure I-27 shows the capacitor boxes with wires going into the conduit that leads to the outside IPT charging pad.

Figure 1-27

Capacitor Boxes used
to Tune Circuit



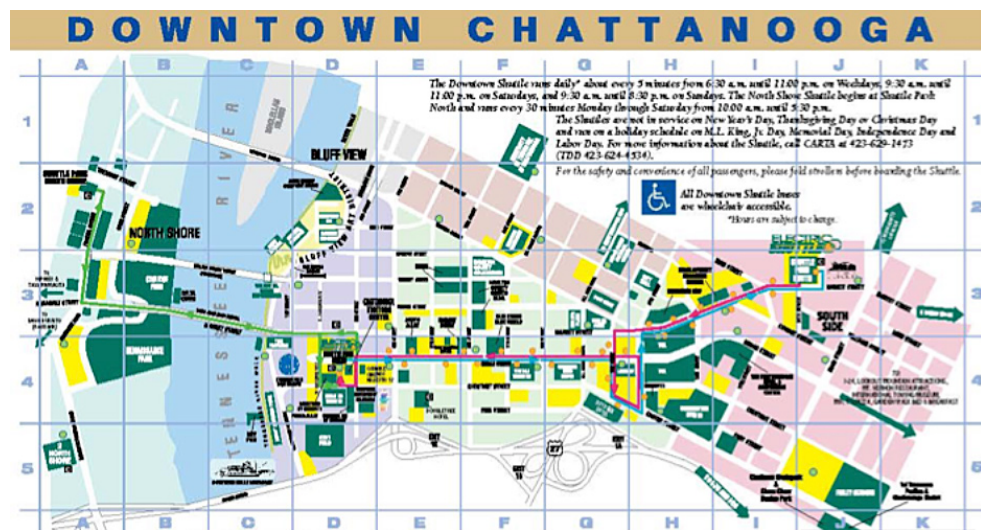
Experimental Results

Test Protocol

The CARTA downtown shuttle route, shown in Figure 1-28, consists of approximately 3 miles of relatively flat city streets with 20 stops.

Figure 1-28

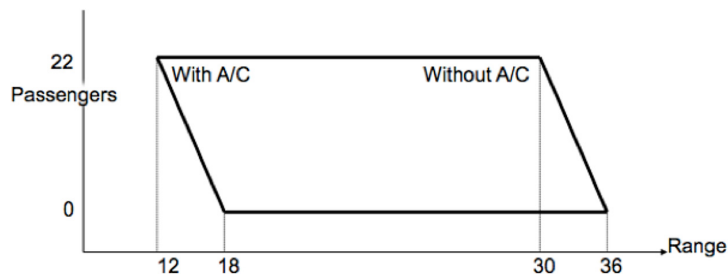
Downtown
Chattanooga
Shuttle Route



The number of trips that can be made with the existing fleet of lead acid (PbA) battery-powered shuttles depends upon number of passengers, traffic conditions, ambient temperature, and the driving habits of the operator. An overall range envelope for the existing shuttles is shown in Figure 1-29.

Figure 1-29

*Range Envelope
for Existing CARTA
Shuttles with
PbA Batteries*



For testing purposes, it was recognized that the bus does not stop unless a passenger signals or someone is waiting for the bus. On average, the bus stops about nine times for each loop around the downtown route. Since the test track is a one-mile oval, the test protocol adopted was to begin each test at the AVTF building with a full state of charge (SOC), drive the bus for three laps around the track, and stop three times on each lap to simulate a single trip of three miles with nine stops around the downtown shuttle route, then ending back at the AVTF charging station.

To simulate passenger load, water barrels were placed along the centerline of the passenger compartment, as shown in Figure 1-30, representing the weight of approximately 22 passengers.

Figure 1-30

*Water Barrels
Equivalent to 22
Passengers*



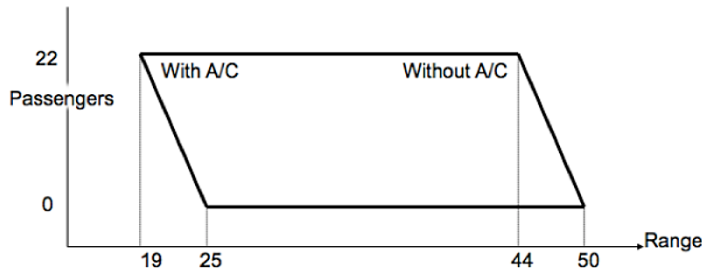
Baseline Testing

After reconditioning the original Ni-Cd batteries, a range of more than 70 miles was recorded for travel around the test track at the AVTF at a constant speed of 25 mph without stopping. The measured performance envelope for the Ebus shuttle running on Ni-Cd batteries alone on the simulated downtown route (three miles with nine stops) is shown in Figure 1-31. It can be seen that the Ebus shuttle with Ni-Cd batteries alone significantly increased the range when compared with

the existing shuttles that are powered with PbA batteries. However, the range is still not sufficient to cover the daily distance without swapping buses or changing batteries.

Figure 1-31

Baseline Range with Ni-Cd Batteries



Range with Wireless Charging

Simulation suggested that a single charge at 60 kW for 3 minutes after each 3-mile trip would provide enough energy to extend the range to the required distance. Therefore, the Track Supply was programmed for a three-minute charge and then testing began, using three laps around the test track with three stops each lap.

The on-board data acquisition system was used to record SOC, battery voltage, energy consumed, and Amp hours consumed during each trip. Prior knowledge set the parameters for defining maximum range to be when the SOC dropped to 20% or the voltage dropped to 280 volts.

Test results, shown in Figures 1-32 and 1-33, indicate changes in SOC and voltage as a function of distance for the baseline bus and the bus with wireless charging. It can be seen that the range has been extended to more than 100 miles. Some of the irregularity in the plots is because the operator was not allowed to back the bus to achieve an acceptable position for charging. This is a safety rule. To compensate for a missed charging opportunity, the operator had the option of taking a double charge for six minutes duration at the next opportunity.

Figure 1-32

SOC as a Function of Distance

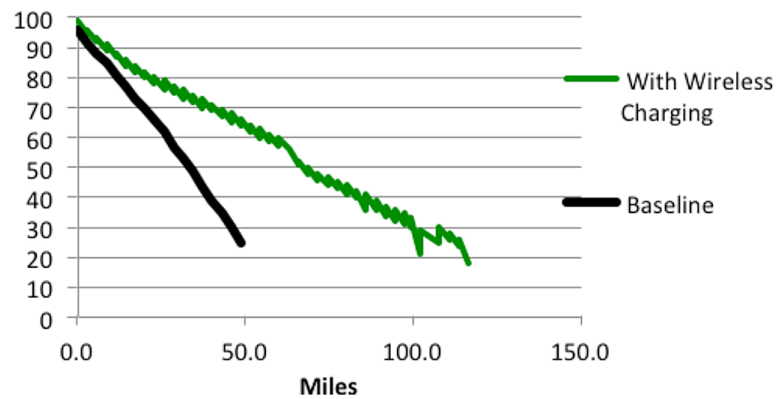
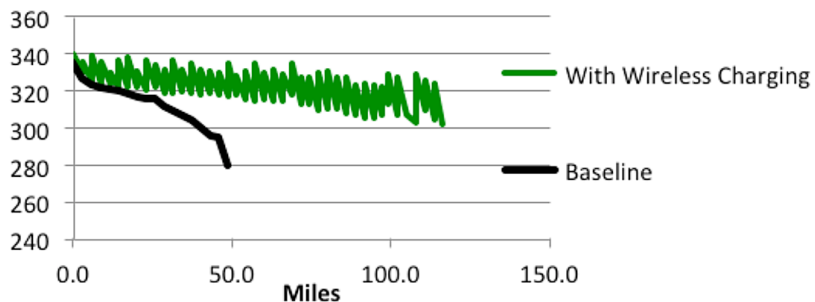


Figure 1-33

Battery Voltage as a Function of Distance



It can also be seen that the voltage collapses as the bus approaches the end of its range. SOC seems to be better behaved, but SOC is a derived number. Since a disabled bus with dead batteries in the middle of a trip would cause unacceptable inconvenience for passengers and a recovery operation by CARTA, it was decided that counting Amp hours (Coulombs) would be a better way of eliminating range anxiety for the operator. By starting with a full charge of 200 Amp hours and counting Amp hours consumed, the operator can know how many more trips can be made without losing power, which occurs when voltage collapse causes the current limiting features built into the drive system to reduce power as a means of protecting the batteries and on-board power electronics.

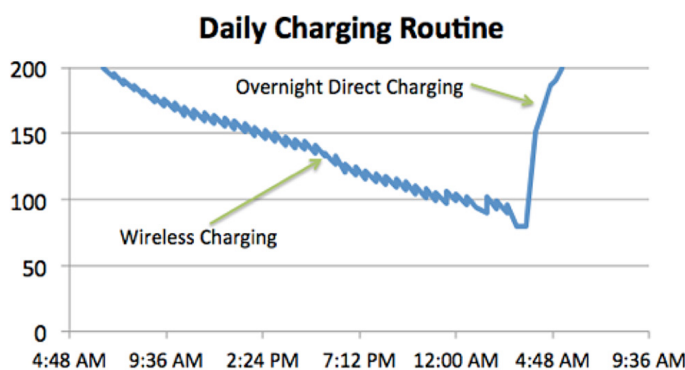
In theory, the range could also be extended by increasing the power level or increasing the frequency or duration of each opportunity charge; however, $C_s = 0.3$ is the maximum recommended charging rate for these batteries. From an operational standpoint, the wireless charging should meet, but not exceed, the level and duration needed to achieve the required range, allowing the batteries to reach a relatively low SOC at the end of the day, with slow overnight charging used to restore the batteries to a full SOC while allowing the individual cell voltages to equalize, thereby increasing the life of the batteries.

Charging the Batteries

DC Amp hours consumed and replaced over a 24-hour day is shown in Figure 1-34. It should be noted that regenerative braking provided some of the energy put back into the batteries during the day. It can also be seen that the direct charger used for overnight charging was programmed to restore automatically the batteries to a full charge of 200 Amp hours.

Figure 1-34

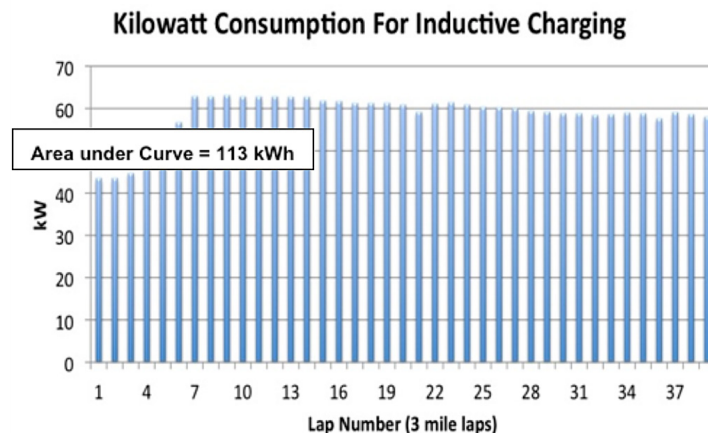
DC Amp Hours Consumed and Replaced over 24-Hour Day



Labview was used to monitor AC voltage and current on each of the three phase lines connected to the power grid. Real AC power was calculated by applying a power factor of 0.95 for the Track Supply. Results for the driving phase of a 24-hour day are shown in Figure 1-35.

Figure 1-35

AC Power for Day of
Wireless Charging
Covering 39 Trips
(117 miles)

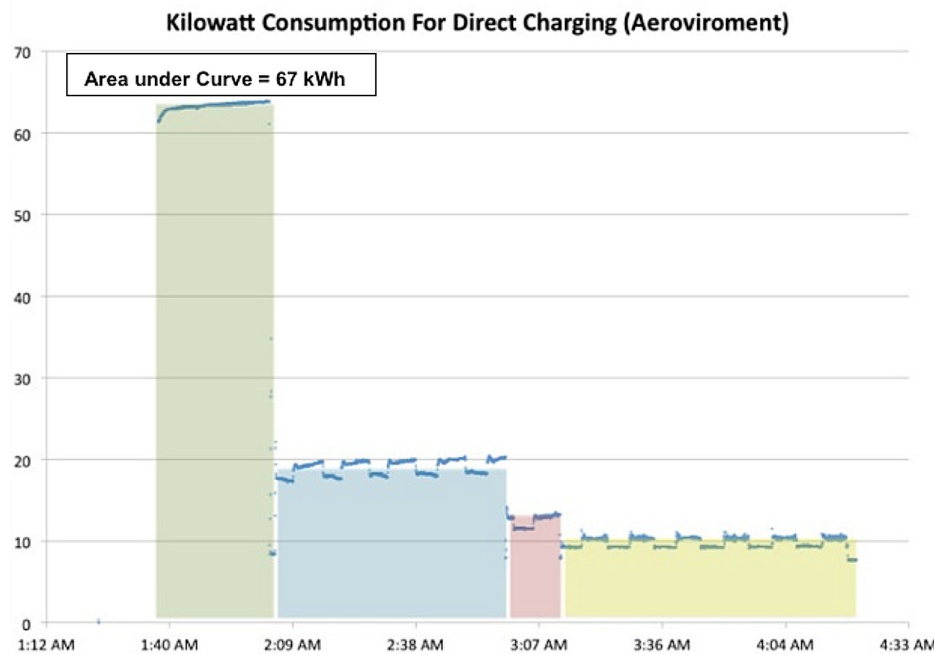


It can be seen that full charging does not occur until the seventh trip. Until then, the SOC of the batteries is too high to accept a full charge. During this period, the wireless charging is truncated automatically. As a practical matter, wireless charging could be skipped until the SOC dropped to about 80%, at which time the batteries become more receptive to charging.

Two types of chargers were available for overnight charging. Both were programmed to charge at their maximum charge rate until the SOC reaches 80%, followed by a lower rate of charge until the SOC reaches 95%, followed by a lower rate until SOC reaches 100%, followed by trickle charging until the SOC is slightly above 100%. The grid energy consumed by the Aerovironment 60 kW charger is shown in Figure 1-36. The area under the curve represents the kilowatts consumed. Analysis of the data confirmed that the automatic overnight charging not only restored the batteries to 100% SOC but also replenished the Amp hours consumed during the previous day of driving.

Figure 1-36

Power Consumed by Overnight Charging

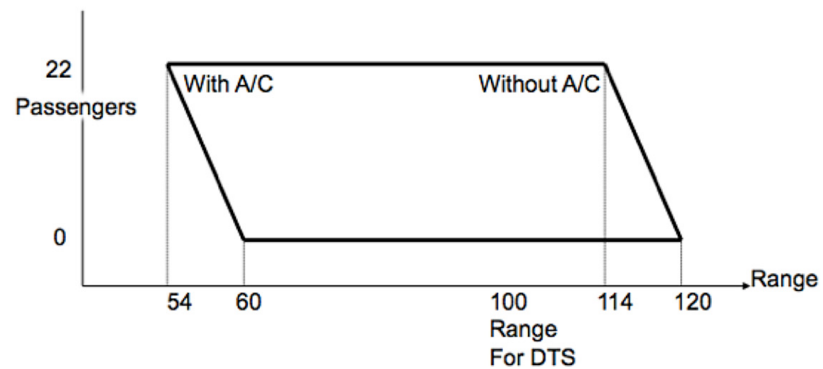


The efficiency for direct charging depends upon the phase, with the most efficient operation occurring during the initial phase. During this phase, while the batteries were at a relatively low (<25%) SOC, the measured efficiency was more than 85%. Efficiency at other times was lower, but never below 80%. Efficiency during the discharge cycle can be estimated to be approximately 90%.

The above data were recorded for an empty bus without air conditioning. The measured performance envelope for other operating conditions is shown in Figure 1-37. It can be seen that the range varies from 54 miles with a full load of passengers on a hot day to 120 miles with no passengers on a cool day. The climate in Chattanooga is mild enough most of the year that air conditioning has never been used on the CARTA electric shuttles. Should air conditioning be required, the charging profile could be modified or the operator could simply initiate double charges during the part of the day when air conditioning is needed.

Figure 1-37

Range Envelope with Wireless Charging



Operating Cost Estimates

Overall energy consumption for traction and operation of auxiliary equipment can be estimated by summing the energy supplied from the grid during wireless and direct charging. Using the data from the above test, the total energy supplied was 113 kWh + 67 kWh for a total of 180 kWh during a day when the bus was driven 120 miles. This results in a specific energy consumption rate of 1.5 kWh per mile.

The present retail rate for electricity at the AVTF is 8.5 cents per kWh. However, large commercial customers such as CARTA pay a lower rate. For a typical month, CARTA will pay 8.25 cents per kWh for the first 15,000 kWh and 3.43 cents per kWh for the balance of 21,000 kWh. This results in an average cost per kWh of 5.43 cents per kWh. The total cost of electricity used by the bus can be calculated as follows:

$$\begin{aligned}\text{Daily cost of electricity} &= 180 \times \$0.0543 = \$9.77/\text{day} \\ \text{Cost/mile} &= \$9.77/120 = \$0.08/\text{mile} \\ &\quad (\text{Empty, no A/C})\end{aligned}$$

A fully-loaded bus, operating on the same route on a hot day with the air conditioning running continuously will consume approximately 2.6 kWh per mile. This results in an estimated cost given by:

$$\begin{aligned}\text{Cost/mile} &= 2.6/1.5 \times \$0.08 = \$0.14/\text{mile} \\ &\quad (\text{Full with A/C})\end{aligned}$$

However, these conditions exist for only a few afternoons during the tourist season in Chattanooga. Furthermore, it should be noted that driving habits can have a significant impact on specific energy consumption. Taking all of these factors into account, it would be reasonable to conclude that one goal for this project has been met:

$$\text{Average cost/mile} < \$0.10/\text{mile} \text{ (year round)}$$

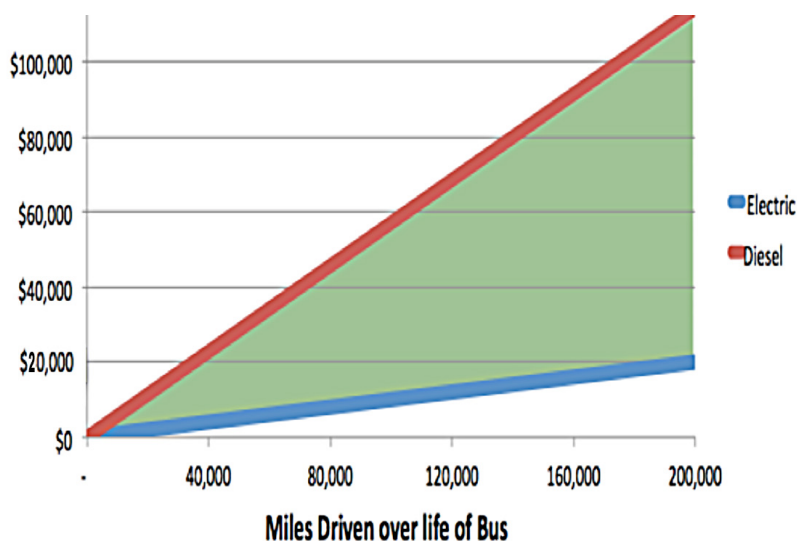
This can be compared with the cost of fuel for a diesel bus that will average about 7 mpg. The present cost of diesel fuel for CARTA is \$3.23 per gallon. This yields the following estimates for a diesel bus:

$$\begin{aligned}\text{Daily cost for diesel fuel} &= 120/7 \times \$3.23 = \$55.37/\text{day} \\ \text{Cost/mile for diesel bus} &= \$3.23/7 = \$0.46/\text{mile}\end{aligned}$$

A typical shuttle bus is designed for a useful life of seven years. Over that time, the bus will travel approximately 30,000 miles per year. Figure I-38 shows a comparison of fuel costs for an electric shuttle and a comparable diesel shuttle at today's prices. It can be seen that an electric shuttle will save more than \$100,000 on fuel costs over a 7-year life.

Figure 1-38

Comparison of Fuel Costs

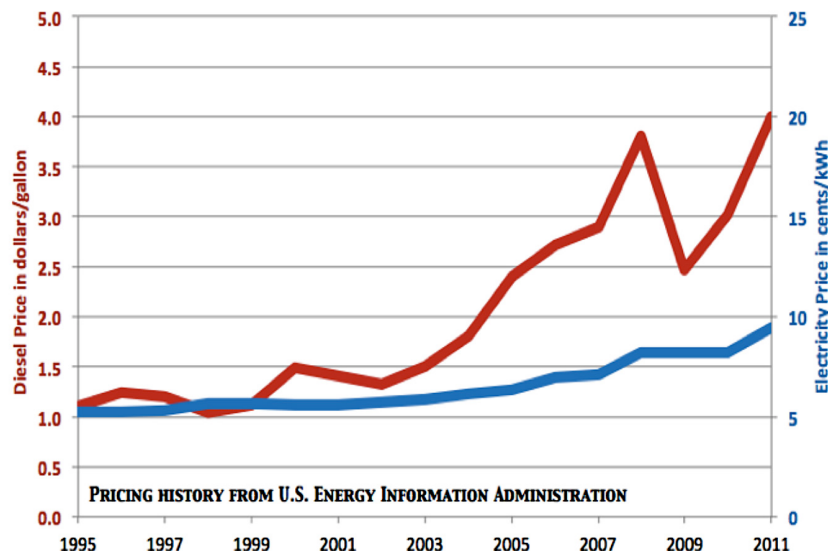


Perhaps more important, elimination of the need to swap batteries or buses during the day has the potential to reduce the total number of buses needed from 13 to 5. It can also reduce the number of batteries since present operations require one set to be in the bus while a second set is being charged and a third set is cooling down.

Also worth noting is a comparison of the changes in cost for electricity and diesel fuel over time. Since 1995, the cost of oil and electricity both have increased, as shown in Figure 1-39. It can be seen that the cost of diesel fuel quadrupled over this period, while the cost of electricity doubled. It can also be seen that the price for diesel fuel has been much more volatile, making it difficult to budget for fuel costs. The impact of this volatility can be characterized by noting that a 10% increase in the price of diesel fuel would increase CARTA's annual fuel bill by more than \$160,000.

Figure 1-39

Cost Comparison of Diesel Fuel with Electricity



Measurement of Efficiency

Since most of the wireless charging takes place after the batteries are able to accept a full charge, the most meaningful measurements of the rate of power transfer and the overall efficiency should be made during a charge cycle that occurs after the system has stabilized. The results given in the Table I-1 were measured during a wireless charging cycle that took place in the middle of the day after approximately 49 miles of service.

Table 1-1
Voltage and Current during Wireless Charging

AC Voltage	AC Current	Apparent Power (kVA)	Battery	Utility Load	Battery + Utility
272.9	74.1	20.2	382 V	325 V	-
272.8	73.2	20.0	137 A	-7A	-
272.6	74.6	20.3	-	-	-
Total	-	60.5	52.3	2.3	54.6

It can be seen that the total power being delivered across the air gap, including the utility load on the bus, was 55 kW when the grid was supplying apparent power of 60.5 kVA. A true indication of overall electrical efficiency would be the ratio of real power delivered to the bus divided by the real power provided by the grid. By definition, real power is the product of apparent power and power factor, which takes into account both phase displacement and harmonic distortion. A Fourier series representation of the current input to the rectifier yields a theoretical value for power factor of $3/\pi = 0.955$. This would yield the following estimate for theoretical efficiency:

$$\text{Theoretical efficiency} = 54.6/(60.5 \times 0.955) = 94.5\%$$

Magnetic Flux Emissions

Public safety must be paramount in all transit operations. Documentation provided with the equipment suggested that the electromagnetic field strength around the charging coils would be safe for human exposure. However, since the actual field strength depends upon the installation, Dr. John Boys, Professor of Electrical Engineering, University of Auckland, New Zealand, was retained to measure electromagnetic flux to ensure public safety.

Flux measurements were taken while the vehicle was on charge at maximum power. There is, in fact, a rather small window during which the measurements can be made and, after this short time, the charging current reduces quite significantly. The measurements were made with a Narda Safety Test Solutions ELT, Model ELT-400, P/N 2304/01, S/N M-0282. The instrument was equipped with a B Field Probe P/N 2300/90 10, S/N M-0301. This instrument has been specifically designed for this type of measurement and is ideally set up for it. It

was manufactured in Germany before the International Commission on Non-Ionizing Radiation Protection (ICNIRP) guidelines were revised upwards, so the scales based on ICNIRP measurements were not used here. The measurements were all taken by Dr. Boys using the probe directly under the edge of the vehicle, as shown in the Figure I-40.

Figure 1-40

*Dr. John Boys
Measuring EMF*



To ensure safety for the general public, measurements of flux density were made at locations outside the bus that might be representative of the places where passengers or pedestrians might stand. Variations in the flux density in any particular site occur at different positions along the site and depending on how close to the ground the probe is. The flux on the side of the vehicle above the air-gap is much smaller than the flux at ground level near the air-gap and does not contribute to the ICNIRP measurement. Results for maximum measurements taken outside the bus are given in Table I-2.

Table 1-2

*EMF Measurements
Outside the Bus*

Position	Flux Range
Forward of front wheels	<0.5 µT
Driver's side, between wheels	2.3-7.2µT
Door side, between wheels	7.2-7.5 µT
Behind the rear wheels	<0.5 µT

Inside the bus, the background level with the charging equipment off was observed to be 0.13 µT. With the charging equipment operating at maximum output, flux levels varied with location, having a maximum value at floor level directly above the coils. Results are shown in Table I-3.

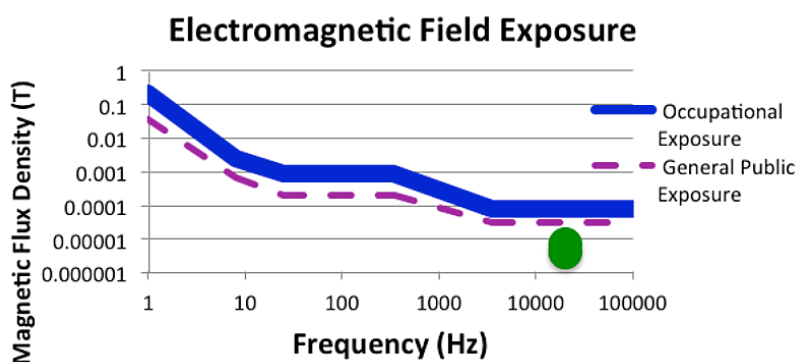
Table 1-3
*EMF Measurements
Inside the Bus*

Position	Flux Range
Background	0.13 μT
Inside bus at floor level directly above coils	4. 1 μT
Inside bus 3 ft above floor directly above coils	0.41 μT
Inside bus 6 ft above floor directly above coils	0.21 μT
Inside bus at all other locations	< 0.2 μT

Maximum values from Tables I-2 and I-3 are also shown in Figure I-41, which indicates that measured flux levels are well below the recommended limits for both public and occupational exposure to electromagnetic fields.

Figure 1-41

*Comparison of
Observed Levels of
Flux with ICNIRP
Recommendations*



Since the general public is unlikely to be familiar with the nomenclature and meaning of the ICNIRP recommendations for exposure to electromagnetic fields, the poster in Figure I-42 was produced to explain to the general public that wireless charging of buses using IPT is not harmful to humans.

Figure 1-42

Poster on Safety for
Wireless Charging

Wireless Charging Q & A

What is wireless charging?

Wireless charging is a hands-free charging system, using an Electromagnetic Field (EMF) to charge the battery in an electric vehicle, or other device, without having to plug it into a power source. It is controlled using a radio link.

Is wireless technology new?

No. Wireless technology is used in radios, televisions, cell phones, satellite based navigation systems, wireless internet access used in buildings, homes and the bus you will be riding.

Is wireless charging safe?

The magnetic field of the Earth is more than 100 times greater than what passengers are exposed to when boarding or riding the bus. The EMF exposure for passengers is no greater than would be experienced when using common household appliances.

Will the magnetic field affect my credit cards, cell phone, and other electric devices?

No. The wireless charging primary coil is enclosed and its range is specifically limited, so that it only interacts with the second coil on the vehicle. The stationary in-ground coil only emits a field when the vehicle is correctly positioned above it, so there is no interaction with the personal electronics of pedestrians.

Source	Magnetic Field Strength in micro Tesla (μT)
Earth at the magnetic poles	60
Wireless charging electric bus	less than 0.2
Electric blanket at surface	1.0 to 3.0
Hairdryer at 12 inches	0.1 to 7.0
Toaster at 12 inches	0.6 to 7.0

Do the coils get hot?

No. The coils are water cooled and will not exceed the ambient temperature of the pavement, so there is no danger to pedestrians or vehicles when the bus departs the charging station. However, metal objects left on the coil during charging may become warm to the touch.

Environmental Considerations

Compliance with the Clean Air Act

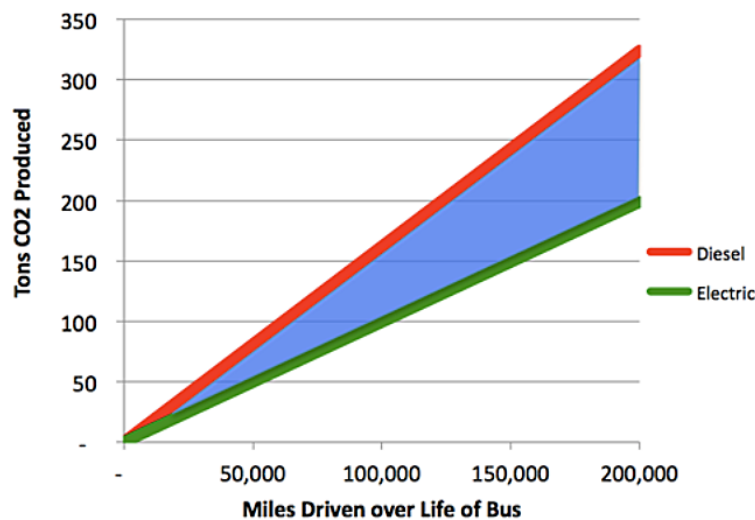
Elimination of tailpipe emissions makes electric shuttle buses particularly friendly to the environment. When the electric shuttles were introduced in Chattanooga, the primary driving force was to assist Chattanooga to attain compliance with the Clean Air Act. This meant significant reductions in all the emissions normally associated with diesel buses, including hydrocarbons (NHO_x, NMHC, or THC), Oxides of Nitrogen (NO_x), particulate matter (PM), Carbon Monoxide (CO), and Formaldehyde (HCHO). Today, Chattanooga has not only attained full compliance with the Clean Air Act but also has created enough "headroom" to accommodate economic development projects such as the new automobile manufacturing plant recently built in Chattanooga.

Reduction in Greenhouse Gases

In addition to reducing smog, there will also be a corresponding reduction in greenhouse gases (GHG). Using the method recommended by the American Bus Association, it can be estimated that combustion of a gallon of diesel fuel will produce 10,274 grams of CO₂, whereas the U.S. average for production of 1 kWh of electricity is 600 grams. A diesel bus will average 7 mpg. An electric bus will consume approximately 1.5 kWh per mile for traction. Using these values, an electric bus will reduce CO₂ emissions by approximately 567 grams per mile. Reductions over the design life of an electric shuttle are shown in Figure 1-43.

Figure 1-43

Comparison of CO₂ Emissions for Diesel and Electric Shuttle Buses (22 ft)



It can be seen that an electric shuttle will reduce CO₂ emissions by at least 125 tons. Total GHG emissions would be higher for diesel buses because of emitted hydrocarbons and particulate matter in addition to CO₂. It should also be noted that electric buses are virtually silent, thereby reducing noise pollution that can be particularly annoying in those areas normally served by transit buses.

Summary of Wayside Charging Results

A comparison of the goals and results for this project are given in Table 1-4. While there was no specific goal for efficiency, it was found that the overall grid to vehicle efficiency was greater than 90%. It was also demonstrated that electromagnetic flux emissions were well below ICNIRP standards for all locations.

Table 1-4
Summary of Results

Objective	Goal	Results
Charge time	1 minute	1 minute
Distance per charge	1 mile	1 mile
Cost per mile	\$0.10	\$0.08
Range w/o charging	100 miles	120 miles
Tail Pipe Emissions	0	0

Lessons Learned about Wireless Charging

It has been demonstrated that the range of an electric shuttle bus can be increased to more than 100 miles by wireless charging during times that the bus is stopped to load and unload passengers. It also has been shown that the electromagnetic flux produced by wireless charging is well below the safe exposure limits recommended by international standards. When compared to diesel bus operation for the same deployment, wireless charging can reduce fuel costs by more than \$90,000 over the life of the bus while reducing GHGs by more than 120 tons.

SECTION
2

Hydrogen Hybrid Bus Demonstration

Background

The objective for this project was to extend the range of an electric shuttle bus by a combination of improved batteries and an on-board generator to be powered by a hydrogen-fueled internal combustion engine and used as an auxiliary power unit (APU) to provide energy and power for the non-traction loads on the bus.

The goal was to achieve a minimum range of 100 miles for a battery-centric shuttle bus without recharging. This range would allow a CARTA electric shuttle bus to operate for a full day without swapping batteries.

Prior to the start of this project, Ebus had developed two hybrid buses. The rear compartment of one of these buses is shown in Figure 2-1. This bus has a 19 kW fuel cell (lower left in photo) as a range extender. It was tested at the University of Texas at Austin where it was shown to have a range in excess of 200 miles. However, this hybrid bus costs more than \$1,000,000, and the fuel cell had to be replaced twice during testing.

Figure 2-1
Fuel Cell Hybrid Bus
Built by Ebus and
Tested at UT Austin



The rear compartment of a second type of hybrid bus is shown in Figure 2-2. This bus has been deployed by the City of Sevierville, Tennessee, with CETE providing technical assistance to the City. The bus has a 20 kW capstone gas turbine fueled with propane as a range extender.

Figure 2-2

Hybrid Ebus with a 20 kW Gas Turbine as a Range Extender



University of Tennessee at Chattanooga (UTC) students, with assistance from CARTA, installed and evaluated the performance of an identical capstone gas turbine as a student project at the AVTF. Their analysis confirmed data from the field that indicated reasonably efficient performance of the gas turbine when operating at peak capacity, but poor efficiency when operating at less than full speed.

Prior to the onset of this project, UTC students had converted a Saturn Vue to run on hydrogen as a student project. This project suggested that an internal combustion engine running on hydrogen could provide a clean, inexpensive alternative to either previous approach.

Organization

A multidisciplinary team was formed for this project. The partnership is represented graphically in Figure 2-3.

Figure 2-3

Partnership for Development of Hydrogen Hybrid Bus Demonstration



Roles of the Partners

The role of the partners in this project was as follows:

- FTA provided funding through this cooperative agreement number TN-26-7034.
- CARTA provided expertise in transit operations and equipment.

- EVAmerica provided design, fabrication, and integration capability.
- United Hydrogen of Tennessee provided hydrogen backup capability.
- CETE provided ICE expertise and overall project management.

The project was managed through weekly design review meetings, usually held at the EVAmerica site in Ringgold. A photograph showing participants at a design review for the generator is shown in Figure 2-4.

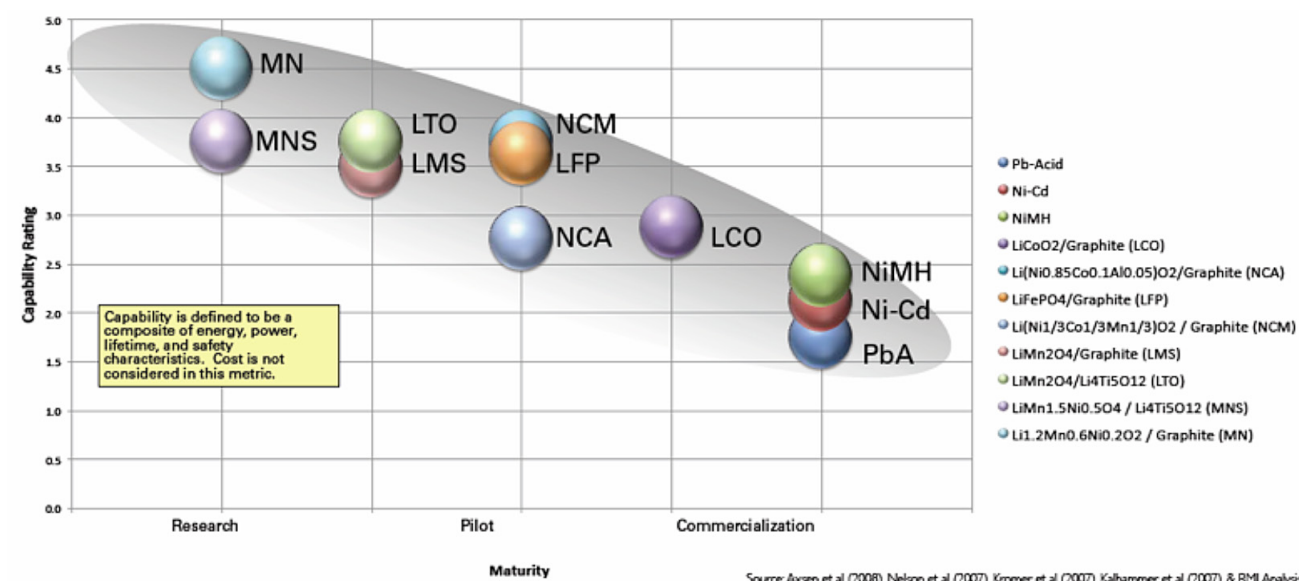
Figure 2-4
Design Review Meeting



Battery Selection

Energy density, cost, and level of maturity must be considered in selecting the optimal batteries for this project. Figure 2-5 shows a comparison of capacity rating with level of maturity for various batteries.

Figure 2-5
Comparison of Capacity Rating with Level of Maturity for Various Batteries



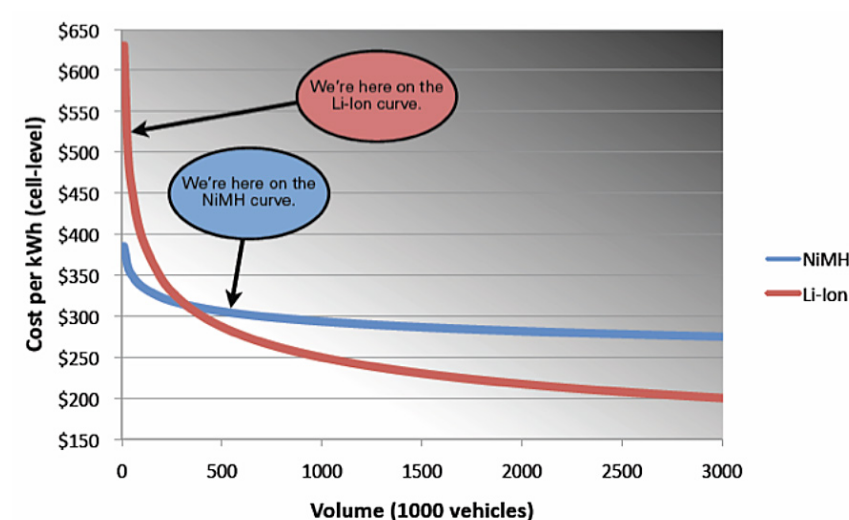
The Ebus shuttles transferred from Emory University have a nominal range of 50 miles with the original Ni-Cd batteries. Since these buses were built in 2003, newer batteries have been developed that provide certain advantages, as indicated in Table 2-1.

Table 2-1*Battery Considerations*

Variant	Advantages	Disadvantages
Li-Iron Phosphate LiFePO ₄ /Graphite	Lower cost Thermal stability Overcharge resistance Wide SOC window	Lower energy Performance at low temps
Manganese Spinel LiMn ₂ O ₄ /Graphite	Lower cost Environmentally friendly Safety (no O ₂ at high temp)	Lower energy Performance at extreme temp Cycle life
Titanate LiMn ₂ O ₄ /Li ₄ Ti ₅ O ₁₂	Cycle life Performance at low temp Thermal stability	Lower energy Lower power High cost
NCA Li(Ni _{0.85} CO _{0.1} Al _{0.05})O ₂ /Graphite	Proven technology Highest energy & power Long life	Thermally unstable Degrades at fast charge Higher cost

At the time the Ebus was built, the cost of Li-Ion batteries was prohibitively high, as indicated in Figure 2-6, because of the relatively small number of vehicles using these batteries.

Figure 2-6
Cost Projections with Increased Volume for Li-Ion Batteries



As a number of automotive manufacturers began to select Li-ion batteries, it was anticipated that the cost would come down significantly to a level that would be competitive for buses. Advantages and disadvantages for Li-Ion batteries are as follows:

- Advantages
 - Highest specific energy and power density relative to other batteries
 - Long cycle life

- Less sensitive to metal prices
- No memory effect
- Low self-discharge rate
- Disadvantages
 - More expensive than PbA or Ni-Cd batteries
 - Thermal instability in some variants
 - Poor overcharge tolerance in some variants
 - Poor lot temperature performance in some variants
- Still under development

Comparisons of various battery manufacturers and products are given in Table 2-2.

Table 2-2

Battery Manufacturers

Manufacturer	Location	Variant	2009 Price per kWh
Thunder Sky	China	Li-Iron-Phosphate	\$375
BYD Auto	China	Li-Phosphate	\$500
Ener1	Indiana	Li-Polymer	\$660
K2 Energy Solutions	Nevada (China)	Li-Phosphate	\$700
Valance	Texas (China)	Li-Phosphate	\$1,000
Altair Nanotechnologies	Nevada (China)	Li-Titanate	\$1,000
AI23 Systems	Massachusetts (Korea and China)	Li-Phosphate	\$1,228

After due consideration and comparison of all available alternatives, Thunder Sky was selected as the vendor for the battery cells. EVAmerica designed and fabricated the battery packs using cells from Thunder Sky to be compatible with the space available while providing adequate power and energy storage. A photograph of the finished battery pack is shown in Figure 2-7. The boxes on top of the yellow battery cells are part of a proprietary system that is designed to keep the individual cells balanced. Forced air cooling is also provided with the packaging designed and built by EVAmerica. These batteries can deliver of 330 Amp hours at a maximum voltage of 330 volts, which results in a nominal energy storage capacity of 109 kWh.

The cost for the cells alone was \$40,000 for a capacity of 109 kWh. The cost per kWh is given by:

$$\text{Cost per kWh} = \$40,000 / 109 \text{ kWh} = \$367 \text{ per kWh}$$

This value demonstrates the validity of Figure 2-6 while confirming that some cost reductions have occurred due to increased acceptance of these batteries.

Figure 2-7
*LiFePO₄ Batteries
 Mounted in Battery Box
 at EVAmerica*



Improvement in Range from LiFePO₄ Batteries

Tests were conducted at the AVTF track using the same driving protocol as previously developed for measuring the performance of the wireless charging bus, namely driving the bus continuously around the 1-mile test track at a maximum speed of 25 miles per hour and stopping 3 times each lap to simulate actual service on the downtown shuttle route. However, since these were new batteries, the termination criterion for ending the range test was unknown. For this reason, care was taken to monitor individual cell voltages on a real-time basis so that the point of voltage collapse could be observed before any damage was done to the batteries.

As a precaution, individual cell temperatures (highest and lowest cells) were also monitored while driving. Results are shown in Figure 2-8. The unexpected drop in temperature can be attributed to having stored the bus inside the building at approximately 23°C. The outdoor ambient temperature ranged from 13°C at the start of testing to 19°C at the end. The built-in cooling fans were programmed to come on at 20°C, so it is clear that the cooling system was adequate to take care of any heating due to current losses during driving.

Figure 2-8
Cell Temperature vs. Distance

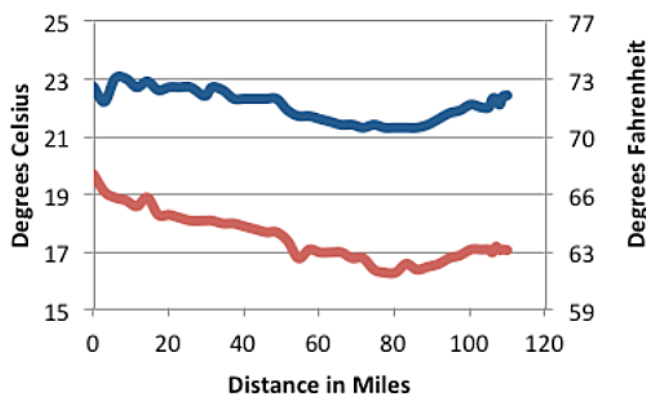
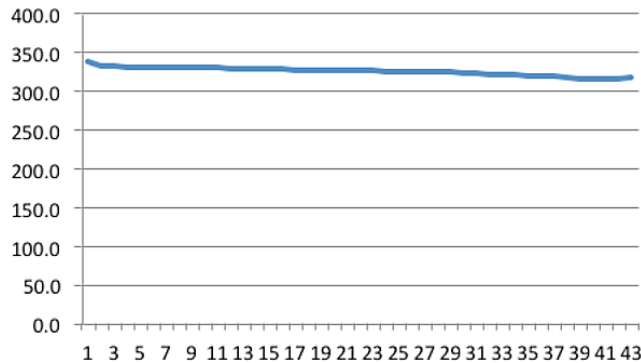


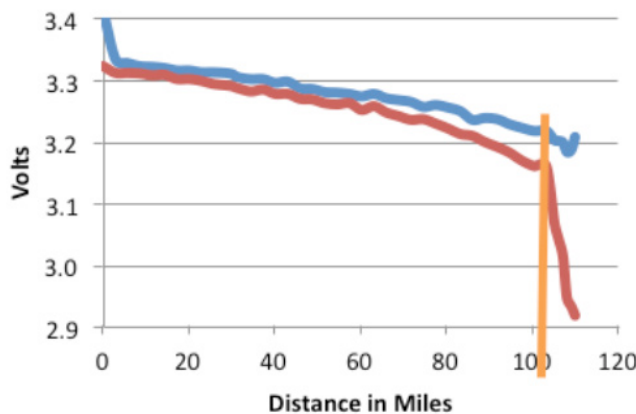
Figure 2-9 shows battery voltage as displayed on the operator panel at the end of each trip around the test track. It can be seen that the overall voltage drops only slightly from start to finish.

Figure 2-9
Pack Voltage after
Each Trip (~3 miles)



It should be noted that the voltage displayed for the operator is the value of 100 individual cells connected in series. It is known that the individual cells do not charge and discharge at the same rates. For this reason, individual cell voltage was monitored during range testing. Values for the highest and lowest cell voltage are shown in Figure 2-10.

Figure 2-10
High and Low Cell
Voltage vs. Distance



It can be seen that the cell with the lowest voltage experienced a voltage collapse after trip 39, which corresponds to 102 miles. The criterion for minimum cell voltage recommended by the manufacturer was 2.8 volts, which allowed the bus to be driven to an ultimate range of 110 miles, but that would not be recommended for daily driving because the small addition in range would not be worth the risk associated with causing permanent damage to individual cells if discharged below the recommended cell voltage of 2.8 volts.

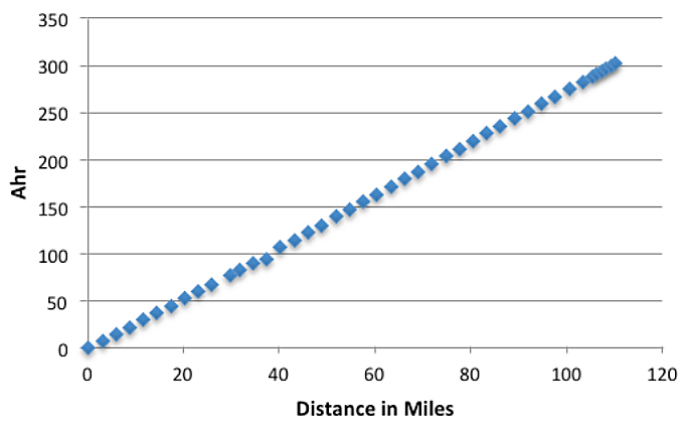
It would be unreasonable and distracting to expect the driver to monitor individual cell voltages to watch for the beginning of voltage collapse. The usual way for determining when to take the bus out of service would be to monitor

the SOC display or overall battery voltage. However, the SOC indicator for this bus was calibrated for the original Ni-Cd batteries and could not be recalibrated without changes to the firmware. Likewise, it was observed that the overall battery voltage did not collapse at the same time as the weakest cell voltage collapsed.

Since neither voltage nor SOC provide an adequate way for the driver to know when the bus is approaching the end of its range, an alternative method was explored. Shown in Figure 2-11 is a plot of Amp hours (Coulombs) consumed by the bus as a function of distance.

Figure 2-11

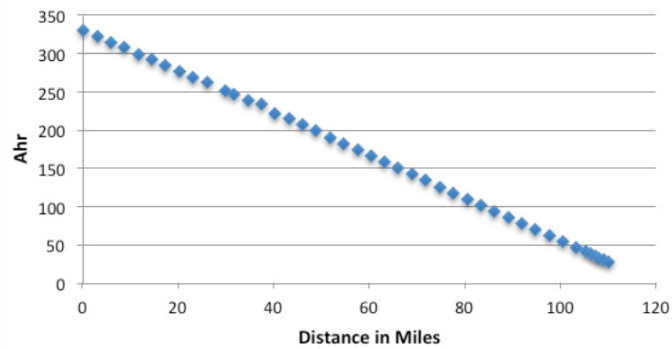
High and Low Cell Voltage vs. Distance



An alternative way of viewing this data is to subtract the Amp hours consumed from 330 Amp hours that would be available in a fully-charged battery. This would be analogous to a fuel gage on a conventional vehicle. This result can be seen in Figure 2-12.

Figure 2-12

Remaining Amp Hours vs. Distance



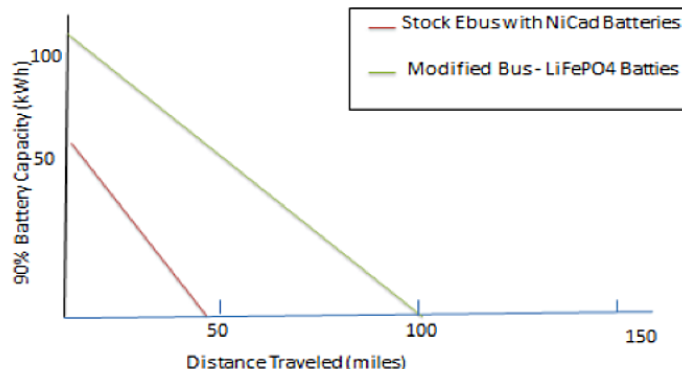
It can be seen that a linear relationship exists between Amp hours consumed and distance traveled, making this a much more reliable way of determining range. Since voltage collapse was observed to occur at approximately 100 miles, this would correspond to consumption of approximately 280 Amp hours, leaving 50 Amp hours of energy remaining from the original 330 Amp hours, which is sufficient to drive the bus approximately 17 miles before the weakest cell reaches voltage collapse.

Looking at this from the driver's point of view, a maximum of two data points can be observed simultaneously with the on-board driver's display. Since the bus must have enough reserve for the trip from the terminal point of the route back to the depot, the batteries cannot be drained beyond the point that would put the driver at risk of not being able to return the bus to the depot for recharging. Assuming that the bus begins with a full SOC, the best indication that the bus needs to be taken out of service would be when the Trip Amp Hour display reaches 280 Amp hours or the Trip Odometer reaches 100 miles, whichever comes first.

The improvement in range from replacement of the original Ni-Cd batteries with 60 kWh of capacity with the new LiFePO₄ batteries with a capacity of 109 kWh can be seen in Figure 2-13 when the operating range is limited to 90% of capacity.

Figure 2-13

Improvement in Range with LiFePO₄ Batteries



Development of Battery Charging Profile

The original Ebus came equipped with Ni-Cd batteries that were packaged in two parallel strings. The chargers that came with this bus from Emory University were programmed to charge the two strings in parallel. The new batteries were packaged in a single string, which made it impossible to use these chargers. Before purchasing a new charger for these batteries, the ABC-150, shown in Figure 2-14, was used to develop and test a charging profile that could be used to specify a purpose-built charger for these batteries.

Figure 2-14

ABC-150 Used to Develop Charge Profile for LiFePO₄ Batteries



The battery manufacturer provided a recommended charge profile for individual cells that allowed charging to be done at 0.5C until cell voltage reached 4.0 volts. For a string of 100 cells, this would have allowed the battery pack to be charged at 54.5 kW until the pack voltage reached 400 volts. To provide a margin of safety, the ABC-150 was programmed to charge at 50 amps with a maximum power output of 20 kW, at which point the ABC-150 would automatically switch to a voltage source type charger, holding voltage constant at 400 volts while letting the current drop in response to the change in impedance that would occur as the battery approached a full SOC. This rate is less than half the maximum allowable rate but fast enough to fully recharge the battery pack in five hours, which is within the time allowed between 11:30 PM and 6:30 AM for overnight charging.

Current and voltage during a typical charging operation are shown in Figures 2-15 and 2-16.

Figure 2-15

Current during Charging

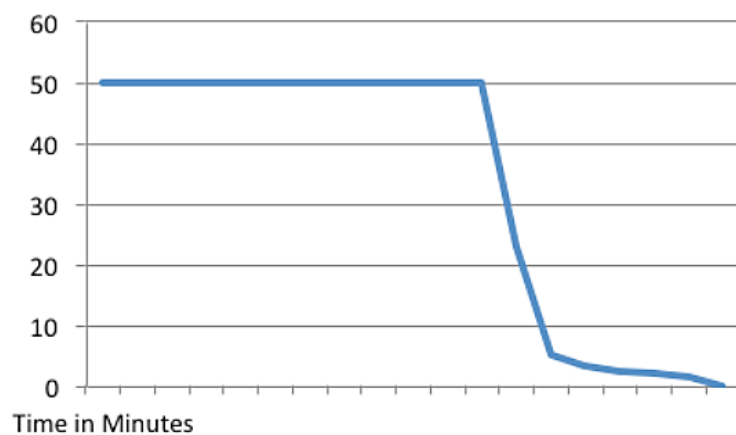
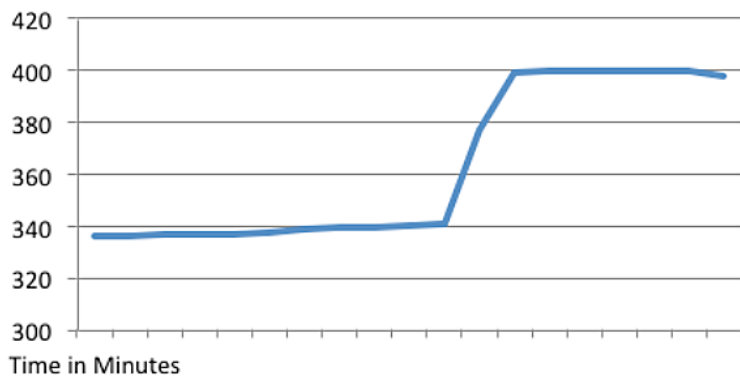
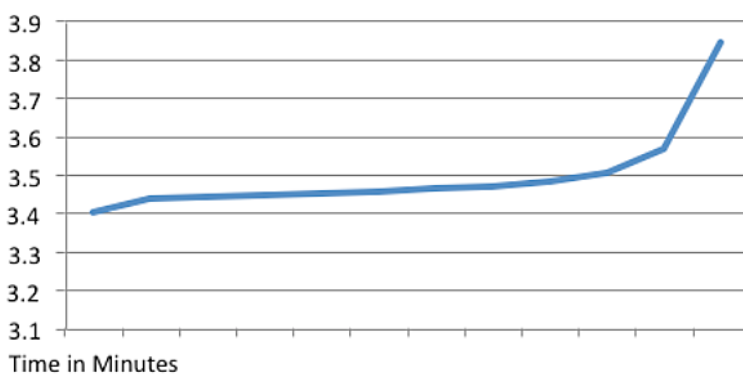
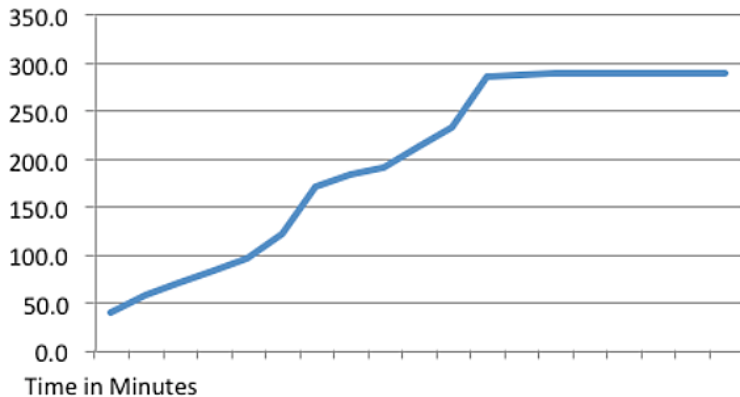


Figure 2-16*Voltage during Charging*

Individual cell voltages were monitored during the charging process to make sure that no single cell was overcharged. The highest individual cell voltage is shown in Figure 2-17.

Figure 2-17*Highest Cell Voltage during Charging at 100 Amps*

It should be noted that the rate of increase in cell voltage accelerated as the battery pack approached a full SOC. To establish a cut-off point for the design of a purpose-built charger, it was noted that very little energy was restored to the battery during the final stage when the rate of voltage increase began to accelerate. Figure 2-18 shows the cumulative amp hours restored to the battery.

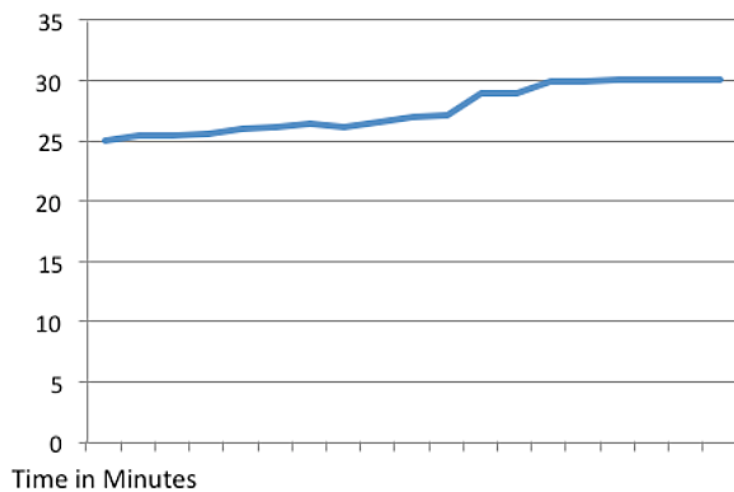
Figure 2-18*Cumulative Amp Hours during Charging*

Since so little energy is restored to the battery after the pack voltage reaches 400 volts, the recommended profile for a purpose-built charger would be to charge at 100 amps until voltage reaches 400 volts and then cut off charging immediately rather than risk cell damage after that point while attempting to add an insignificant amount of charge to the battery pack.

As safety precaution, individual cell temperatures were also monitored during charging. The results are shown in Figure 2-19 for the cell with the highest temperature. It can be seen that the batteries do not experience a significant increase in temperature, mirroring the behavior observed earlier during discharging.

Figure 2-19

Cell Temperature
(Highest)
during Charging



Lessons Learned about LiFePO₄ Batteries

For same space and less weight, LiFePO₄ batteries have been demonstrated to increase range by a factor of 2.3 (from 44 miles to more than 100 miles). These batteries also have a faster charge rate (0.5 C vs. 0.3), which reduces the recharge time by 40%. These batteries run cooler, which means that an on-board chiller is not needed, saving weight and energy. The batteries do not overheat when being charged, which means they can be safely charged without removing them from the bus, again saving time.

The combination of increased range and recharging time has the potential to reduce significantly the number of shuttle buses that must be maintained in order to meet the daily demand for service. For CARTA, this could mean a reduction in the number of shuttle buses needed to operate the downtown route from 13 to 5 or 6, depending on reliability and maintainability of all bus components.

Overall grid-to-motor efficiency will be the product of efficiency for charging and efficiency during discharging which can be estimated as follows:

$$\text{Grid-to-motor efficiency} \sim 0.85 \times 0.9 = 76.5\%$$

Auxiliary Power Unit (APU) Considerations

To comply with the Clean Air Act, any engine used for traction on public roadways must be certified by EPA and can be issued only to a vehicle manufacturer. At present, the only hydrogen-fueled engines that have EPA certification are large diesel conversions that are too big for this project. To proceed without violating the Clean Air Act, the generator can be used only for the auxiliary services and not for traction.

These auxiliary services (“hotel loads”) include air conditioning, power steering, lighting, air compressor (power brakes), and the cooling system for the batteries, if required. For the Ebus, the maximum power required for all auxiliary services is approximately 10 kW. However, CARTA does not intend to use the air conditioner, and new batteries do not require a separate cooling system. This would leave an auxiliary load of approximately 5 kW. However, a slightly larger unit was chosen because the power rating of the engine will be somewhat lower when running on hydrogen because of the higher air-fuel ratio required for complete combustion. For these reasons, a relatively small 10 kW generator, shown in Figure 2-20, was chosen to serve as an APU for this project.

Figure 2-20

10 kW Polar Power APU



This generator was selected based on the following features:

- Maximum continuous output of 10 kW at 2600 rpm
- Available in all voltages from 24 to 500 Volts dc
- Variable speed with a typical 500 rpm span from no load to full load
- Lower speed option available
- 3-cylinder water-cooled engine originally designed for diesel operation
 - Water-cooled
 - Outstanding durability: 20,000 to 30,000 hour life expectancy
- Easy to maintain
 - Oil change at 200 hours
- Temperature-compensated battery charging
- Alternator efficiency in excess of 85%
- Military specifications met without extra cost

Engine Modifications

Shown in Figure 2-21 is the APU installed in the rear compartment of the bus. It has been converted to run on hydrogen and compressed natural gas (CNG).

Figure 2-21
H₂/CNG APU Installed
in Modified Bus



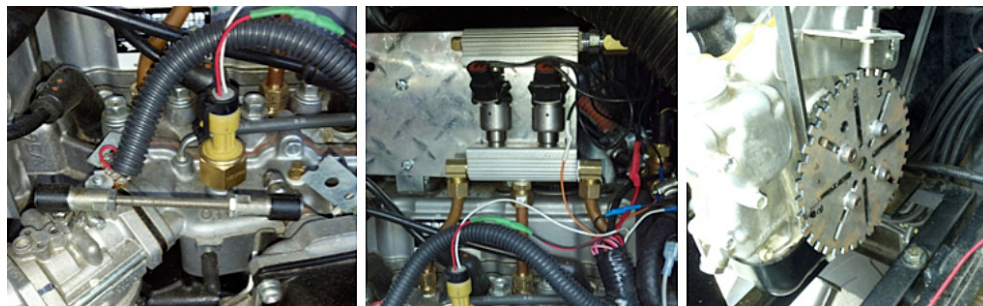
Major modifications to the APU for hydrogen operation were the additions of a separate, independent fuel and ignition system, a turbocharger, and a series of relays to switch inputs from the Daihatsu ignition module (IM) to the AEM® EMS-4 stand-alone engine control unit (ECU) to the ignition coils. This design allows the engine to be switched between CNG and hydrogen electronically.

without making any major mechanical changes to the engine or affecting the engine performance with respect to each fuel. The switchability of the unit also allows for the customer to use whichever fuel is the most economically viable at the time. Modifications made for CNG operation were the exchange of the propane regulators for CNG/methane regulators. The stock Daihatsu carburetor/mixer was designed to handle either fuel.

Other modifications to the engine include the installation of various sensors for the EMS-4 and the fabrication and installation of a fuel manifold. Figure 2-22 shows pictures of the modifications made to the APU for hydrogen operation.

Figure 2-22

Various Hydrogen Fuel and Ignition System Components and Sensors



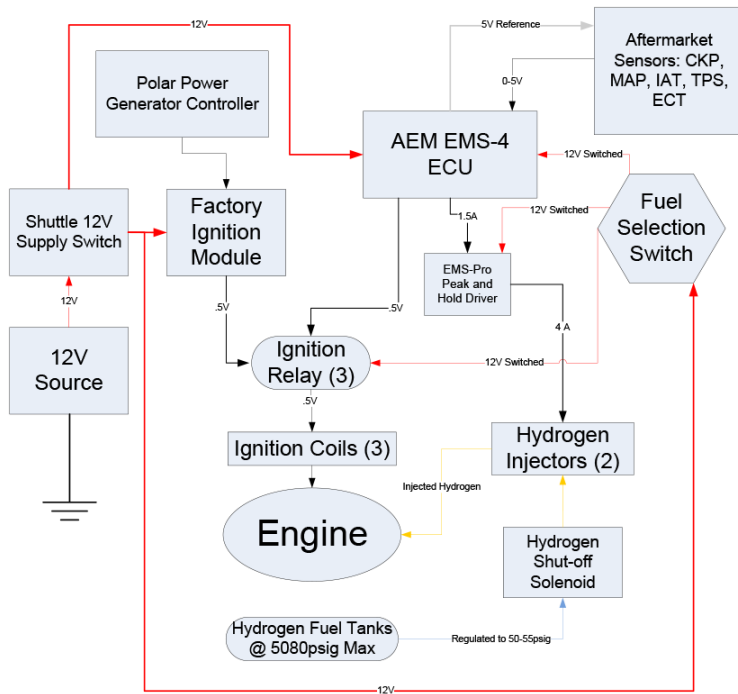
Fuel and Ignition

In designing an engine that is capable of operating on CNG and hydrogen independent of one another, two separate fuel systems must be in place to deliver each fuel efficiently. This operation is executed using a series of switchable relays to discern which ignition signal will be delivered to the ignition coils. When the selection is switched ON to use hydrogen, the EMS-4 and relays are energized and the ignition signals are switched to the EMS-4 rather than the Daihatsu ECM. The fuel selection switch is left in the OFF position for CNG operation as the Daihatsu IM and Polar Power engine controller controls the engine.

Figure 2-23 is a simplified schematic of the aftermarket and factory systems.

Figure 2-23

Dual Engine Management Diagram

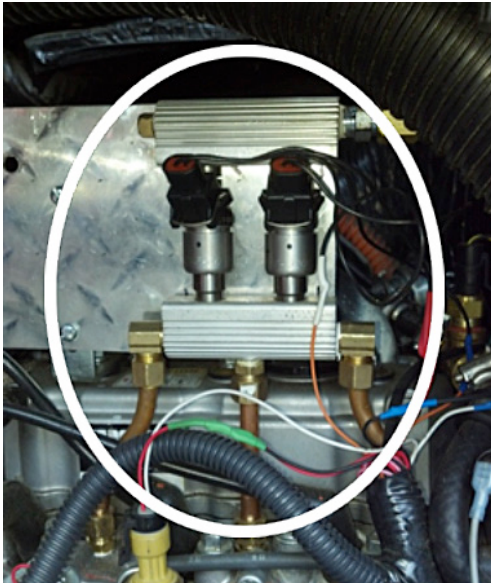


Fuel Delivery Apparatus

The hydrogen is injected into the engine for combustion by two injectors through three points in the slightly modified cylinder head using copper tubes, as shown in Figures 2-24.

Figure 2-24

Hydrogen Delivery Manifold



Dual Fuel Feature

Since hydrogen-fueling infrastructure has not been fully developed, the APU conversion was done in such a way that the engine could be switched from CNG to hydrogen, as previously mentioned. Shown in Figure 2-25 is a view of the engine management panel, which contains the fuel selection switch, EMS-4, and ignition control relays.

Figure 2-25

Engine Management Panel

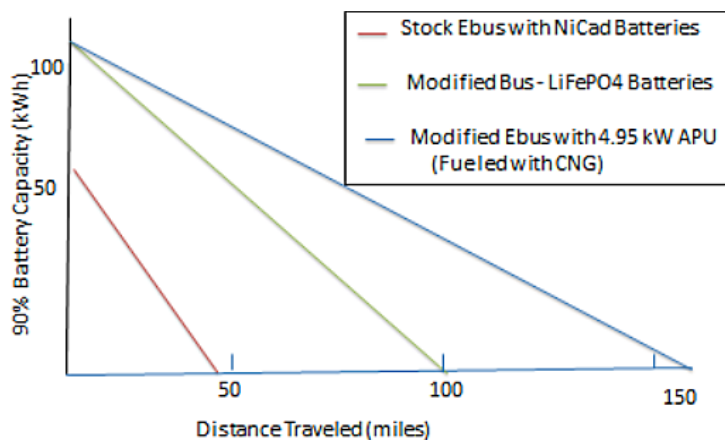


Test Results with CNG

The Ni-Cd batteries on the original Ebus shuttle were cooled with a 2.5 kW unit that was removed when the new batteries were installed. Likewise, the 2.5 kW air conditioning unit was also removed, thereby reducing the auxiliary load from a maximum of 10 kW to 5 kW. For this reason, the capacity of the APU had to be limited to no more than 5 kW to provide power for the auxiliary services only. Results for an empty bus with the APU set to deliver 4.95 kW are shown in Figure 2-26.

Figure 2-26

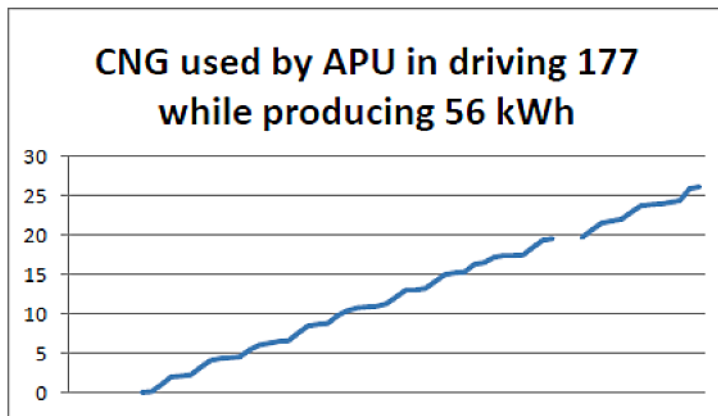
Improvement in Range with 4.95 kW APU Fueled by CNG



Fuel consumed during this test is shown in Figure 2-27. Note that the APU was not started until the SOC was reduced to 95% to protect the batteries from overcharging.

Figure 2-27

CNG Used by APU in Driving 177 miles



The overall efficiency of the APU can be estimated as follows:

$$Q_{in} = \text{mass of CNG consumed} \times \text{lower heating value}$$

$$Q_{in} = 26.1 \text{ kg} \times 12.8 \text{ kWh/kg} = 334 \text{ kWh}$$

$$Q_{out} = \text{APU Output} = 56 \text{ kWh}$$

$$\text{Efficiency APU} = Q_{out} / Q_{in} = 56 / 334 = 16.8\%$$

During this range test, the batteries provided 103 kWh of additional energy, so the total energy used for traction and auxiliary power can be estimated as follows:

$$\text{Total energy} = E_{\text{BATTERIES}} + Q_{\text{APU}} = 103 \text{ kWh} + 56 \text{ kWh} = 159 \text{ kWh}$$

The measured efficiency for charging the batteries has been found to be 85%. Assuming the efficiency during discharge is 90%, the overall grid to motor efficiency for this modified bus can be estimated as follows:

$$\text{Overall grid-to-motor efficiency} \sim ((0.85 \times 0.9 \times 103) + 0.168 \times 56) / 159 = 55.5\%$$

Test Results with Hydrogen

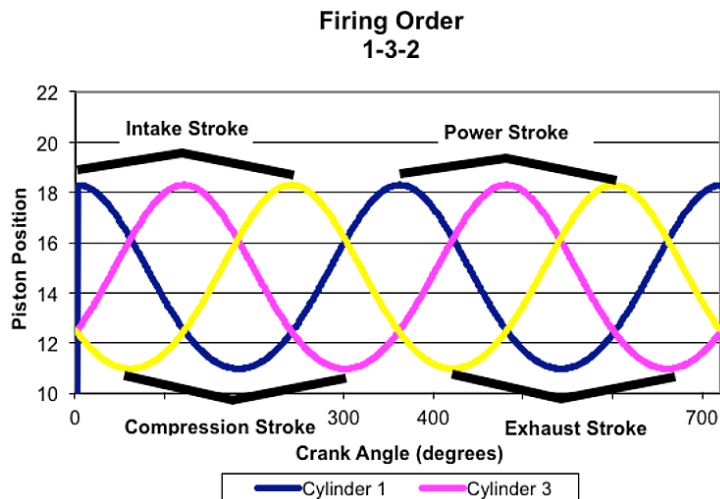
In theory, the thermodynamic efficiency of an internal combustion engine should be higher when fueled with hydrogen because of the higher flame temperature. However, the cooling system for this engine was not adequate to handle the higher flame temperatures without overheating.

This engine management system (EMS) was originally designed for a four-cylinder vehicle, but it can be reprogrammed and adapted to engines as large as ten cylinders using an ignition scheme called “wasted spark.” This scheme

fires multiple spark plugs simultaneously. In designing the ignition system, a wasted spark ignition scheme was used in which only three of the four available ignition channels were used on the EMS-4. When operating using a wasted spark ignition, it is important to know which stroke each cylinder is on at any given time to prevent pre-ignition and detonation. This would inhibit engine operation and could cause severe engine damage. The desired wasted spark operation had one cylinder fire on the power stroke while the wasted spark fires on the exhaust stroke where there is no combustible fuel available. To prevent this, a graphical representation of the cylinder motion for all six cylinders was created using the equations of motion for a slider crank mechanism with an arbitrary connecting rod length. This is shown graphically in Figure 2-28.

Figure 2-28

Firing Diagram



In practice, the wasted spark design of the ignition system limited operation to speeds below 2500 rpm to avoid pre-ignition caused when the wasted spark ignited hydrogen left in the combustion chamber from the previous power stroke of the engine. This problem was compounded by the relatively high air fuel ratio required for stoichiometric combustion of hydrogen. This prevented operation of the engine at rated capacity because it was impossible to get enough air into the cylinder, even with turbocharging, for complete combustion of the hydrogen charge that was needed to supply enough chemical energy to operate at rated capacity. This rich combustion also caused unacceptable levels of hydrocarbons to be emitted from the engine, thereby effectively erasing any gains in tailpipe emissions from burning hydrogen, and perhaps creating a fire hazard should the exhaust gases pass near an open flame. For all of these reasons, the maximum sustainable output of the APU running on hydrogen was limited to 2.5 kW, which was well below the average auxiliary load of approximately 7 kW. Results for operating the APU with hydrogen are shown in Figure 2-29. The hydrogen consumed during this test is plotted in Figure 2-30.

Figure 2-29
Range Improvement with
2.5 kW APU
Fueled by Hydrogen

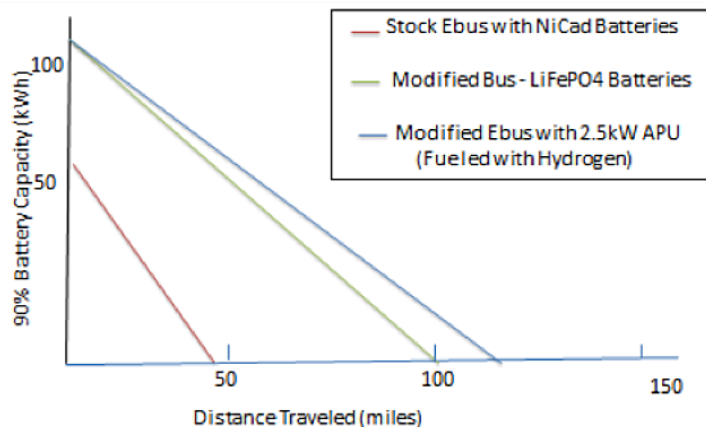
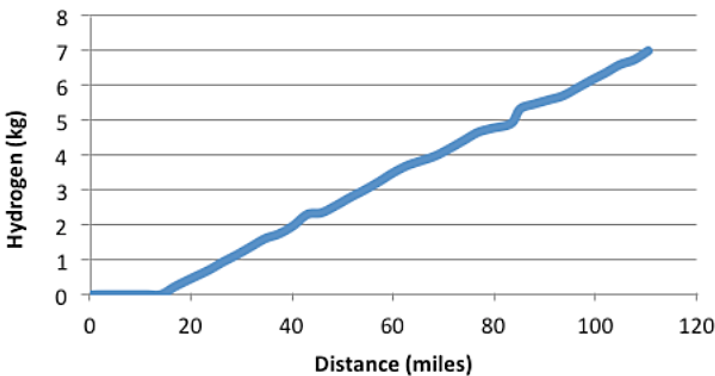


Figure 2-30
Hydrogen Used by APU
While Driving 117 Miles



It can be seen that 7.0 kg of hydrogen were consumed to increase the range by 20 miles. The overall efficiency of the APU can be estimated as follows:

$$\begin{aligned} Q &= 7 \text{ kg} \times 39 \text{ kWh/kg} = 273 \text{ kWh} \\ \text{APU output} &= 18.8 \text{ kWh} \\ \text{Efficiency} &= 18.8/273 = 7\% \end{aligned}$$

The fuel cost for this extra 20 miles would be approximately \$49.00 at an average commercial price of \$7.00 per kg, for an average of \$2.45 per extra mile. This can be compared with approximately \$0.10 per mile for fuel when running on batteries alone and approximately \$0.40 per mile for fuel for an equivalent diesel bus. Clearly, the cost for this modest gain in range is prohibitively expensive.

During this test, the batteries also supplied 86 kWh of energy with charging efficiency of approximately 85% and discharge efficiency of 90%. This would result in an overall grid-to-motor efficiency given by the following calculation:

$$\text{Overall grid-to-motor efficiency} = ((0.85 \times 0.9 \times 86) + 0.07 \times 18.8)/104.8 = 64\%$$

Lessons Learned about Use of an APU to Improve Range

It has also been shown that the range can be increased to a distance of more than 170 miles when the APU was operated at 4.95 kW with CNG. In theory, the range could have been extended to more than 200 miles if the APU had operated at its rated capacity of 10 kW, but this would have exceeded the power required by the auxiliary loads, which would have resulted in some of the energy being used for traction which would require certification by the EPA for roadway use. It was beyond the scope of this project to seek EPA certification, but the information may be of interest for future development of a true battery-centric hybrid bus.

Results were less promising when the APU was fueled with hydrogen, which increased the range by a modest 15 miles. This failure was due primarily to inability to tune the ICE for an output greater than 2.5 kW because the relatively high air-fuel ratio required for complete combustion limited the amount of hydrogen that could be injected into the combustion chamber for each power stroke. Even with turbocharging, it was impossible to tune the engine to run at speeds higher than 2500 rpm without experiencing pre-ignition that could have been caused by either hot spots from the higher flame temperature of hydrogen or hydrogen left in the combustion chamber that could be ignited by the wasted spark ignition system. It is possible that these tuning problems could have been overcome by implementation of an alternative ignition system, but that was beyond the scope of this project.

SECTION
3

Technical Support

The first technical support task was to provide technical assistance for a fleet of electric shuttle buses being operated by the City of Sevierville, Tennessee. After extensive analysis of the problems being encountered, it was determined that a dedicated technician was needed to keep the fleet of buses running smoothly. This task was accomplished by transferring funds to enable Sevierville to hire a technician.

The second support task was to assist Emory University with selecting and procuring new chargers for its fleet of electric shuttle buses. CETE had previously determined a number of issues with Emory's existing chargers and its general maintenance operation; however, task was rendered unnecessary when the university decided to replace its fleet of electric shuttle buses with diesel buses running on biodiesel to be manufactured from used cooking oil used in the campus food services. When that decision was made, Emory also agreed to transfer its fleet of electric shuttle buses to CARTA with assistance from FTA under Cooperative Agreement TN-26-7035. The lessons learned in supporting Emory University were applied to the current research project, which provided the information that CARTA needed to procure a proper charger for the buses transferred to it. CETE transferred funds originally intended for Emory to CARTA to purchase an appropriate charger for the Ni-Cd batteries used on the buses transferred to CARTA. One of these buses is now in regular service. One was used for the wireless charging project, and another was used for the hydrogen hybrid bus project described previously; a third was used for the battery-centric hydrogen hybrid bus project. The other two shuttle buses are being evaluated for possible future deployment as replacements for CARTA's aging fleet of electric shuttle buses.

Lessons Learned about Technical Support

It has been shown that the success of electric shuttle operation is highly dependent upon technical support in the maintenance operation. At Sevierville, the problem was solved by employment of a dedicated electric bus technician. Emory University decided to go another direction rather than dedicate technical support resources to its fleet of electric shuttles. During the course of this program, CETE had many opportunities to observe and interact with the maintenance personnel at CARTA. Its success in operating a fleet of electric shuttles continuously for more than 20 years can be attributed in part to the skill and level of dedication exhibited by its maintenance organization. Similar observations were made with regard to the successful operation of electric

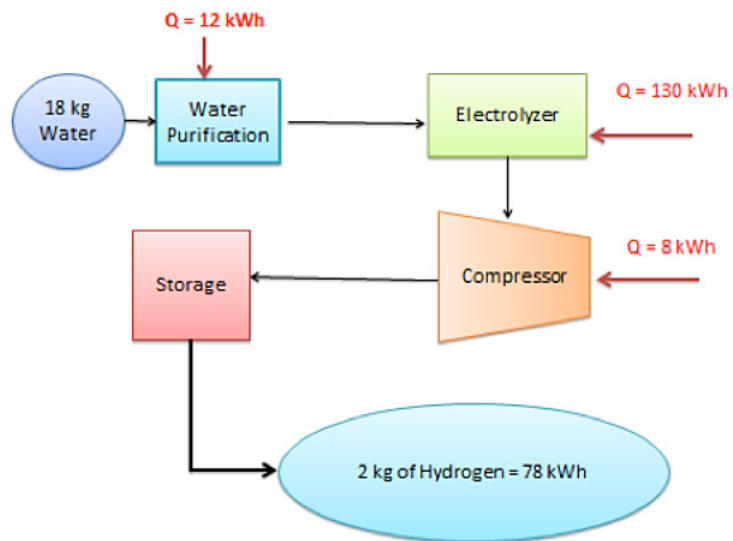
shuttles at Santa Barbara, California. The lesson here is that even the best technology will fail if not supported in the field.

SECTION
4

Acquire and Install Hydrogen Electrolyzer

The hydrogen fuelling station that was started under FTA Cooperative Agreement TN-26-7032, East Tennessee Hydrogen Initiative, was completed and commissioned in December 2009. The basic components of the fueling station are shown in Figure 4-1, which also shows the daily inputs and outputs for the as-built system.

Figure 4-1
Components of Hydrogen Fueling Station



The deionizer used for water purification is shown in Figure 4-2. The Proton Exchange Membrane (PEM) Fuel Cell shown in Figure 4-3 uses electrolysis to generate hydrogen from deionized water. The compressor shown in Figure 4-4 was used to compress the hydrogen from to 6,000 psi.

Figure 4-2
Water Deionizer



Figure 4-3

PEM Fuel Cell Electrolyzer
supplied by
Proton Energy Systems

**Figure 4-4**

Hydrogen Compressor



The hydrogen flows from the compressor through the wall and underground to the storage tanks and dispensing system shown in Figure 4-5. The tanks and dispensing system were set back 20 feet from the building and enclosed by a chain-link fence with a locking gate to comply with recommended standards for hydrogen storage and local fire codes. The dispensing system was also used

for filling the bus with CNG, which was supplied from tanks that were installed behind the red hydrogen tanks. The fueling station is capable of producing 2 kg of hydrogen per day and storing 10 kg at 6,000 psi. This system was completed and commissioned in December 2009.

Figure 4-5
Hydrogen Storage Tanks
(red) and Dispensing
System (in blue cabinet)



The energy required to produce 2 kg of hydrogen was found to be 140 kWh. The useful chemical energy in 1kg of hydrogen is equal to the lower heating value of 78 kWh. Thus, the overall efficiency of the system can be calculated as follows:

$$\text{Efficiency} = \text{Output/input} = 78 \text{ kWh}/140 \text{ kWh} = 56\%$$

At the present retail cost of electricity at the AVTF of \$0.0757 per kWh, the energy cost to produce one kg of hydrogen can be estimated as follows:

$$\text{Energy cost/kg of hydrogen} = 39 \text{ kWh/kg} \times \$0.0757/\text{kWh} = \$2.95 \text{ per kg}$$

Lessons Learned about the Hydrogen Electrolyzer

The system has the advantage of being able to produce fuel for transportation from water and electricity. In an ideal environment, the electricity to run the system could be provided by solar panels, so an electric vehicle could be said to run on sunlight and water. However, the capital cost of the equipment without solar panels is in excess of \$220,000. If these capital expenses were amortized over 20 years, the fully-burdened cost of producing hydrogen with this system would be more than \$17 per kg compared with delivered commercial price of approximately \$7 per kg or the current price of \$4 per gallon of diesel fuel, which has approximately the same energy as 1 kg of hydrogen.

It should be noted that the compressor failed three times during the first two years of operation. In each instance, the failure was traced to the O-rings used to seal the diaphragm. The first repair was done under warranty so original equipment type O-rings were installed. The second failure occurred after the warranty had expired. Repairs were made locally this time, with the same type of O-ring. When the compressor failed a third time, the material used for the O-rings was examined and found to be incompatible with hydrogen. Hydrogen-rated silicone O-rings were substituted for the original equipment type of O-rings. No further problems have been encountered with the compressor. The vendor of the compressor has been advised of the problem.

Safety was paramount throughout the design and build stages of the project, which was conducted in strict compliance with standards for the safe handling of hydrogen. For example, care was taken to avoid electrostatic discharge by grounding everything near the dispenser. A photograph of fuel being dispensed into the bus is shown in Figure 4-6. Note the green ground wire, which is required to eliminate the possibility that a spark from electrostatic discharge could ignite the fuel tank.

Figure 4-6

*Fueling the Bus
with Hydrogen*



An attractive alternative to on-site electrolysis is to deliver hydrogen from commercial producers by tube trailers like the one shown in Figure 4-7. Depending on distance between the production site and the delivery point, these trailers can deliver hydrogen at very competitive prices

Figure 4-7*Hydrogen Tube Trailer*

In anticipation that greater volumes of hydrogen would be required if CARTA decided to deploy the hydrogen hybrid bus, an arrangement was made with United Hydrogen Group of Tennessee to provide commercial hydrogen with a tube trailer similar to the one shown in Figure 4-6. Since CARTA decided that the range provided by the new batteries alone was sufficient for use of the modified bus on its downtown shuttle route, this capability was not needed; but it does offer a more cost-effective way to deliver hydrogen as a motor fuel. The cost of hydrogen delivered by this method depends upon the distance between the source and delivery point.

SECTION
5

Outreach

The goal of this task was to share lessons learned with the transit industry through an outreach program that would include publication of technical reports and participation in industry-sponsored events that promote advanced transportation.

CETE has participated in a number of regional, national, and international conferences that focus on advanced transportation. These include making presentations and publishing papers in the proceedings of Electric Vehicle Symposium (EVS) conferences in California, Norway, and China. These publications are listed in the References section of this document. CETE also accepted responsibility for publishing the second edition of the World Electric Vehicle Journal, with Dr. Bailey serving as editor-in chief. Dr. Bailey is also a member of an international task force charged by the Society of Automotive Engineers (SAE) with writing a standard for wireless charging. He is currently co-chair of the subcommittee for buses and trucks.

Over the course of this investigation, it became obvious that a better method was needed to specify the performance of vehicles used for public transit. Whether the task was to determine the suitability of a particular bus for a given route or to design a bus for service over a given route, few tools were available to assist the decision makers. What began as a rather tedious mathematical modeling exercise using formulas and spreadsheets eventually evolved into a sophisticated, easy-to-use simulator that can be used to match the physical demands of deployment with the particular attributes of vehicles to reduce risk of failure.

Description of EViSim

The Electric Vehicle Visualization and Simulator (EViSim) incorporates topographical and curvature of the planned route, vehicle weight, requirements for acceleration and instantaneous speed, aerodynamic drag, rolling resistance, and overall energy efficiencies to predict performance over selected routes. A screen shot of EViSim is provided in Figure 5-1.

Figure 5-1

Screen Shot of EViSim



Functionality

Three primary functions of EViSim have been identified: range prediction, EV comparisons, and charging infrastructure planning.

- *Range Prediction* – By calculating the power use of specific electric vehicles along custom user-entered routes, EViSim provides the very important functionality of range prediction. The simulator predicts the energy use of the vehicle along a designated route, taking into account vehicle characteristics, terrain information, charging and loading stops, traffic, and driving behavior. This allows the end-user to answer questions such as how many times a bus can run a route prior to requiring a full charge or how far along an interstate an electric vehicle can travel before needing to recharge.
- *EV Comparison* – By allowing for vehicle input from the end-user, the simulator can effectively compare the performance and energy-use characteristics of different vehicles. This functionality is highly useful to individuals such as transportation officials who must select a particular bus for a planned electric shuttle route or as a tool for consumers to determine which electric vehicle most ideally suits their driving habits and geographic location.
- *Charging Infrastructure Planning* – The EViSim application, when used to simulate a large number of electric vehicles along a wide range of common routes, can assist infrastructure planners to determine the most desirable and cost-effective locations for charging stations. By identifying points along

each simulated route where each vehicle is in need of a recharge and then applying a clustering algorithm, candidate locations for high-speed charging stations can be identified. These candidate station areas can then be analyzed by infrastructure planners using other variables such as power grid layout and real estate availability to intelligently place charging stations.

Promising Applications

Four applications of EViSim have been identified that could lead to increased adoption of electric vehicles: manufacturer sales tool, mass-transit implementation analysis tool, infrastructure planning tool, and end-user trip planning tool.

- *Manufacturer Sales Tool* – EViSim can be used to demonstrate to potential electric vehicle buyers how well an electric vehicle would suit their daily lives. Potential buyers would be able to see how far their electric vehicle would be able to take them on a single charge and how far they would be able to drive using the area's existing charging infrastructure. Custom simulations could be run that demonstrate the vehicle's performance on routes from the potential buyer's home to their place of work, recreational destinations, and other common driving points. This would make an unsure customer feel much more comfortable in their decision to purchase an EV.
- *Mass-Transit Implementation Analysis* – EViSim can assist government (or private) planners to decide the most efficient routes for EV transit solutions, aid in vehicle selection, determine running times between charges, and determine the number of EVs required to provide uninterrupted service.
- *Infrastructure Planning Tool* – The performance of EVs along an area's commonly-traveled routes can help in deciding where to place charging stations and where to encourage the early adoption of EVs.
- *Trip-Planning Tool* – EViSim can help EV owners feel more comfortable with driving to areas where charging stations may not be available. By accurately calculating the range of the vehicle, owners will know if they can safely complete a trip along a previously untested route.

Implementation

EViSim relies on vehicle data including weight, battery and charging properties, frontal surface area and drag coefficient, rolling resistance, and acceleration characteristics provided by vehicle manufacturers. It uses this information in conjunction with road information, traffic patterns, speed limits, individual driving behavior, dynamic driving route calculations, and elevation data. To calculate the energy use of EVs, the following formulas are used:

$$P_{Inertia} = m * \frac{\Delta v^2}{2\Delta t}$$

$$P_{Hill} = v * m * g * \frac{\Delta e}{\Delta d}$$

$$P_{Roll} = \mu * v * m * g * \frac{\Delta h}{\Delta t}$$

$$P_{Drag} = \frac{p}{2} * v^3 * C_d * A_f$$

Where:

- P power consumption
- v current speed
- m vehicle mass
- g gravity
- e elevation
- d distance over land
- h distance horizontal
- μ rolling resistance
- p air density
- C_d coefficient of drag
- A_f vehicle frontal area
- t time

The simulator refines calculation results by taking into account varying acceleration behaviors, peak power output limits, road conditions, and terrain conditions such as steepness of ascent or descent. Elevation and driving route information are obtained using the public application programming interfaces (APIs) provided by Google.

Design and Features

One shortcoming of many vehicle simulation programs is the end-user's detachment from the route being driven. By combining EViSim with visualization components, the user can see the energy-use and performance of a vehicle while watching it traverse the route virtually. EViSim is presented using both 2D overhead maps (Figure 5-2) and 3D fly-behind views (Figure 5-3). The 2D overview map provides for quick location reference, and the 3D visualization

provides the user with a sense of immersion and locality reference along the simulated route(s).

Figure 5-2
Two-Dimensional (2d)
Overhead Map

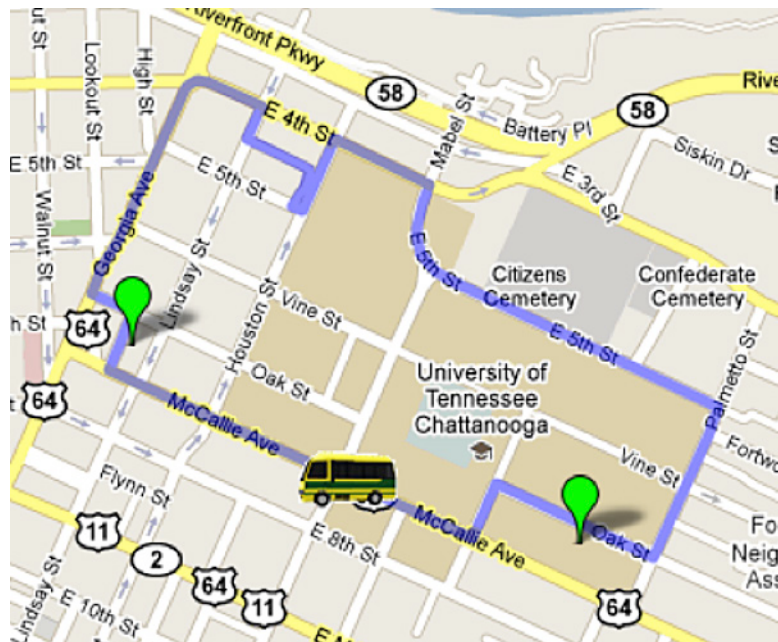


Figure 5-3
Three-Dimensional (3-d)
Fly-behind View



Charts and gauges visualize otherwise difficult to interpret numerical data. The vehicle's energy level, energy level history, current speed, and elevation information are all displayed in easy-to-understand formats. Other vital statistics are shown in a simple, centrally-located display. The charts are able to be expanded to view more detail, and raw numerical data can be accessed if necessary. The current location of the vehicle is also represented on the

elevation graph, so current elevation gradient can quickly be seen. These features are shown in Figures 5-4, 5-5, 5-6, and 5-7.

Figure 5-4

Energy Level and Speed Gauges

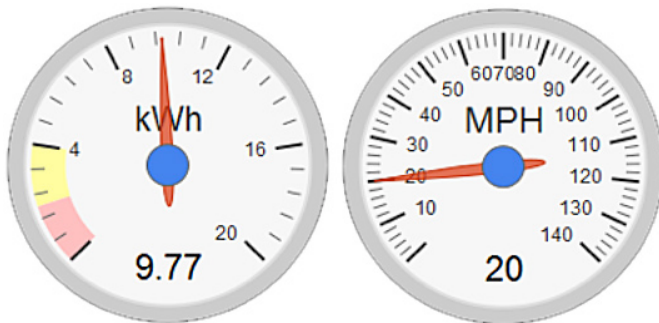


Figure 5-5

*Energy Level History
(Time vs. Energy Level)*

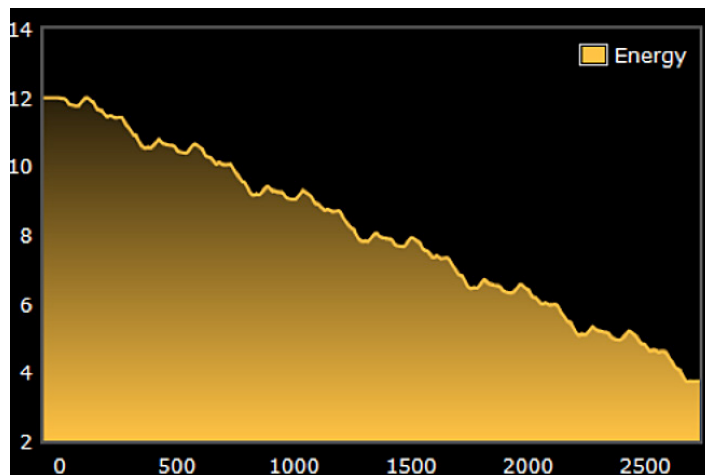


Figure 5-6

*Elevation Profile of Route
(Distance vs. Elevation)*

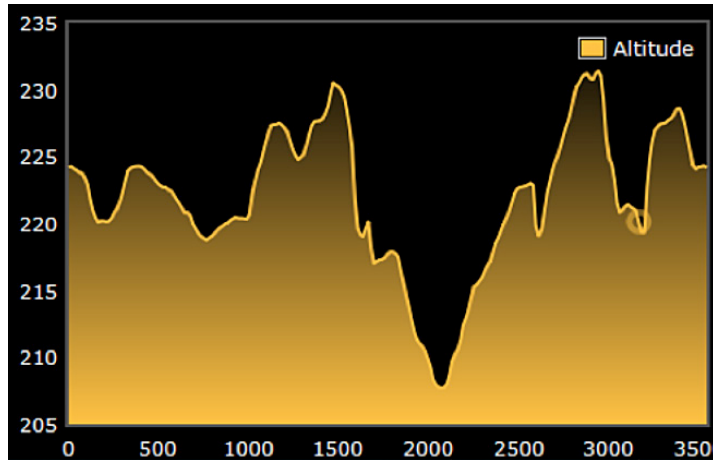


Figure 5-7
Central Status Display



Route Creation

The simulator is designed for dynamic input. Routes are specified by the end-user selecting starting and ending locations, and optionally, several waypoints in between. Points along the route can be added to represent charging stations, stopping points, and simulated traffic, and, in the case of mass transit vehicles, passenger loading. Figure 5-8 shows a customized route.

Figure 5-8
Customized Driving
Route Creation



Analysis

To provide real-world data for comparison with the simulation, an electric shuttle bus was driven over the above route on the UTC campus. Instantaneous readings of power required for the bus to navigate up the steep grades on campus were compared with predicted values from the simulator. Likewise, actual total energy consumption over this route was compared with predicted values. The bus was then driven around the downtown shuttle route. Data from extensive testing at the AVTF test track were also available for comparison with predictions from the simulator. Through a process of iteration, correction factors were built into the simulator to account for unknown efficiencies of the various subsystems to align predicted outcomes with actual data from these experiments. Our analysis shows that EViSim provides a viable method to predict the energy use of vehicles to a high-enough degree of accuracy to be a valuable tool in the types of EV-related decisions. Our goal was to provide a tool that encourages the adoption of electric vehicles. The inventors of this technology have filed a patent disclosure with the University of Tennessee Research Foundation. Going forward, the intent is to make this tool available to assist public transit stakeholders understand the full potential for electric and hybrid vehicles.

References

- Bailey, J. Ronald, Justin McBath, and Mark E. Hairr. 2012. "Increasing the Range of Electric Shuttle Buses with Wireless Charging." Paper presented at EVS 26 International Battery, Hybrid and Fuel Cell Electric Vehicle Symposium, Los Angeles, California, May 6–9.
- Bailey, J. Ronald, Mark E. Hairr, Thomas Dugan, Albert E. Curtis III, and Dick Boothe, 2012. "Wireless Charging of Electric Shuttle Buses." Paper presented at Conference on Electric Roads and Vehicles, Park City, Utah, February 3–6.
- Bailey, J. Ronald, Wayne Davis, and Cliff Ricketts. 2010. "East Tennessee Hydrogen Initiative." Paper presented at the NHA Hydrogen Conference & Expo, Long Beach, California, May 3–6.
- Gasior, Wade, Li Yang, Ignatius Fomunung, Mark Hairr, and Ronald Bailey. 2010. "So You Want to Drive an Electric Vehicle." Paper presented at EVS 25, the 25th World Battery, Hybrid and Fuel Cell Vehicle Symposium and Exhibition, Shenzhen, China, November 5–9.
- Hairr, Mark E., Paul Griffith, J. Ronald Bailey, and Woodlyn Madden. 2009. "Data Acquisition System for Electric and Hybrid-Electric Buses." Paper presented at EVS 24 International Battery, Hybrid and Fuel Cell Electric Vehicle Symposium, Stavanger, Norway, May 13–16.
- Hairr, Mark E., Paul Griffith, Tom Dugan, and J. Ronald Bailey. 2010. "Development of a Hydrogen Hybrid Internal Combustion Engine Bus." Paper presented at APTA Conference, Washington, DC, May 4.
- Hairr, Mark E., Ron D. Sweeney, J. Ronald Bailey, and Ignatius Fomunung. 2010. "Developing Hydrogen Hybrid ICE and Inductive Power Transfer Technologies for Buses: Chattanooga, Tennessee, USA Continues to Lead in Advanced Transit Technologies After Twenty Years." Paper presented at EVS 25, the 25th World Battery, Hybrid and Fuel Cell Vehicle Symposium and Exhibition, Shenzhen, China, November 5–9.
- Madden, Woodlyn, J. Ronald Bailey, and Mark Hairr. 2009. "Topographical Inertial Energy Simulator for Hybrid Electric Vehicle." Paper presented at EVS 24 International Battery, Hybrid and Fuel Cell Electric Vehicle Symposium, Stavanger, Norway, May 13–16.
- McBath, Justin, Roger LeMond, Mark Hairr, and J. Ronald Bailey. 2011. "ICE Conversions as a Bridge to the Hydrogen Economy." Paper presented at NHA Fuel Cell & Hydrogen Conference, Washington, DC, February 13–16.
- Thomas, Tricia, Mark Hairr, Paul Griffith, Woodlyn Madden, and J. Ronald Bailey. 2009. "Using Topographical and State of Charge Information to Predict the Actual Range of Electric Vehicles." Paper presented at EVS 24 International Battery, Hybrid and Fuel Cell Electric Vehicle Symposium, Stavanger, Norway, May 13–16.



**U.S. Department of Transportation
Federal Transit Administration**

U.S. Department of Transportation
Federal Transit Administration
East Building
1200 New Jersey Avenue, SE
Washington, DC 20590
<http://www.fta.dot.gov/research>

COVER PHOTO

Courtesy of Center for Energy, Transportation and the Environment

DISCLAIMER

This document is disseminated under the sponsorship of the U.S. Department of Transportation in the interest of information exchange. The United States Government assumes no liability for its contents or use thereof. The United States Government does not endorse products or manufacturers. Trade or manufacturers' names appear herein solely because they are considered essential to the objective of this report.

Wayside Charging and Hydrogen Hybrid Bus

Extending the Range
of Electric Shuttle Buses

SEPTEMBER 2012

FTA Report No. 0027

PREPARED BY

J. Ronald Bailey and Mark E. Hairr
Center for Energy, Transportation and the Environment
University of Tennessee at Chattanooga

SPONSORED BY

Federal Transit Administration
Office of Research, Demonstration and Innovation
U.S. Department of Transportation
1200 New Jersey Avenue, SE
Washington, DC 20590

AVAILABLE ONLINE

<http://www.fta.dot.gov/research>

Metric Conversion Table

SYMBOL	WHEN YOU KNOW	MULTIPLY BY	TO FIND	SYMBOL
LENGTH				
in	inches	25.4	millimeters	mm
ft	feet	0.305	meters	m
yd	yards	0.914	meters	m
mi	miles	1.61	kilometers	km
VOLUME				
fl oz	fluid ounces	29.57	milliliters	mL
gal	gallons	3.785	liters	L
ft ³	cubic feet	0.028	cubic meters	m ³
yd ³	cubic yards	0.765	cubic meters	m ³
NOTE: volumes greater than 1000 L shall be shown in m ³				
MASS				
oz	ounces	28.35	grams	g
lb	pounds	0.454	kilograms	kg
T	short tons (2000 lb)	0.907	megagrams (or "metric ton")	Mg (or "t")
TEMPERATURE (exact degrees)				
°F	Fahrenheit	5 (F-32)/9 or (F-32)/1.8	Celsius	°C

REPORT DOCUMENTATION PAGE		<i>Form Approved OMB No. 0704-0188</i>	
<p>Public reporting burden for this collection of information is estimated to average 1 hour per response, including the time for reviewing instructions, searching existing data sources, gathering and maintaining the data needed, and completing and reviewing the collection of information. Send comments regarding this burden estimate or any other aspect of this collection of information, including suggestions for reducing this burden, to Washington Headquarters Services, Directorate for Information Operations and Reports, 1215 Jefferson Davis Highway, Suite 1204, Arlington, VA 22202-4302, and to the Office of Management and Budget, Paperwork Reduction Project (0704-0188), Washington, DC 20503.</p>			
1. AGENCY USE ONLY	2. REPORT DATE	3. REPORT TYPE AND DATES COVERED	
	September 30, 2012	Final Report, October 1, 2008—September 30, 2012	
4. TITLE AND SUBTITLE		5. FUNDING NUMBERS	
Wayside Charging and Hydrogen Hybrid Bus: Extending the Range of Electric Shuttle Buses			
6. AUTHOR(S) J. Ronald Bailey, Ph.D., P.E., and Mark E. Hairr			
7. PERFORMING ORGANIZATION NAME(S) AND ADDRESSE(ES)		8. PERFORMING ORGANIZATION REPORT NUMBER	
Center for Energy, Transportation and the Environment University of Tennessee at Chattanooga 615 McCallie Avenue 214 EMCS Building, Department 2522 Chattanooga, Tennessee 37403-2598		FTA Report No. 0027	
9. SPONSORING/MONITORING AGENCY NAME(S) AND ADDRESS(ES)		10. SPONSORING/MONITORING AGENCY REPORT NUMBER	
U.S. Department of Transportation Federal Transit Administration Office of Research, Demonstration and Innovation East Building 1200 New Jersey Avenue, SE Washington, DC 20590		FTA Report No. 0027	
11. SUPPLEMENTARY NOTES [http://www.fta.dot.gov/research]			
12A. DISTRIBUTION/AVAILABILITY STATEMENT		12B. DISTRIBUTION CODE	
Available from: National Technical Information Service (NTIS), Springfield, VA 22161. Phone 703.605.6000, Fax 703.605.6900, email [orders@ntis.gov]		TRI-20	
13. ABSTRACT			
<p>This report documents the results completed by the Center for Energy, Transportation and the Environment (CETE) at the University of Tennessee at Chattanooga (UTC) under Federal Transit Administration Cooperative Agreement TN-26-7034. This research has addressed the limited range of electric shuttle buses by two different methods: first, by wayside charging using inductive power transfer, and second, by adding a small (10 kW) on-board generator set powered by an internal combustion engine (ICE) fueled by hydrogen. Wayside charging reduced fuel costs to less than \$0.10 per mile while eliminating tailpipe emissions that would have been produced by a similar diesel bus. The hydrogen hybrid bus eliminated emission of CO₂, but the cost was found to be prohibitive because of the relatively poor thermodynamic efficiency of the ICE and the high cost of hydrogen. Better results were obtained when the ICE was fueled with compressed natural gas (CNG), which resulted in a range in excess of 170 miles at a lower fuel cost per mile than a comparable diesel-fueled hybrid bus.</p>			
14. SUBJECT TERMS		15. NUMBER OF PAGES	
Public transportation, electric buses, wayside charging, inductive power transfer, hydrogen, range extension		80	
16. PRICE CODE			
17. SECURITY CLASSIFICATION OF REPORT	18. SECURITY CLASSIFICATION OF THIS PAGE	19. SECURITY CLASSIFICATION OF ABSTRACT	20. LIMITATION OF ABSTRACT
Unclassified	Unclassified	Unclassified	

TABLE OF CONTENTS

1	Executive Summary
4	Section 1: Wayside Charging
4	Background
4	Statement of the Problem
5	Advanced Vehicle Test Facility
6	Overview of Wireless Charging By Inductive Power Transfer
7	Organization
7	Roles of the Partners
7	Preliminary Testing
9	Sensitivity to Misalignment and Air Gap Between the Coils
11	Systems Integration
15	Site Preparation
17	Tuning the System
18	Experimental Results
18	Test Protocol
19	Baseline Testing
20	Range with Wireless Charging
21	Charging the Batteries
24	Operating Cost Estimates
26	Measurement of Efficiency
26	Magnetic Flux Emissions
30	Environmental Considerations
30	Compliance with Clean Air Act
30	Reduction in Green House Gases
31	Summary of Wayside Charging Results
31	Lessons Learned About Wireless Charging
32	Section 2: Hydrogen Hybrid Bus Demonstration
32	Background
33	Organization
34	Battery Selection
37	Improvement in Range from LiFePO ₄ Batteries
40	Development of Battery Charging Profile
44	Auxiliary Power Unit (APU) Considerations
45	Engine Modifications
46	Fuel and Ignition
47	Fuel Delivery Apparatus
48	Dual Fuel Feature
48	Test Results with CNG
49	Test Results with Hydrogen
52	Lessons Learned About Use of an APU to Improve Range

53	Section 3: Technical Support
53	Lessons Learned About Technical Support
55	Section 4: Acquire and Install Hydrogen Electrolyzer
57	Lessons Learned about the Hydrogen Electrolyzer
60	Section 5: Outreach
60	Description of EViSim
61	Functionality
62	Promising Applications
62	Implementation
63	Design and Features
66	Route Creation
66	Analysis
67	REFERENCES

LIST OF FIGURES

4	Figure 1-1:	Statement of the Problem
5	Figure 1-2:	Test Track at Advanced Vehicle Test Facility
5	Figure 1-3:	Research Building at Advanced Vehicle Test Facility
6	Figure 1-4:	Bus Being Tested at Advanced Vehicle Test Facility Track in Chattanooga
6	Figure 1-5:	Wireless Charging System Using Inductive Power Transfer
7	Figure 1-6:	Partnership Formed for Wireless Charging using Inductive Power Transfer
8	Figure 1-7:	Power Electronics Components
8	Figure 1-8:	Stationary Coils, Pick-Up Coils, and Rectifiers
9	Figure 1-9:	Laboratory Setup for Component Testing at Advanced Vehicle Test Facility
9	Figure 1-10:	Power Transfer as Function of Air Gap
10	Figure 1-11:	Power Transfer as Function of Misalignment with 0.5" (1.27cm) Air Gap
10	Figure 1-12:	Power Transfer as Function of Misalignment with 2" (5.08cm) Air Gap
11	Figure 1-13:	Rectifiers and Heat Exchanger Installation
11	Figure 1-14:	Battery Management System Control Board behind the Driver's Seat
12	Figure 1-15:	Communication Equipment Installed on Bus
12	Figure 1-16:	Mechanism for Lowering Pickup Coils
13	Figure 1-17:	EVAmerica Assembly Area in Ringgold, Georgia
13	Figure 1-18:	Electric Shuttle Bus with Wireless Charging
13	Figure 1-19:	View of Coils under Bus and Alignment Scheme
14	Figure 1-20:	Electronic Components of Guidance System
14	Figure 1-21:	Display Used to Guide Horizontal Alignment
14	Figure 1-22:	Bus Entering Wireless Charging Area
15	Figure 1-23:	Switch Gear, Voltage Transducer, and Data Acquisition System
16	Figure 1-24:	Labview Screen for Monitoring AC Power
16	Figure 1-25:	Track Supply
17	Figure 1-26:	Simplified RLC Model for Primary Side of IPT Circuit
18	Figure 1-27:	Capacitor Boxes Used to Tune Circuit
18	Figure 1-28:	Downtown Chattanooga Shuttle Route
19	Figure 1-29:	Range Envelope for Existing CARTA Shuttles with PbA Batteries
19	Figure 1-30:	Water Barrels Equivalent to 22 Passengers
20	Figure 1-31:	Baseline Range with Ni-Cd Batteries
20	Figure 1-32:	SOC as a Function of Distance
21	Figure 1-33:	Battery Voltage as a Function of Distance
21	Figure 1-34:	DC Amp Hours Consumed and Replaced over 24-Hour Day

22	Figure 1-35: AC Power for Day of Wireless Charging Covering 39 Trips (117 Miles)
23	Figure 1-36: Power Consumed by Overnight Charging
23	Figure 1-37: Range Envelope with Wireless Charging
25	Figure 1-38: Comparison of Fuel Costs
25	Figure 1-39: Cost Comparison of Diesel Fuel with Electricity
27	Figure 1-40: Dr. John Boys Measuring EMF
28	Figure 1-41: Comparison of Observed Level of Flux with ICNIRP Recommendations
29	Figure 1-42: Poster on Safety for Wireless Charging
30	Figure 1-43: Comparison of CO ₂ Emissions for Diesel and Electric Shuttle Buses
32	Figure 2-1: Fuel Cell Hybrid Bus Built by Ebus and tested at UT Austin
33	Figure 2-2: Hybrid Ebus with a 20 kW Gas Turbine as a Range Extender
33	Figure 2-3: Partnership for Development of Hydrogen Hybrid Bus Demonstration
34	Figure 2-4: Design Review Meeting
34	Figure 2-5: Comparison of Capacity Rating with Level of Maturity for Various Batteries
35	Figure 2-6: Cost Projections with Increased Volume for Li-Ion Batteries
37	Figure 2-7: LiFePO ₄ Batteries Mounted in Battery Box at EVAmerica
37	Figure 2-8: Cell Temperature vs. Distance
38	Figure 2-9: Pack Voltage after Each Trip (~ 3 miles)
38	Figure 2-10: High and Low Cell Voltage vs. Distance
39	Figure 2-11: Trip Amp Hours vs. Distance
39	Figure 2-12: Remaining Amp Hours vs. Distance
40	Figure 2-13: Improvement in Range with LiFePO ₄ Batteries
41	Figure 2-14: ABC-150 Used to Develop Charge Profile for LiFePO ₄ Batteries
41	Figure 2-15: Current during Charging
42	Figure 2-16: Voltage during Charging
42	Figure 2-17: Highest Cell Voltage during Charging at 100 Amps
42	Figure 2-18: Cumulative Amp Hours during Charging
43	Figure 2-19: Cell Temperature (Highest) during Charging
44	Figure 2-20: 10 kW Polar Power APU
45	Figure 2-21: H2/CNG APU Installed in Modified Bus
46	Figure 2-22: Various Hydrogen Fuel and Ignition System Components and Sensors
47	Figure 2-23: Dual Engine Management Diagram
47	Figure 2-24: Hydrogen Delivery Manifold
48	Figure 2-25: Engine Management Panel
48	Figure 2-26: Improvement in Range with 4.95 kW APU Fueled by CNG

49	Figure 2-27: CNG Used by APU in Driving 177 Miles
50	Figure 2-28: Firing Diagram
51	Figure 2-29: Range Improvement with 2.5 kW APU Fueled by Hydrogen
51	Figure 2-30: Hydrogen Used by APU while Driving 117 Miles
55	Figure 4-1: Components of Hydrogen Fueling Station
55	Figure 4-2: Water Deionizer
56	Figure 4-3: PEM Fuel Cell Electrolyzer Supplied by Proton Energy Systems
56	Figure 4-4: Hydrogen Compressor
57	Figure 4-5: Hydrogen Storage Tanks and Dispensing System
58	Figure 4-6: Fueling Bus with Hydrogen
59	Figure 4-7: Hydrogen Tube Trailer
61	Figure 5-1: Screen Shot of Simulator
64	Figure 5-2: Two-Dimensional Overhead Map
64	Figure 5-3: Three-Dimensional Fly-Behind View
65	Figure 5-4: Energy Level and Speed Gauges
65	Figure 5-5: Energy Level History (Time vs. Energy Level)
65	Figure 5-6: Elevation Profile of Route (Distance vs. Elevation)
66	Figure 5-7: Central Status Display
66	Figure 5-8: Customized Driving Route Creation

LIST OF TABLES

26	Table 1-1:	Voltage and Current during Wireless Charging
27	Table 1-2:	EMF Measurements Outside Bus
28	Table 1-3:	EMF Measurements Inside Bus
31	Table 1-4:	Summary of Wayside Charging Results
35	Table 2-1:	Battery Considerations
36	Table 2-2:	Battery Manufacturers

ACKNOWLEDGMENTS

This project was conducted under Federal Transit Administration (FTA) Cooperative Agreement TN-26-7034. Special recognition and appreciation is extended to the Chattanooga Enterprise Center staff and board and the Chattanooga Area Regional Transportation Authority (CARTA), both of which contributed greatly in the completion of this research program. EVAmerica, Embedded Power Controls, Conductix Wampfler, and the University of Auckland, New Zealand, have also contributed to the success of this program.

The project team also wishes to thank Mr. Henry Nejako, FTA Program Management Officer; Patrick Centolanzi, FTA Transportation Program Engineer; Lisa Colbert, FTA Project Manager; and numerous UTC students, faculty, and staff who assisted with many aspects of the projects completed under this work program.

ABSTRACT

The research completed under Federal Transit Administration Cooperative Agreement TN-26-7034 has focused on demonstration of ways to improve the range of electric buses. Methods include wireless charging, installation of better batteries, and use of an auxiliary power unit fueled by compressed natural gas or hydrogen. Results show that the range can be increased to more than 100 miles by any one of these three methods. However, wireless charging using inductive power transfer appears to be the best choice for immediate deployment when the range requirement exceeds 100 miles between overnight chargings. The improved batteries, in combination with wireless charging, should enable use of larger electric buses operating over longer, more difficult routes than previously possible.

EXECUTIVE SUMMARY

The Center for Energy, Transportation and the Environment (CETE) at the University of Tennessee at Chattanooga (UTC) in partnership with the Chattanooga Area Regional Transportation Authority (CARTA) conducted research and outreach tasks aimed at increasing the range of electric shuttle buses. The objectives for this work program are to:

- Demonstrate the use of wireless charging using inductive power transfer (IPT) to increase the range of electric shuttle buses
- Demonstrate the use of advanced batteries and an auxiliary power unit (APU) powered by an internal combustion engine (ICE) running on hydrogen to increase the range of an electric shuttle bus
- Provide assistance to the City of Sevierville to improve operation of its fleet of hybrid electric shuttle buses
- Provide assistance to Emory University to improve operation of its fleet of electric shuttle buses
- Complete procurement and installation of a hydrogen fueling station needed to provide fuel for the APU
- Conduct an outreach program to share lessons learned with stakeholders in public transit

In the first research project, the range of an electric shuttle bus was increased from less than 50 miles on batteries alone to more than 120 miles by wireless charging during the period when passengers are normally boarding the bus. CETE in partnership with CARTA demonstrated wireless charging for electric shuttle buses using IPT technology provided by Conductix Wampfler, AG. This short “opportunity” charge of 3 minutes duration at 60 kilowatts provides enough traction energy to power the bus for approximately 3 miles, thereby eliminating the normal range constraint that, until now, has required battery swapping during the day to cover the required daily route of 100 miles. Overall efficiency from the grid to the vehicle was found to be more than 90%, resulting in an energy cost per mile of less than \$0.10 while producing zero tailpipe emissions. Measurements of electromagnetic field strength at the edge of the coils near street level and at all locations inside the bus were found to be well below draft international standards for exposure.

In the second research project, the range of a battery-centric electric shuttle was increased from less than 50 miles to more than 120 miles by a combination of improved batteries and the addition of an on-board generator powered by a hydrogen-fueled ICE. Because of recent interest in CNG as a fuel for transportation, the ICE controls were made to be switchable between hydrogen and CNG, which produced an increase in range to more than 170 miles when running on CNG with a fuel cost significantly less than hydrogen. However, it should be noted that replacing the original Ni-Cd batteries with LiFePO₄ batteries alone increased the range from less than 50 miles to more than 100 miles. Since

this exceeded the daily range required by CARTA, the added complication and cost of having to establish hydrogen or CNG fueling capability and maintain a unique hybrid bus resulted in a decision by CARTA to remove the generator and deploy the shuttle with the new batteries alone. Perhaps more significantly, this research demonstrated that these new batteries, in combination with wayside charging, have the potential to greatly expand the opportunity for electric buses by making it possible for larger electric buses to travel over longer routes than previously possible.

CETE in partnership with the City of Sevierville evaluated operational problems with its fleet of hybrid electric shuttle buses and reached a mutual agreement that a dedicated technician was needed to maintain these buses. This was accomplished by transferring funds to enable Sevierville to hire a technician.

At Emory University, CETE discovered that the performance of its fleet of electric shuttle buses had deteriorated to such an extent that the operational range had been reduced to less than 25 miles with fully-charged batteries. It was determined that the batteries were in severe need of reconditioning and that the battery chargers being used were the proximate cause of the problem. CETE developed a specification for a new battery charger and was prepared to transfer funds to Emory University to procure this charger when it decided to abandon its fleet of electric shuttles in favor of converting its fleet of diesel buses to run on bio-diesel produced from cooking oil used in the campus food service. With assistance from FTA through Cooperative Agreement TN-26-7035, Emory University's fleet of five electric shuttle buses was transferred to CARTA. One of these buses was equipped with wireless charging equipment and used to demonstrate wayside charging as described above. A second was converted into a hydrogen hybrid bus as part of the second research project described above. A third was put into regular service after an extensive effort to recondition the batteries, which were abused at Emory by use of incorrect charging equipment. The other two are being held in reserve for possible deployment by CARTA. The transfer of these five buses to CARTA made it possible to avoid the cost of purchasing new buses for the wireless charging and hydrogen hybrid bus research projects described previously.

The hydrogen fueling station that was started under FTA Cooperative Agreement TN-26-7032, East Tennessee Hydrogen Initiative, was completed and commissioned in December 2009. It is now capable of producing 2 kg per day and storing 10 kg of hydrogen at 6,000 psi.

The outreach task included publication of a number of peer reviewed journal articles; presentations at regional, national, and international professional society technical meetings; and frequent demonstrations at the Advanced Vehicle Test Facility (AVTF) and elsewhere to showcase wayside charging and hydrogen as a fuel for transportation. The director of CETE has also served as Editor-in-Chief

of the *World Electric Vehicle Journal* and is currently serving as a member and chair of the bus subcommittee of an international taskforce that is charged by the Society of Automotive Engineers (SAE) with drafting a standard for wireless charging of vehicles.

The demonstration of wireless charging has opened up new opportunities for deployment of electric buses with larger buses over routes, which was heretofore impossible for electric buses. The demonstration of an inexpensive APU as a means of building a battery-centric bus could open up opportunities for deployment, especially where transit operators already use hydrogen or CNG. Technical support for the City of Sevierville enabled it to continue successful operation of its fleet of hybrid electric buses. Work with Emory University enabled the transfer of five electric buses to CARTA, saving money on this project by forgoing the expense of purchasing new buses while also giving CARTA some lightly-used buses that could be deployed immediately. Lessons learned have been published and presented at national and international conferences.

SECTION
1

Wayside Charging

Background

The Chattanooga Area Regional Transportation Authority (CARTA) has been operating a fleet of electric shuttle buses since May 1, 1992. The decision to convert to electric buses was driven by a community effort to improve the air quality in Chattanooga and to comply with all provisions of the Clean Air Act. Anyone visiting Chattanooga today who has not visited lately would have difficulty recognizing it because of the remarkable improvements in air quality that not only have put Chattanooga into a state of attainment with all U.S. Environmental Protection Agency (EPA) air quality regulations but also has allowed for continued economic development, such as the new Volkswagen assembly plant that is now in full production in Chattanooga, partly because of the strong community commitment to the environment. CARTA now carries approximately one million passengers each year on its electric shuttles. To remove the CARTA shuttles from Chattanooga today would be as unthinkable as removing the cable cars from San Francisco.

Over the years, CARTA experimented with virtually every new product that promised to extend the range of electric buses. This included various combinations of new battery chemistries, more efficient drive systems, and gas turbines running on diesel fuel or propane as range extenders that could recharge the batteries during operations.

Statement of the Problem

After almost 20 years of continuous operation of electric shuttles, the problem for CARTA is shown in Figure I-1.

Figure 1-1
Statement of Problem



- Shuttle runs every thirty minutes from 6:30 AM until 11:00 PM
- Downtown Route is approximately 3 miles
- Range requirement is ~100 miles
- Limitations
 - Downtown Routes Only
 - Not enough Power to climb hills on UTC campus
 - Not enough Range
 - Batteries Swapped at Mid-Day for Downtown Route
 - Other Routes Out of the Question for Electric Shuttle
 - Fleet is beyond original design life
 - Newest Shuttle is over fifteen years old
 - Manufacturer is no longer in business

Advanced Vehicle Test Facility

This demonstration project was conducted at the Advanced Vehicle Test Facility (AVTF), which consists of a 1-mile banked asphalt test track and a 9,400-square-foot research building located on 52 acres approximately 6 miles from the University of Tennessee campus in Chattanooga. An aerial photograph of the test track is shown in Figure I-2. The research building at the AVTF is shown in Figure I-3. A photograph of a bus being tested at the AVTF track is shown in Figure I-4.

Figure 1-2

Test Track at AVTF



Figure 1-3

*Research Building
at AVTF*



Figure 1-4

*Bus Being Tested
at AVTF*

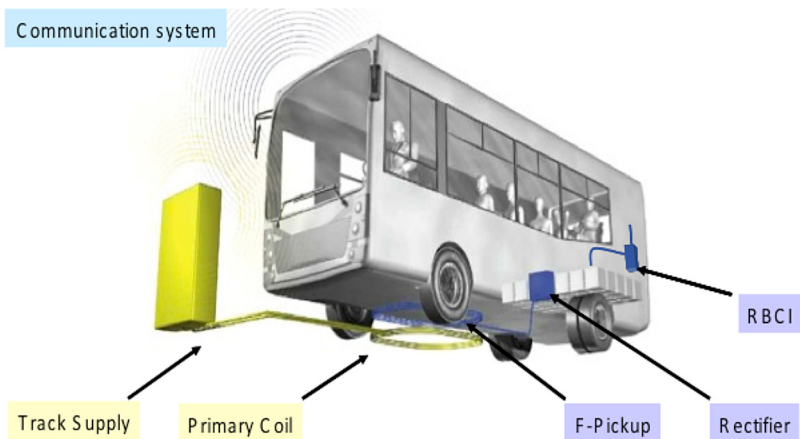


Overview of Wireless Charging by Inductive Power Transfer

Wireless charging by inductive power transfer (IPT) is accomplished by providing power to a stationary (primary coil) buried in the pavement, which induces a current in a pickup coil mounted on the bottom of the vehicle. The major systems components are shown in Figure 1-5.

Figure 1-5

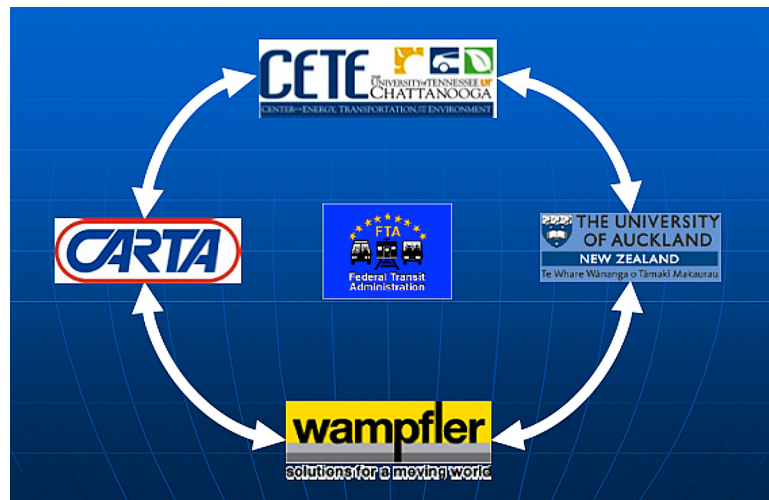
Wireless Charging System using Inductive Power Transfer



Organization

A multidisciplinary team was assembled to conduct this research project. The project partnership is represented graphically in Figure 1-6.

Figure 1-6
Partnership Formed
for Wireless Charging
using Inductive
Power Transfer



Roles of the Partners

Roles of the partners in the project were the following:

- FTA provided funding under FTA Cooperative Agreement TN-26-7034.
- CARTA provided experience and expertise in transit operations and equipment.
- EVAmerica provided systems integration and fabrication capability.
- Embedded Power Controls provided power electronics expertise.
- Conductix Wampfler, AG provided technical assistance and all of the inductive power transfer equipment.
- University of Auckland, New Zealand, provided expertise in wireless charging.
- Center for Energy, Transportation and the Environment (CETE) provided overall project management.

Preliminary Testing

All of the components for the wireless charging system were tested in the laboratory before installing them on the bus. Some of the components are shown in Figure 1-7.

Figure 1-7

Power Electronics Components



The equipment shown in Figure I-7 includes the battery management system circuit board, the inductors, and the communications module with wireless modem. The switch board on the right was used to simulate the controls that would be installed on the bus to allow the operator to initiate charging. Most of these components were designed and built by Embedded Power Control to specifications provided by Conductix Wampfler, AG.

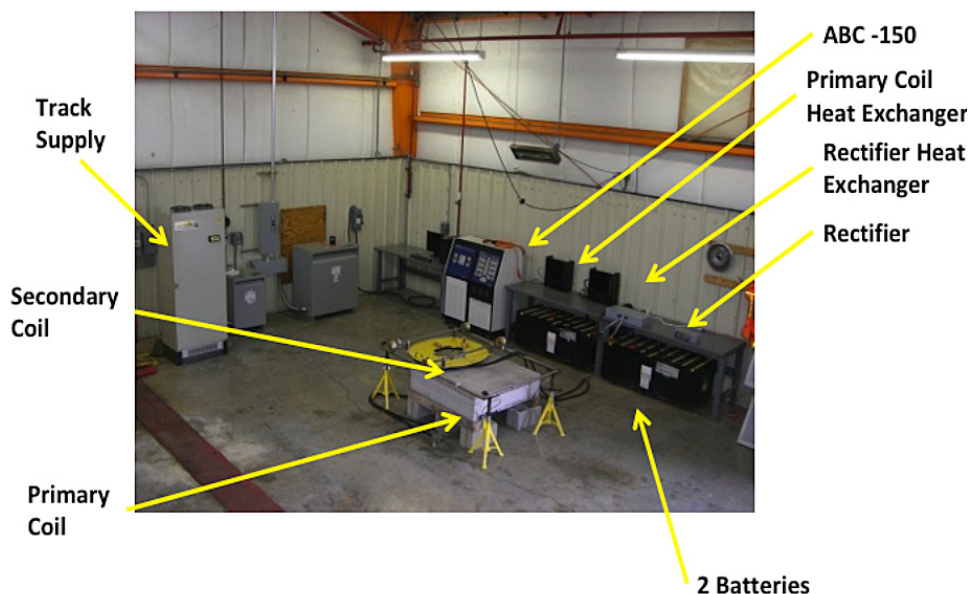
The two stationary coils that are encased in concrete are shown in Figure I-8, which also shows two yellow pick-up coils (one standing on edge) and the rectifiers (with cover removed) in the background. The overall stationary setup that was used for preliminary testing is shown in Figure I-9.

Figure 1-8

Stationary Coils, Pick-Up Coils (yellow) and Rectifiers (covers off)



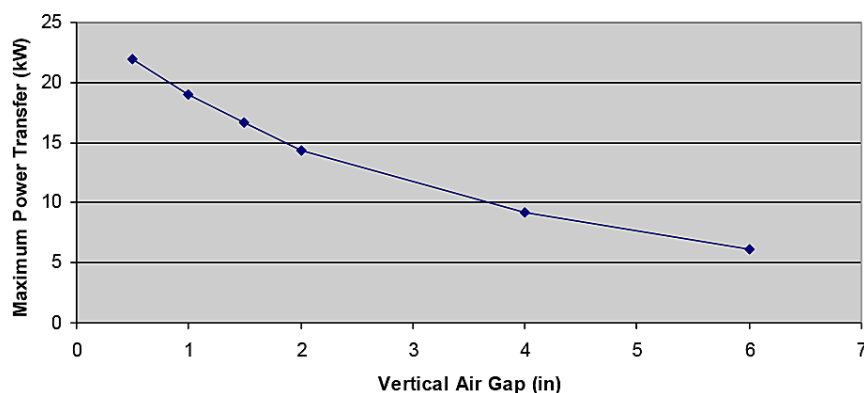
Figure 1-9
Laboratory Setup for Component Testing at Advanced Vehicle Test Facility



Sensitivity to Misalignment and Air Gap between IPT Coils

With near-perfect horizontal alignment between the two coils, the rate of power transfer as a function of vertical air gap is shown in Figure I-10. As expected, the power transfer rate decreases with air gap, dropping to less than 10kW when the gap reaches 4 inches (10.1 cm). The maximum power transfer rate of 22 kW occurred when the two coils were at the centered position. Increasing the misalignment resulted in a decrease in the power transfer rate, falling to 16 kW in the area of misalignment enclosed by 3 inches (7.62 cm) in the X direction (aligned with the major axis of the coil) and about 2.5 inches (6.35 cm) in the Y direction. As expected, the power transfer rate decreased rapidly as the misalignment increased. This led to the conclusion that it would not be possible to achieve a satisfactory rate of power transfer without either lowering the bus or installing a positioning mechanism under the bus that would lower the coils.

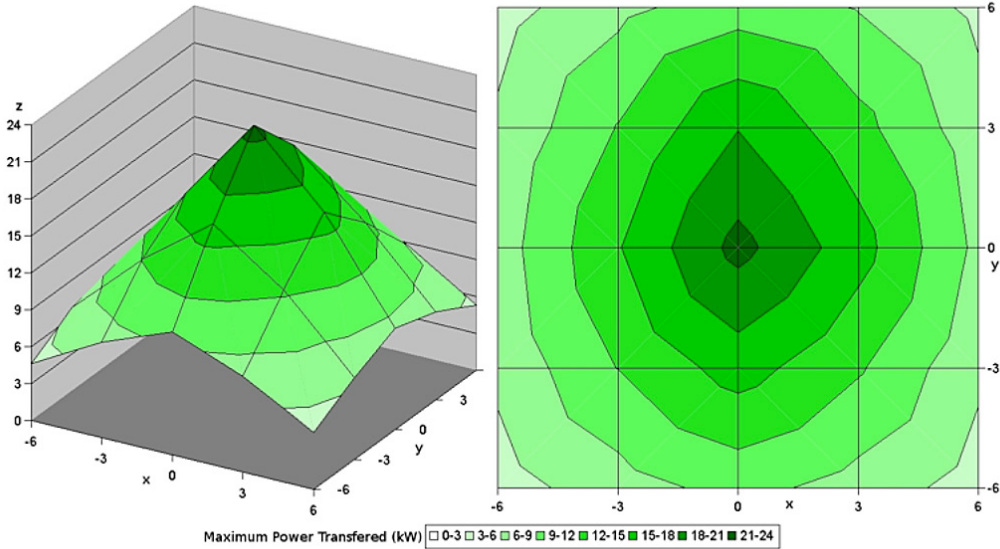
Figure 1-10
Power Transfer as Function of Air Gap



Tests were also conducted to determine the sensitivity of power transfer at various air gaps when the coil is misaligned. Power transfer rates were collected at 0.5 inch (1.27 cm) intervals between a 0.5 inch (1.27 cm) air gap and 4 inches (10.1 cm). Results for testing with a 0.5 inch (1.27 cm) air gap are shown in Figure 1-11.

Figure 1-11

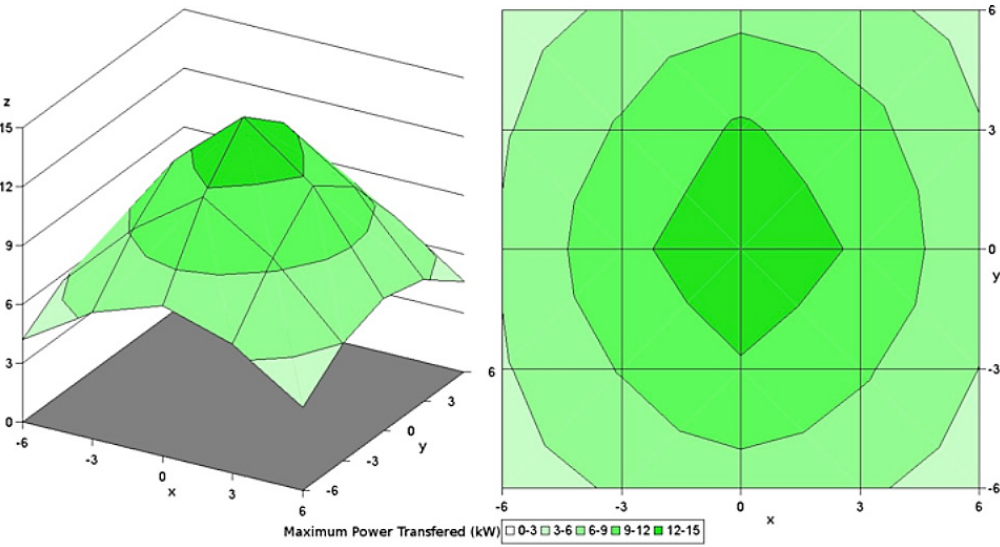
*Power Transfer
as Function of
Misalignment with 0.5”
(1.27cm) Air Gap*



With larger separation between the primary and secondary coils, the rate of power transfer was reduced as expected, but the larger air gap also reduced the gradient for horizontal misalignment. Typical results are shown in Figure 1-12 for an air gap of 2 in. (5.08 cm). This characteristic may enable larger air gaps for future generations of IPT equipment, especially if interoperability between and among equipment from multiple suppliers becomes important.

Figure 1-12

*Power Transfer
as Function of
Misalignment with 2”
(5.08 cm) Air Gap*



Systems Integration

After component testing, duplicates of all the power electronics equipment shown in Figure I-6 and Figure I-7 were installed on the bus by EVAmerica.

The rectifiers and heat exchanger were placed in an open compartment on the side of the bus, as shown in Figure I-13. The output of each coil is connected to an associated rectifier module. The rectifier modules are configured in parallel for charging the batteries. The battery pack consists of 100 amp-hour, Ni-Cd, 6 voltage modules. Modules of 0.25 are connected in series to form a string. Two pairs of parallel strings make up the 100-cell traction battery with a total nominal capacity of 200 A-hrs. The battery management system control board was installed inside the bus behind the operator's seat, as shown in Figure I-14.

Figure 1-13
Rectifiers and Heat Exchanger Installation



Figure 1-14
Battery Management System Control Board behind Driver's Seat



The communications equipment shown in Figure I-15 was installed in the passenger compartment directly behind the operator and includes an on-board wireless modem and an antenna for communications with the stationary Track Supply.

Figure 1-15

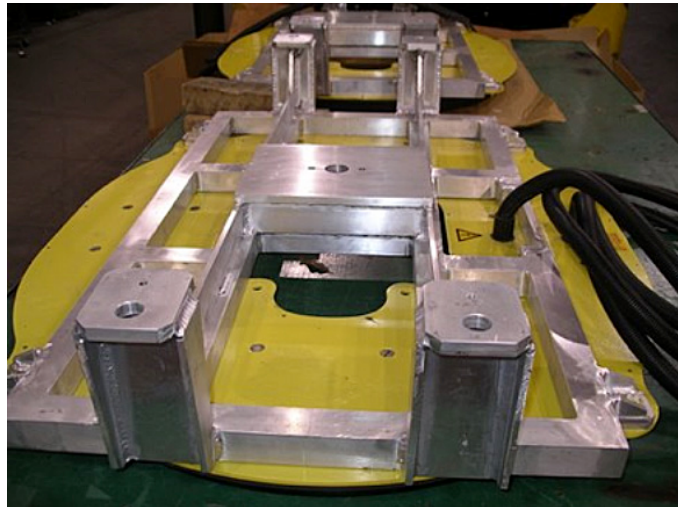
Communication Equipment Installed on Bus



To achieve the optimum air gap for charging, two pneumatically-actuated mechanisms were designed and built by EVAmerica to lower the pickup coils into place. Figure 1-16 shows the pickup coils (yellow) and pneumatic mechanism ready for installation at the EVAmerica vehicle manufacturing plant in Ringgold, Georgia. The frame for the mechanism was made of aluminum to avoid interference with the electromagnetic field generated when charging

Figure 1-16

Mechanisms for Lowering Pickup Coils



All of the power electronics equipment shown in Figures 1-10 through 1-13 was installed on the bus and integrated with on-board systems by EVAmerica at their plant in Ringgold, as shown in Figure 1-17. The fully integrated bus shown in Figure 1-18 was delivered by EVAmerica to UTC in May 2011.

Figure 1-17

EVAmerica
Assembly Area in
Ringgold, Georgia

**Figure 1-18**

*Electric Shuttle Bus
with Wireless Charging*



UTC students designed and installed a guidance system outlined in Figure 1-19 to assist the operator in positioning the bus for charging. Components of the guidance system are shown in Figure 1-20. These are off-the-shelf commercial components commonly used in recreational vehicles. The camera was mounted inside the bus near the center of the windshield. The display was mounted on the dashboard as shown in Figure 1-21.

Figure 1-19

*View of Coils under
Bus (left) and
Alignment Scheme
(right)*

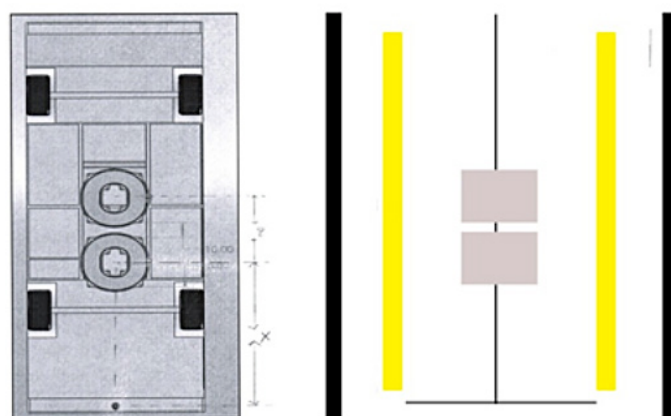
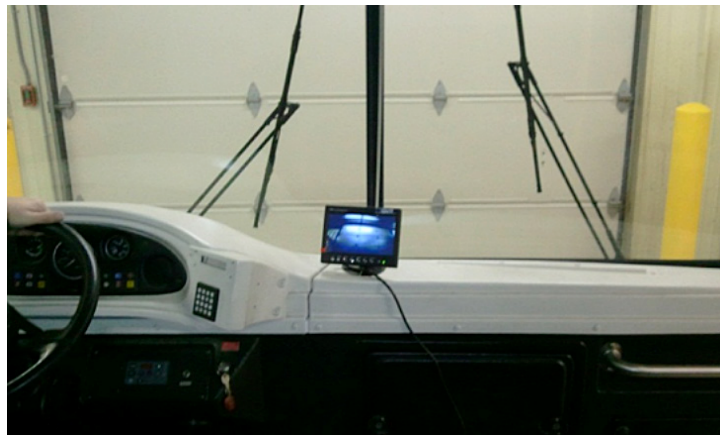


Figure 1-20

Electronic Components of Guidance System

**Figure 1-21**

Display Used to Guide Horizontal Alignment



The white lane markers are used by the operator to get the bus started toward alignment, as indicated in the photograph in Figure 1-22, which shows the bus entering the charging area. Secondary guidance for final alignment is accomplished by a camera mounted inside the windshield aimed at the yellow line down the center of the charging area. When the bus is properly positioned, the vertical yellow line representing the centerline of the charging pad and a horizontal line representing the correct stopping point will be aligned with cross hairs on the camera display, indicating to the operator that the bus is in the correct position for charging.

Figure 1-22

Bus Entering Wireless Charging Area



Site Preparation

In parallel with the design and integration work being done by EVAmerica, UTC installed all the stationary equipment on the grid side of the air gap at the AVTF. Beginning at the power grid, pull-down switches were installed to provide connection to a 100 KVA, 480V, 3-phase circuit. A second switch was installed to allow power to be directed toward the inductive power transfer system or the direct chargers, which were each equipped with individual disconnect switches that are necessary to comply with national and local electric codes.

Voltage transducers and current transformers were installed inside the main power switch to monitor grid voltage and current. These signals were fed through a data acquisition board into a PC that was equipped with Labview for data collection and analysis. Power from the grid was monitored by a voltage transformer. The photograph in Figure I-23 shows the switch gear in the background, the data acquisition board in the upper left, the voltage transformer in the lower center, and the Labview data acquisition system in the lower left. The Labview screen for monitoring AC voltage and current is shown in Figure I-24. The Track Supply shown in Figure I-25 provides up to 60 kW of power at 20 kHz.

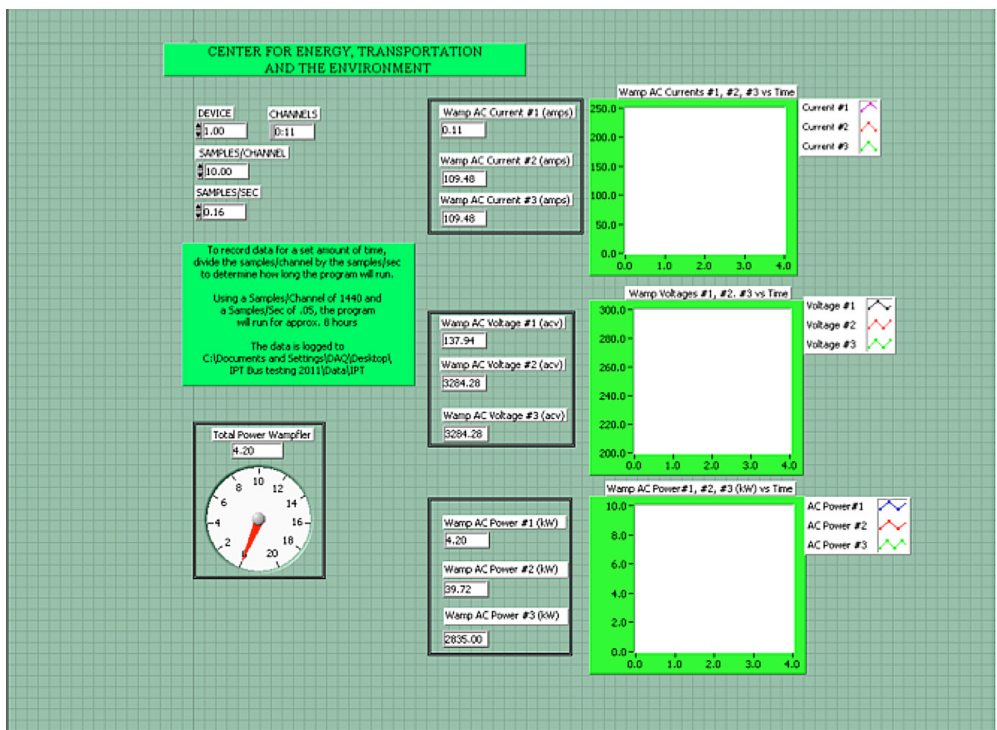
Figure 1-23

Switch Gear, Voltage Transformer, and Data Acquisition System



Figure 1-24

Labview Screen for Monitoring AC Power

**Figure 1-25**

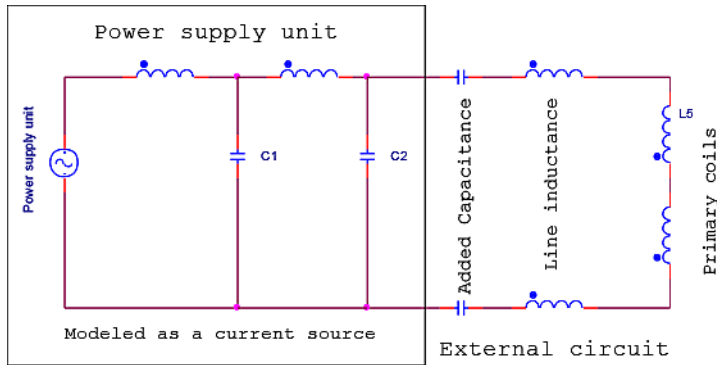
Track Supply



Tuning the System

A simplified circuit diagram for the system is shown in Figure I-26.

Figure 1-26
Simplified RLC Model
for Primary Side
of IPT Circuit



The resonant frequency for this circuit is given by

$$\text{Resonant frequency} = \frac{1}{2\pi\sqrt{LC}}$$

The values of inductance and capacitance that will result in resonance at a given frequency could be derived from the above formula, and is given as

$$L = \frac{1}{4\pi^2 f r^2 C} \quad \text{or} \quad C = \frac{1}{4\pi^2 f r^2 L}$$

Since inductance is fixed as determined by the design of the IPT coils and the length and diameter of the Litz wires that connect the circuit, tuning is accomplished by insertion of capacitors to compensate for the inductance of the Litz cables. In this case, two capacitors were installed in series with the other components to tune the resonant frequency. Note that only finite values of capacitance can be used, so perfect tuning cannot be achieved without also changing the length of the Litz cables, which was not necessary for this installation.

Figure I-27 shows the capacitor boxes with wires going into the conduit that leads to the outside IPT charging pad.

Figure 1-27

Capacitor Boxes used
to Tune Circuit



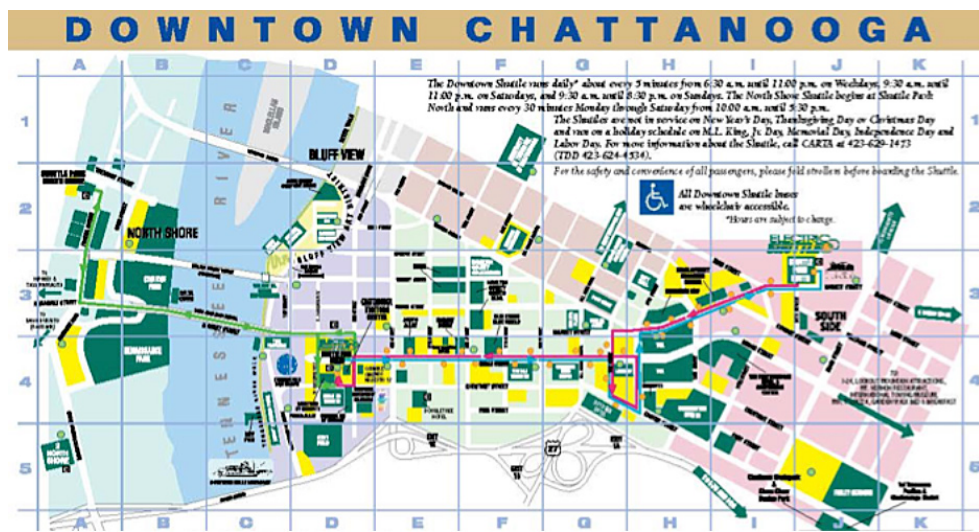
Experimental Results

Test Protocol

The CARTA downtown shuttle route, shown in Figure 1-28, consists of approximately 3 miles of relatively flat city streets with 20 stops.

Figure 1-28

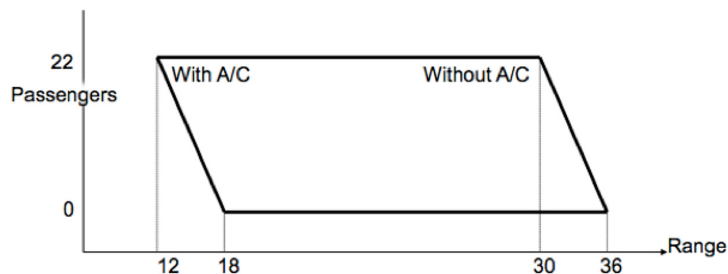
Downtown
Chattanooga
Shuttle Route



The number of trips that can be made with the existing fleet of lead acid (PbA) battery-powered shuttles depends upon number of passengers, traffic conditions, ambient temperature, and the driving habits of the operator. An overall range envelope for the existing shuttles is shown in Figure 1-29.

Figure 1-29

*Range Envelope
for Existing CARTA
Shuttles with
PbA Batteries*



For testing purposes, it was recognized that the bus does not stop unless a passenger signals or someone is waiting for the bus. On average, the bus stops about nine times for each loop around the downtown route. Since the test track is a one-mile oval, the test protocol adopted was to begin each test at the AVTF building with a full state of charge (SOC), drive the bus for three laps around the track, and stop three times on each lap to simulate a single trip of three miles with nine stops around the downtown shuttle route, then ending back at the AVTF charging station.

To simulate passenger load, water barrels were placed along the centerline of the passenger compartment, as shown in Figure 1-30, representing the weight of approximately 22 passengers.

Figure 1-30

*Water Barrels
Equivalent to 22
Passengers*



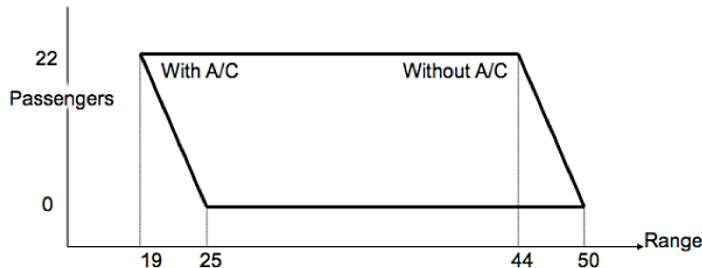
Baseline Testing

After reconditioning the original Ni-Cd batteries, a range of more than 70 miles was recorded for travel around the test track at the AVTF at a constant speed of 25 mph without stopping. The measured performance envelope for the Ebus shuttle running on Ni-Cd batteries alone on the simulated downtown route (three miles with nine stops) is shown in Figure 1-31. It can be seen that the Ebus shuttle with Ni-Cd batteries alone significantly increased the range when compared with

the existing shuttles that are powered with PbA batteries. However, the range is still not sufficient to cover the daily distance without swapping buses or changing batteries.

Figure 1-31

Baseline Range with Ni-Cd Batteries



Range with Wireless Charging

Simulation suggested that a single charge at 60 kW for 3 minutes after each 3-mile trip would provide enough energy to extend the range to the required distance. Therefore, the Track Supply was programmed for a three-minute charge and then testing began, using three laps around the test track with three stops each lap.

The on-board data acquisition system was used to record SOC, battery voltage, energy consumed, and Amp hours consumed during each trip. Prior knowledge set the parameters for defining maximum range to be when the SOC dropped to 20% or the voltage dropped to 280 volts.

Test results, shown in Figures 1-32 and 1-33, indicate changes in SOC and voltage as a function of distance for the baseline bus and the bus with wireless charging. It can be seen that the range has been extended to more than 100 miles. Some of the irregularity in the plots is because the operator was not allowed to back the bus to achieve an acceptable position for charging. This is a safety rule. To compensate for a missed charging opportunity, the operator had the option of taking a double charge for six minutes duration at the next opportunity.

Figure 1-32

SOC as a Function of Distance

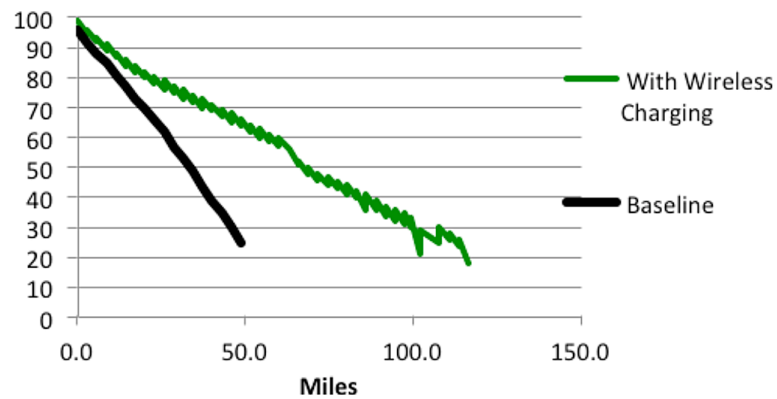
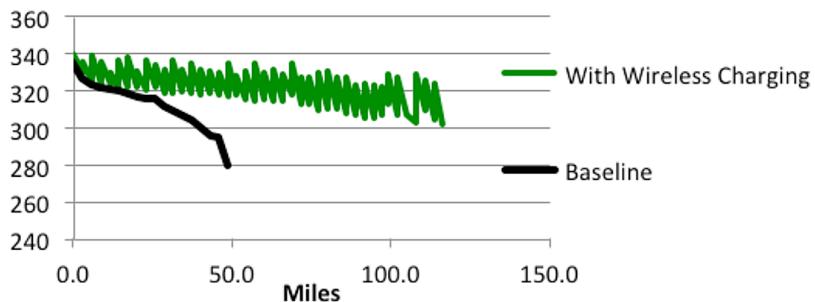


Figure 1-33

Battery Voltage as a Function of Distance



It can also be seen that the voltage collapses as the bus approaches the end of its range. SOC seems to be better behaved, but SOC is a derived number. Since a disabled bus with dead batteries in the middle of a trip would cause unacceptable inconvenience for passengers and a recovery operation by CARTA, it was decided that counting Amp hours (Coulombs) would be a better way of eliminating range anxiety for the operator. By starting with a full charge of 200 Amp hours and counting Amp hours consumed, the operator can know how many more trips can be made without losing power, which occurs when voltage collapse causes the current limiting features built into the drive system to reduce power as a means of protecting the batteries and on-board power electronics.

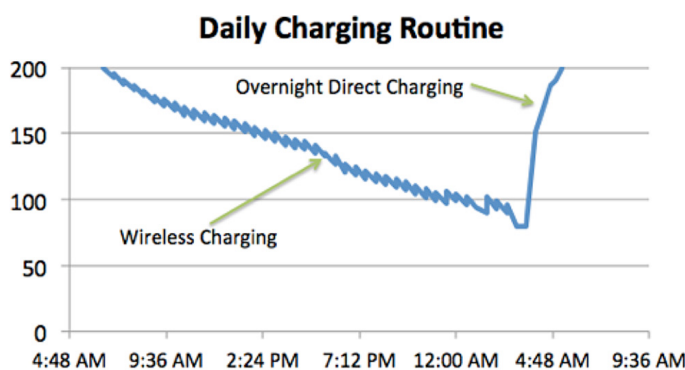
In theory, the range could also be extended by increasing the power level or increasing the frequency or duration of each opportunity charge; however, $C_s = 0.3$ is the maximum recommended charging rate for these batteries. From an operational standpoint, the wireless charging should meet, but not exceed, the level and duration needed to achieve the required range, allowing the batteries to reach a relatively low SOC at the end of the day, with slow overnight charging used to restore the batteries to a full SOC while allowing the individual cell voltages to equalize, thereby increasing the life of the batteries.

Charging the Batteries

DC Amp hours consumed and replaced over a 24-hour day is shown in Figure 1-34. It should be noted that regenerative braking provided some of the energy put back into the batteries during the day. It can also be seen that the direct charger used for overnight charging was programmed to restore automatically the batteries to a full charge of 200 Amp hours.

Figure 1-34

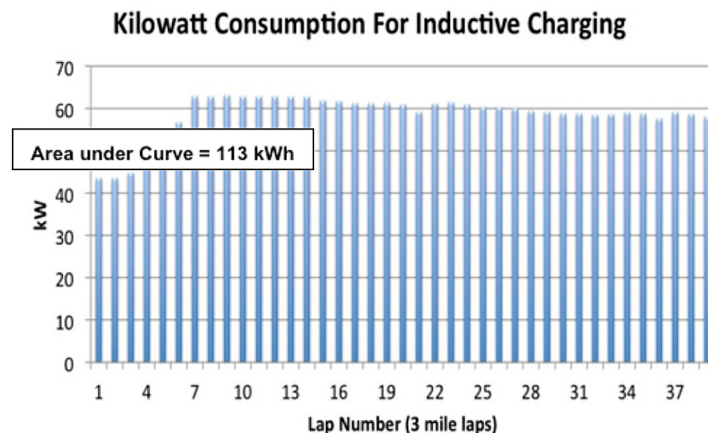
DC Amp Hours Consumed and Replaced over 24-Hour Day



Labview was used to monitor AC voltage and current on each of the three phase lines connected to the power grid. Real AC power was calculated by applying a power factor of 0.95 for the Track Supply. Results for the driving phase of a 24-hour day are shown in Figure 1-35.

Figure 1-35

AC Power for Day of
Wireless Charging
Covering 39 Trips
(117 miles)

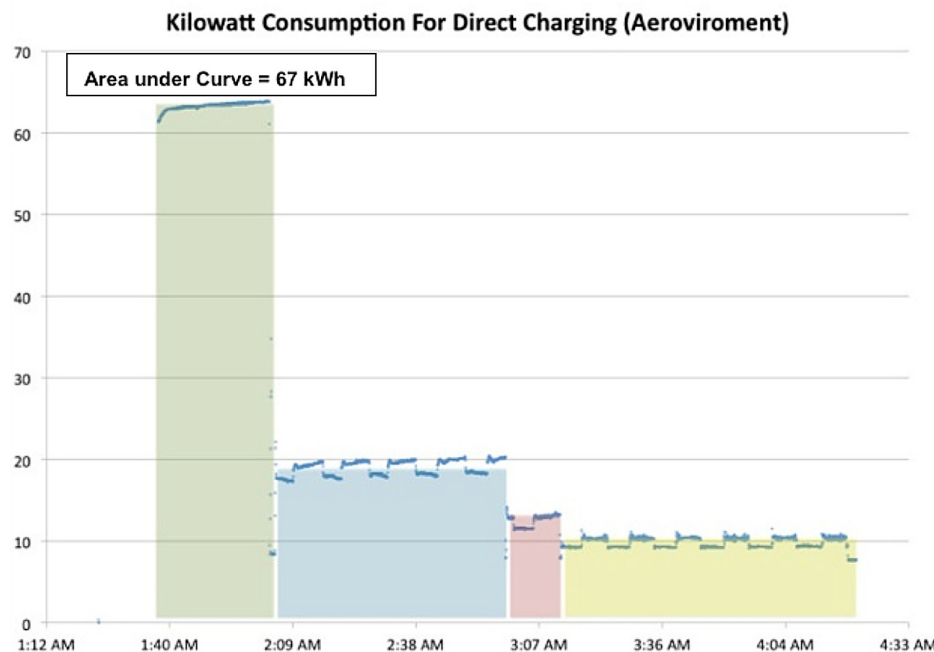


It can be seen that full charging does not occur until the seventh trip. Until then, the SOC of the batteries is too high to accept a full charge. During this period, the wireless charging is truncated automatically. As a practical matter, wireless charging could be skipped until the SOC dropped to about 80%, at which time the batteries become more receptive to charging.

Two types of chargers were available for overnight charging. Both were programmed to charge at their maximum charge rate until the SOC reaches 80%, followed by a lower rate of charge until the SOC reaches 95%, followed by a lower rate until SOC reaches 100%, followed by trickle charging until the SOC is slightly above 100%. The grid energy consumed by the Aerovironment 60 kW charger is shown in Figure 1-36. The area under the curve represents the kilowatts consumed. Analysis of the data confirmed that the automatic overnight charging not only restored the batteries to 100% SOC but also replenished the Amp hours consumed during the previous day of driving.

Figure 1-36

Power Consumed by Overnight Charging

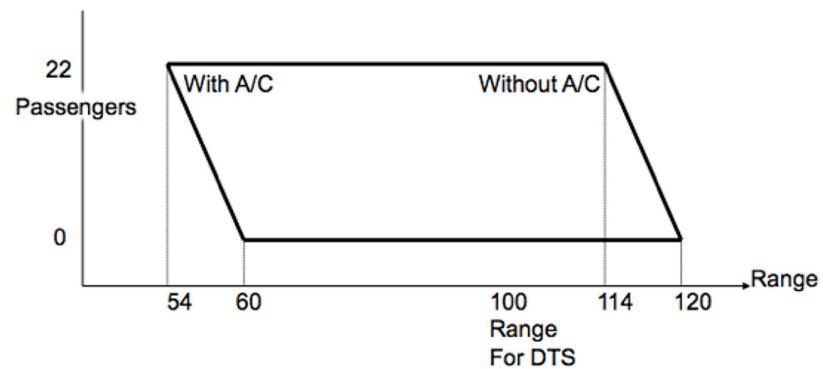


The efficiency for direct charging depends upon the phase, with the most efficient operation occurring during the initial phase. During this phase, while the batteries were at a relatively low (<25%) SOC, the measured efficiency was more than 85%. Efficiency at other times was lower, but never below 80%. Efficiency during the discharge cycle can be estimated to be approximately 90%.

The above data were recorded for an empty bus without air conditioning. The measured performance envelope for other operating conditions is shown in Figure 1-37. It can be seen that the range varies from 54 miles with a full load of passengers on a hot day to 120 miles with no passengers on a cool day. The climate in Chattanooga is mild enough most of the year that air conditioning has never been used on the CARTA electric shuttles. Should air conditioning be required, the charging profile could be modified or the operator could simply initiate double charges during the part of the day when air conditioning is needed.

Figure 1-37

Range Envelope with Wireless Charging



Operating Cost Estimates

Overall energy consumption for traction and operation of auxiliary equipment can be estimated by summing the energy supplied from the grid during wireless and direct charging. Using the data from the above test, the total energy supplied was 113 kWh + 67 kWh for a total of 180 kWh during a day when the bus was driven 120 miles. This results in a specific energy consumption rate of 1.5 kWh per mile.

The present retail rate for electricity at the AVTF is 8.5 cents per kWh. However, large commercial customers such as CARTA pay a lower rate. For a typical month, CARTA will pay 8.25 cents per kWh for the first 15,000 kWh and 3.43 cents per kWh for the balance of 21,000 kWh. This results in an average cost per kWh of 5.43 cents per kWh. The total cost of electricity used by the bus can be calculated as follows:

$$\begin{aligned}\text{Daily cost of electricity} &= 180 \times \$0.0543 = \$9.77/\text{day} \\ \text{Cost/mile} &= \$9.77/120 = \$0.08/\text{mile} \\ &\quad (\text{Empty, no A/C})\end{aligned}$$

A fully-loaded bus, operating on the same route on a hot day with the air conditioning running continuously will consume approximately 2.6 kWh per mile. This results in an estimated cost given by:

$$\begin{aligned}\text{Cost/mile} &= 2.6/1.5 \times \$0.08 = \$0.14/\text{mile} \\ &\quad (\text{Full with A/C})\end{aligned}$$

However, these conditions exist for only a few afternoons during the tourist season in Chattanooga. Furthermore, it should be noted that driving habits can have a significant impact on specific energy consumption. Taking all of these factors into account, it would be reasonable to conclude that one goal for this project has been met:

$$\text{Average cost/mile} < \$0.10/\text{mile} \text{ (year round)}$$

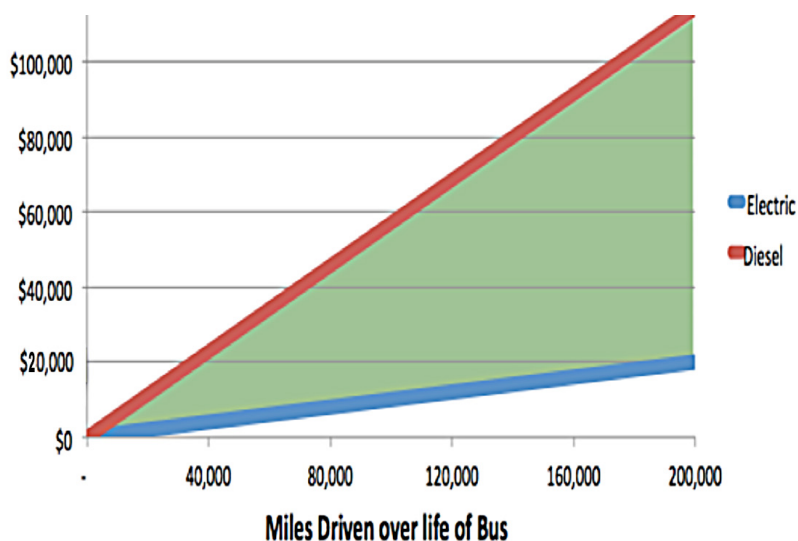
This can be compared with the cost of fuel for a diesel bus that will average about 7 mpg. The present cost of diesel fuel for CARTA is \$3.23 per gallon. This yields the following estimates for a diesel bus:

$$\begin{aligned}\text{Daily cost for diesel fuel} &= 120/7 \times \$3.23 = \$55.37/\text{day} \\ \text{Cost/mile for diesel bus} &= \$3.23/7 = \$0.46/\text{mile}\end{aligned}$$

A typical shuttle bus is designed for a useful life of seven years. Over that time, the bus will travel approximately 30,000 miles per year. Figure I-38 shows a comparison of fuel costs for an electric shuttle and a comparable diesel shuttle at today's prices. It can be seen that an electric shuttle will save more than \$100,000 on fuel costs over a 7-year life.

Figure 1-38

Comparison of Fuel Costs

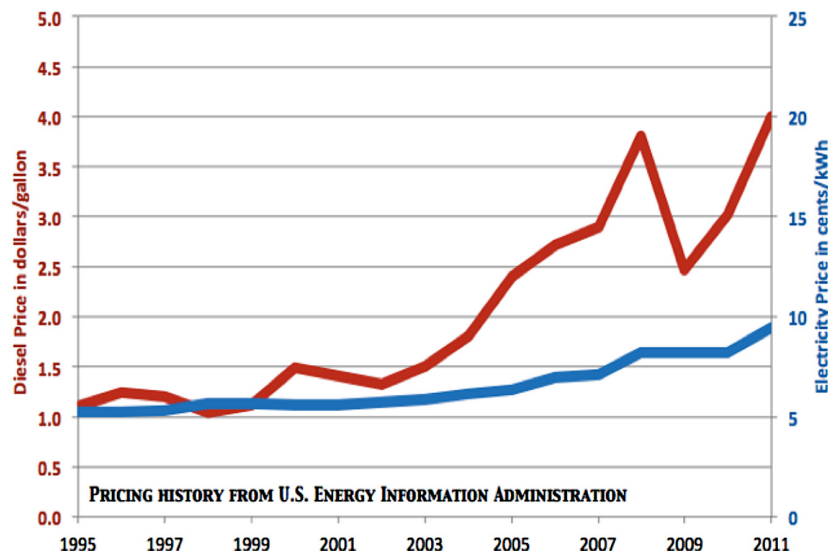


Perhaps more important, elimination of the need to swap batteries or buses during the day has the potential to reduce the total number of buses needed from 13 to 5. It can also reduce the number of batteries since present operations require one set to be in the bus while a second set is being charged and a third set is cooling down.

Also worth noting is a comparison of the changes in cost for electricity and diesel fuel over time. Since 1995, the cost of oil and electricity both have increased, as shown in Figure 1-39. It can be seen that the cost of diesel fuel quadrupled over this period, while the cost of electricity doubled. It can also be seen that the price for diesel fuel has been much more volatile, making it difficult to budget for fuel costs. The impact of this volatility can be characterized by noting that a 10% increase in the price of diesel fuel would increase CARTA's annual fuel bill by more than \$160,000.

Figure 1-39

Cost Comparison of Diesel Fuel with Electricity



Measurement of Efficiency

Since most of the wireless charging takes place after the batteries are able to accept a full charge, the most meaningful measurements of the rate of power transfer and the overall efficiency should be made during a charge cycle that occurs after the system has stabilized. The results given in the Table I-1 were measured during a wireless charging cycle that took place in the middle of the day after approximately 49 miles of service.

Table 1-1
Voltage and Current during Wireless Charging

AC Voltage	AC Current	Apparent Power (kVA)	Battery	Utility Load	Battery + Utility
272.9	74.1	20.2	382 V	325 V	-
272.8	73.2	20.0	137 A	-7A	-
272.6	74.6	20.3	-	-	-
Total	-	60.5	52.3	2.3	54.6

It can be seen that the total power being delivered across the air gap, including the utility load on the bus, was 55 kW when the grid was supplying apparent power of 60.5 kVA. A true indication of overall electrical efficiency would be the ratio of real power delivered to the bus divided by the real power provided by the grid. By definition, real power is the product of apparent power and power factor, which takes into account both phase displacement and harmonic distortion. A Fourier series representation of the current input to the rectifier yields a theoretical value for power factor of $3/\pi = 0.955$. This would yield the following estimate for theoretical efficiency:

$$\text{Theoretical efficiency} = 54.6/(60.5 \times 0.955) = 94.5\%$$

Magnetic Flux Emissions

Public safety must be paramount in all transit operations. Documentation provided with the equipment suggested that the electromagnetic field strength around the charging coils would be safe for human exposure. However, since the actual field strength depends upon the installation, Dr. John Boys, Professor of Electrical Engineering, University of Auckland, New Zealand, was retained to measure electromagnetic flux to ensure public safety.

Flux measurements were taken while the vehicle was on charge at maximum power. There is, in fact, a rather small window during which the measurements can be made and, after this short time, the charging current reduces quite significantly. The measurements were made with a Narda Safety Test Solutions ELT, Model ELT-400, P/N 2304/01, S/N M-0282. The instrument was equipped with a B Field Probe P/N 2300/90 10, S/N M-0301. This instrument has been specifically designed for this type of measurement and is ideally set up for it. It

was manufactured in Germany before the International Commission on Non-Ionizing Radiation Protection (ICNIRP) guidelines were revised upwards, so the scales based on ICNIRP measurements were not used here. The measurements were all taken by Dr. Boys using the probe directly under the edge of the vehicle, as shown in the Figure I-40.

Figure 1-40

*Dr. John Boys
Measuring EMF*



To ensure safety for the general public, measurements of flux density were made at locations outside the bus that might be representative of the places where passengers or pedestrians might stand. Variations in the flux density in any particular site occur at different positions along the site and depending on how close to the ground the probe is. The flux on the side of the vehicle above the air-gap is much smaller than the flux at ground level near the air-gap and does not contribute to the ICNIRP measurement. Results for maximum measurements taken outside the bus are given in Table I-2.

Table 1-2

*EMF Measurements
Outside the Bus*

Position	Flux Range
Forward of front wheels	<0.5 µT
Driver's side, between wheels	2.3-7.2µT
Door side, between wheels	7.2-7.5 µT
Behind the rear wheels	<0.5 µT

Inside the bus, the background level with the charging equipment off was observed to be 0.13 µT. With the charging equipment operating at maximum output, flux levels varied with location, having a maximum value at floor level directly above the coils. Results are shown in Table I-3.

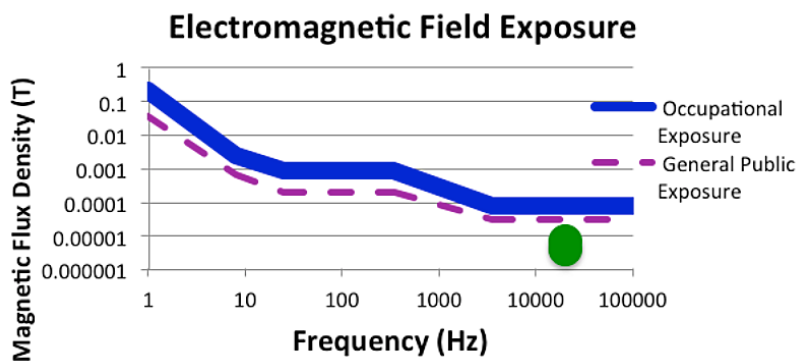
Table 1-3
*EMF Measurements
Inside the Bus*

Position	Flux Range
Background	0.13 μT
Inside bus at floor level directly above coils	4. 1 μT
Inside bus 3 ft above floor directly above coils	0.41 μT
Inside bus 6 ft above floor directly above coils	0.21 μT
Inside bus at all other locations	< 0.2 μT

Maximum values from Tables I-2 and I-3 are also shown in Figure I-41, which indicates that measured flux levels are well below the recommended limits for both public and occupational exposure to electromagnetic fields.

Figure 1-41

*Comparison of
Observed Levels of
Flux with ICNIRP
Recommendations*



Since the general public is unlikely to be familiar with the nomenclature and meaning of the ICNIRP recommendations for exposure to electromagnetic fields, the poster in Figure I-42 was produced to explain to the general public that wireless charging of buses using IPT is not harmful to humans.

Figure 1-42

Poster on Safety for
Wireless Charging

Wireless Charging Q & A

What is wireless charging?

Wireless charging is a hands-free charging system, using an Electromagnetic Field (EMF) to charge the battery in an electric vehicle, or other device, without having to plug it into a power source. It is controlled using a radio link.

Is wireless technology new?

No. Wireless technology is used in radios, televisions, cell phones, satellite based navigation systems, wireless internet access used in buildings, homes and the bus you will be riding.

Is wireless charging safe?

The magnetic field of the Earth is more than 100 times greater than what passengers are exposed to when boarding or riding the bus. The EMF exposure for passengers is no greater than would be experienced when using common household appliances.

Will the magnetic field affect my credit cards, cell phone, and other electric devices?

No. The wireless charging primary coil is enclosed and its range is specifically limited, so that it only interacts with the second coil on the vehicle. The stationary in-ground coil only emits a field when the vehicle is correctly positioned above it, so there is no interaction with the personal electronics of pedestrians.

Source	Magnetic Field Strength in micro Tesla (μT)
Earth at the magnetic poles	60
Wireless charging electric bus	less than 0.2
Electric blanket at surface	1.0 to 3.0
Hairdryer at 12 inches	0.1 to 7.0
Toaster at 12 inches	0.6 to 7.0

Do the coils get hot?

No. The coils are water cooled and will not exceed the ambient temperature of the pavement, so there is no danger to pedestrians or vehicles when the bus departs the charging station. However, metal objects left on the coil during charging may become warm to the touch.

Environmental Considerations

Compliance with the Clean Air Act

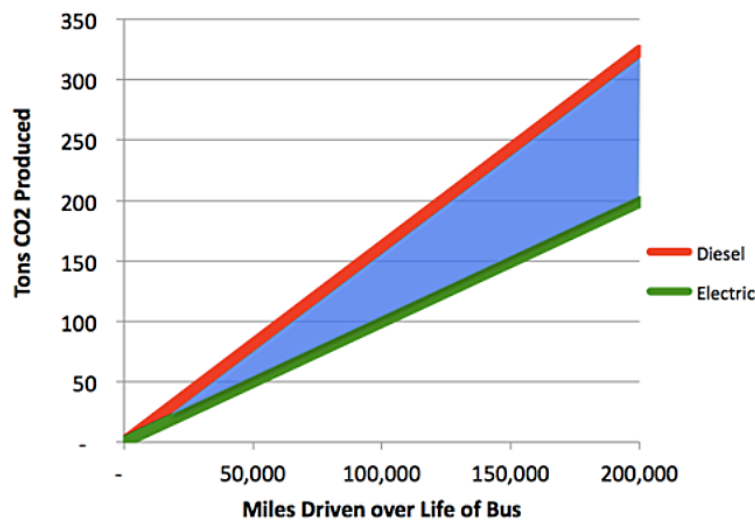
Elimination of tailpipe emissions makes electric shuttle buses particularly friendly to the environment. When the electric shuttles were introduced in Chattanooga, the primary driving force was to assist Chattanooga to attain compliance with the Clean Air Act. This meant significant reductions in all the emissions normally associated with diesel buses, including hydrocarbons (NHO_x, NMHC, or THC), Oxides of Nitrogen (NO_x), particulate matter (PM), Carbon Monoxide (CO), and Formaldehyde (HCHO). Today, Chattanooga has not only attained full compliance with the Clean Air Act but also has created enough "headroom" to accommodate economic development projects such as the new automobile manufacturing plant recently built in Chattanooga.

Reduction in Greenhouse Gases

In addition to reducing smog, there will also be a corresponding reduction in greenhouse gases (GHG). Using the method recommended by the American Bus Association, it can be estimated that combustion of a gallon of diesel fuel will produce 10,274 grams of CO₂, whereas the U.S. average for production of 1 kWh of electricity is 600 grams. A diesel bus will average 7 mpg. An electric bus will consume approximately 1.5 kWh per mile for traction. Using these values, an electric bus will reduce CO₂ emissions by approximately 567 grams per mile. Reductions over the design life of an electric shuttle are shown in Figure 1-43.

Figure 1-43

Comparison of CO₂ Emissions for Diesel and Electric Shuttle Buses (22 ft)



It can be seen that an electric shuttle will reduce CO₂ emissions by at least 125 tons. Total GHG emissions would be higher for diesel buses because of emitted hydrocarbons and particulate matter in addition to CO₂. It should also be noted that electric buses are virtually silent, thereby reducing noise pollution that can be particularly annoying in those areas normally served by transit buses.

Summary of Wayside Charging Results

A comparison of the goals and results for this project are given in Table 1-4. While there was no specific goal for efficiency, it was found that the overall grid to vehicle efficiency was greater than 90%. It was also demonstrated that electromagnetic flux emissions were well below ICNIRP standards for all locations.

Table 1-4
Summary of Results

Objective	Goal	Results
Charge time	1 minute	1 minute
Distance per charge	1 mile	1 mile
Cost per mile	\$0.10	\$0.08
Range w/o charging	100 miles	120 miles
Tail Pipe Emissions	0	0

Lessons Learned about Wireless Charging

It has been demonstrated that the range of an electric shuttle bus can be increased to more than 100 miles by wireless charging during times that the bus is stopped to load and unload passengers. It also has been shown that the electromagnetic flux produced by wireless charging is well below the safe exposure limits recommended by international standards. When compared to diesel bus operation for the same deployment, wireless charging can reduce fuel costs by more than \$90,000 over the life of the bus while reducing GHGs by more than 120 tons.

SECTION
2

Hydrogen Hybrid Bus Demonstration

Background

The objective for this project was to extend the range of an electric shuttle bus by a combination of improved batteries and an on-board generator to be powered by a hydrogen-fueled internal combustion engine and used as an auxiliary power unit (APU) to provide energy and power for the non-traction loads on the bus.

The goal was to achieve a minimum range of 100 miles for a battery-centric shuttle bus without recharging. This range would allow a CARTA electric shuttle bus to operate for a full day without swapping batteries.

Prior to the start of this project, Ebus had developed two hybrid buses. The rear compartment of one of these buses is shown in Figure 2-1. This bus has a 19 kW fuel cell (lower left in photo) as a range extender. It was tested at the University of Texas at Austin where it was shown to have a range in excess of 200 miles. However, this hybrid bus costs more than \$1,000,000, and the fuel cell had to be replaced twice during testing.

Figure 2-1
Fuel Cell Hybrid Bus
Built by Ebus and
Tested at UT Austin



The rear compartment of a second type of hybrid bus is shown in Figure 2-2. This bus has been deployed by the City of Sevierville, Tennessee, with CETE providing technical assistance to the City. The bus has a 20 kW capstone gas turbine fueled with propane as a range extender.

Figure 2-2

Hybrid Ebus with a 20 kW Gas Turbine as a Range Extender



University of Tennessee at Chattanooga (UTC) students, with assistance from CARTA, installed and evaluated the performance of an identical capstone gas turbine as a student project at the AVTF. Their analysis confirmed data from the field that indicated reasonably efficient performance of the gas turbine when operating at peak capacity, but poor efficiency when operating at less than full speed.

Prior to the onset of this project, UTC students had converted a Saturn Vue to run on hydrogen as a student project. This project suggested that an internal combustion engine running on hydrogen could provide a clean, inexpensive alternative to either previous approach.

Organization

A multidisciplinary team was formed for this project. The partnership is represented graphically in Figure 2-3.

Figure 2-3

Partnership for Development of Hydrogen Hybrid Bus Demonstration



Roles of the Partners

The role of the partners in this project was as follows:

- FTA provided funding through this cooperative agreement number TN-26-7034.
- CARTA provided expertise in transit operations and equipment.

- EVAmerica provided design, fabrication, and integration capability.
- United Hydrogen of Tennessee provided hydrogen backup capability.
- CETE provided ICE expertise and overall project management.

The project was managed through weekly design review meetings, usually held at the EVAmerica site in Ringgold. A photograph showing participants at a design review for the generator is shown in Figure 2-4.

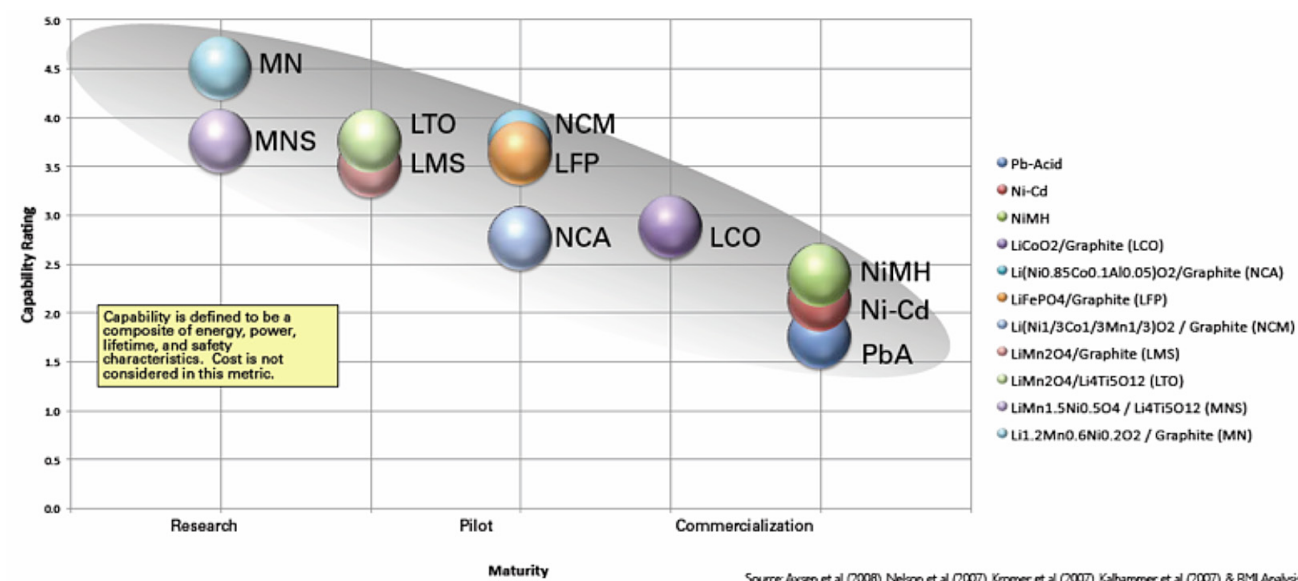
Figure 2-4
Design Review Meeting



Battery Selection

Energy density, cost, and level of maturity must be considered in selecting the optimal batteries for this project. Figure 2-5 shows a comparison of capacity rating with level of maturity for various batteries.

Figure 2-5
Comparison of Capacity Rating with Level of Maturity for Various Batteries



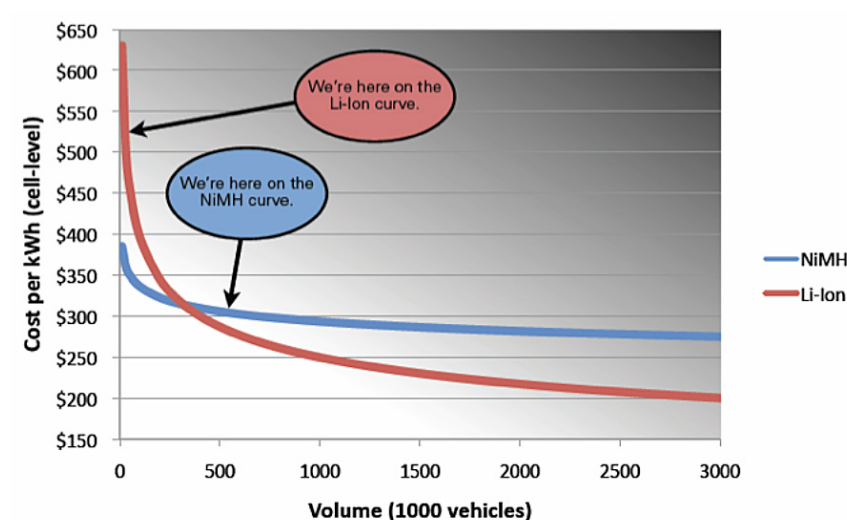
The Ebus shuttles transferred from Emory University have a nominal range of 50 miles with the original Ni-Cd batteries. Since these buses were built in 2003, newer batteries have been developed that provide certain advantages, as indicated in Table 2-1.

Table 2-1*Battery Considerations*

Variant	Advantages	Disadvantages
Li-Iron Phosphate LiFePO ₄ /Graphite	Lower cost Thermal stability Overcharge resistance Wide SOC window	Lower energy Performance at low temps
Manganese Spinel LiMn ₂ O ₄ /Graphite	Lower cost Environmentally friendly Safety (no O ₂ at high temp)	Lower energy Performance at extreme temp Cycle life
Titanate LiMn ₂ O ₄ /Li ₄ Ti ₅ O ₁₂	Cycle life Performance at low temp Thermal stability	Lower energy Lower power High cost
NCA Li(Ni _{0.85} CO _{0.1} Al _{0.05})O ₂ /Graphite	Proven technology Highest energy & power Long life	Thermally unstable Degrades at fast charge Higher cost

At the time the Ebus was built, the cost of Li-Ion batteries was prohibitively high, as indicated in Figure 2-6, because of the relatively small number of vehicles using these batteries.

Figure 2-6
Cost Projections with Increased Volume for Li-Ion Batteries



As a number of automotive manufacturers began to select Li-Ion batteries, it was anticipated that the cost would come down significantly to a level that would be competitive for buses. Advantages and disadvantages for Li-Ion batteries are as follows:

- Advantages
 - Highest specific energy and power density relative to other batteries
 - Long cycle life

- Less sensitive to metal prices
- No memory effect
- Low self-discharge rate
- Disadvantages
 - More expensive than PbA or Ni-Cd batteries
 - Thermal instability in some variants
 - Poor overcharge tolerance in some variants
 - Poor lot temperature performance in some variants
- Still under development

Comparisons of various battery manufacturers and products are given in Table 2-2.

Table 2-2

Battery Manufacturers

Manufacturer	Location	Variant	2009 Price per kWh
Thunder Sky	China	Li-Iron-Phosphate	\$375
BYD Auto	China	Li-Phosphate	\$500
Ener1	Indiana	Li-Polymer	\$660
K2 Energy Solutions	Nevada (China)	Li-Phosphate	\$700
Valance	Texas (China)	Li-Phosphate	\$1,000
Altair Nanotechnologies	Nevada (China)	Li-Titanate	\$1,000
AI23 Systems	Massachusetts (Korea and China)	Li-Phosphate	\$1,228

After due consideration and comparison of all available alternatives, Thunder Sky was selected as the vendor for the battery cells. EVAmerica designed and fabricated the battery packs using cells from Thunder Sky to be compatible with the space available while providing adequate power and energy storage. A photograph of the finished battery pack is shown in Figure 2-7. The boxes on top of the yellow battery cells are part of a proprietary system that is designed to keep the individual cells balanced. Forced air cooling is also provided with the packaging designed and built by EVAmerica. These batteries can deliver of 330 Amp hours at a maximum voltage of 330 volts, which results in a nominal energy storage capacity of 109 kWh.

The cost for the cells alone was \$40,000 for a capacity of 109 kWh. The cost per kWh is given by:

$$\text{Cost per kWh} = \$40,000 / 109 \text{ kWh} = \$367 \text{ per kWh}$$

This value demonstrates the validity of Figure 2-6 while confirming that some cost reductions have occurred due to increased acceptance of these batteries.

Figure 2-7
*LiFePO₄ Batteries
 Mounted in Battery Box
 at EVAmerica*



Improvement in Range from LiFePO₄ Batteries

Tests were conducted at the AVTF track using the same driving protocol as previously developed for measuring the performance of the wireless charging bus, namely driving the bus continuously around the 1-mile test track at a maximum speed of 25 miles per hour and stopping 3 times each lap to simulate actual service on the downtown shuttle route. However, since these were new batteries, the termination criterion for ending the range test was unknown. For this reason, care was taken to monitor individual cell voltages on a real-time basis so that the point of voltage collapse could be observed before any damage was done to the batteries.

As a precaution, individual cell temperatures (highest and lowest cells) were also monitored while driving. Results are shown in Figure 2-8. The unexpected drop in temperature can be attributed to having stored the bus inside the building at approximately 23°C. The outdoor ambient temperature ranged from 13°C at the start of testing to 19°C at the end. The built-in cooling fans were programmed to come on at 20°C, so it is clear that the cooling system was adequate to take care of any heating due to current losses during driving.

Figure 2-8
Cell Temperature vs. Distance

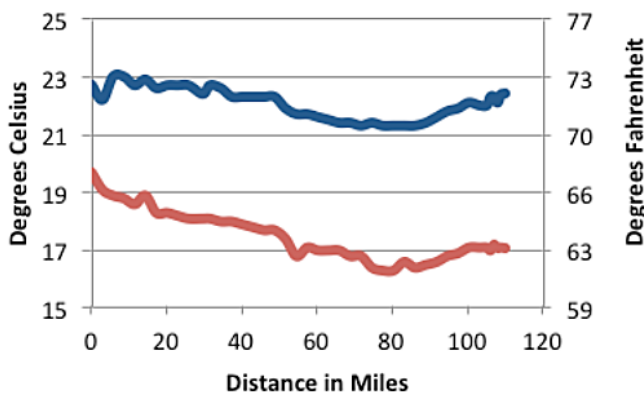
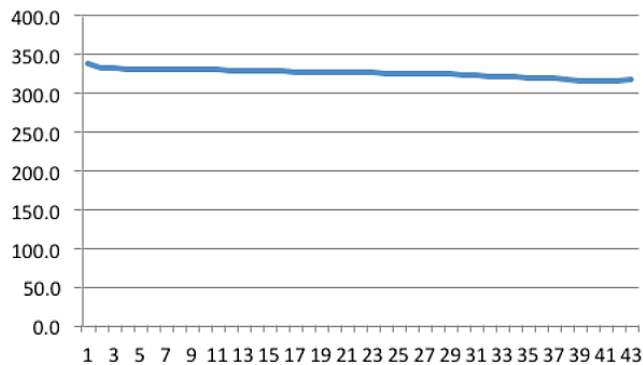


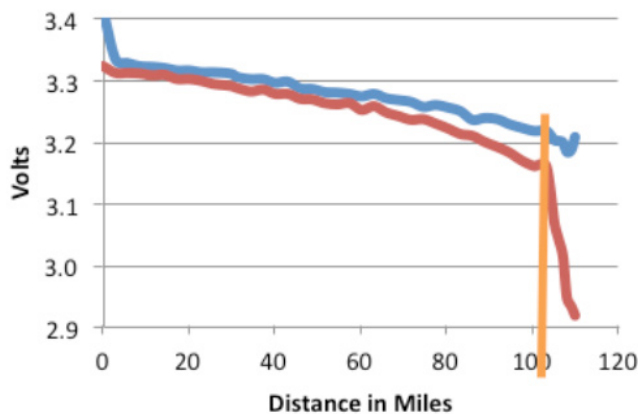
Figure 2-9 shows battery voltage as displayed on the operator panel at the end of each trip around the test track. It can be seen that the overall voltage drops only slightly from start to finish.

Figure 2-9
Pack Voltage after
Each Trip (~3 miles)



It should be noted that the voltage displayed for the operator is the value of 100 individual cells connected in series. It is known that the individual cells do not charge and discharge at the same rates. For this reason, individual cell voltage was monitored during range testing. Values for the highest and lowest cell voltage are shown in Figure 2-10.

Figure 2-10
High and Low Cell
Voltage vs. Distance



It can be seen that the cell with the lowest voltage experienced a voltage collapse after trip 39, which corresponds to 102 miles. The criterion for minimum cell voltage recommended by the manufacturer was 2.8 volts, which allowed the bus to be driven to an ultimate range of 110 miles, but that would not be recommended for daily driving because the small addition in range would not be worth the risk associated with causing permanent damage to individual cells if discharged below the recommended cell voltage of 2.8 volts.

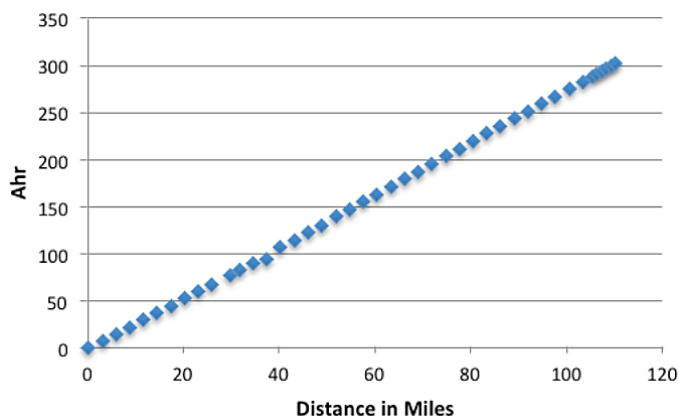
It would be unreasonable and distracting to expect the driver to monitor individual cell voltages to watch for the beginning of voltage collapse. The usual way for determining when to take the bus out of service would be to monitor

the SOC display or overall battery voltage. However, the SOC indicator for this bus was calibrated for the original Ni-Cd batteries and could not be recalibrated without changes to the firmware. Likewise, it was observed that the overall battery voltage did not collapse at the same time as the weakest cell voltage collapsed.

Since neither voltage nor SOC provide an adequate way for the driver to know when the bus is approaching the end of its range, an alternative method was explored. Shown in Figure 2-11 is a plot of Amp hours (Coulombs) consumed by the bus as a function of distance.

Figure 2-11

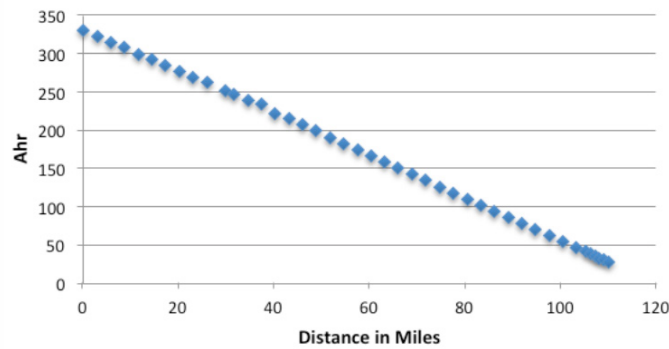
High and Low Cell Voltage vs. Distance



An alternative way of viewing this data is to subtract the Amp hours consumed from 330 Amp hours that would be available in a fully-charged battery. This would be analogous to a fuel gage on a conventional vehicle. This result can be seen in Figure 2-12.

Figure 2-12

Remaining Amp Hours vs. Distance



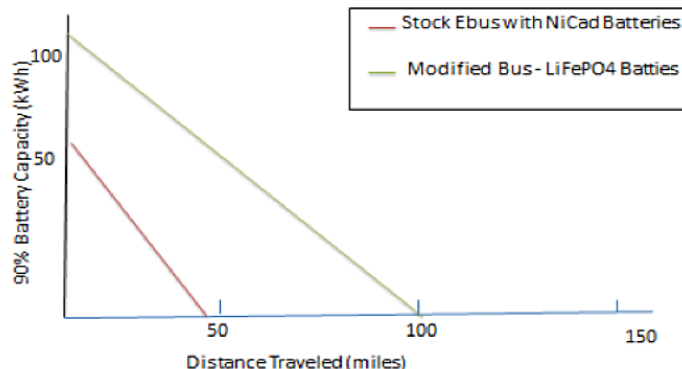
It can be seen that a linear relationship exists between Amp hours consumed and distance traveled, making this a much more reliable way of determining range. Since voltage collapse was observed to occur at approximately 100 miles, this would correspond to consumption of approximately 280 Amp hours, leaving 50 Amp hours of energy remaining from the original 330 Amp hours, which is sufficient to drive the bus approximately 17 miles before the weakest cell reaches voltage collapse.

Looking at this from the driver's point of view, a maximum of two data points can be observed simultaneously with the on-board driver's display. Since the bus must have enough reserve for the trip from the terminal point of the route back to the depot, the batteries cannot be drained beyond the point that would put the driver at risk of not being able to return the bus to the depot for recharging. Assuming that the bus begins with a full SOC, the best indication that the bus needs to be taken out of service would be when the Trip Amp Hour display reaches 280 Amp hours or the Trip Odometer reaches 100 miles, whichever comes first.

The improvement in range from replacement of the original Ni-Cd batteries with 60 kWh of capacity with the new LiFePO₄ batteries with a capacity of 109 kWh can be seen in Figure 2-13 when the operating range is limited to 90% of capacity.

Figure 2-13

Improvement in Range with LiFePO₄ Batteries



Development of Battery Charging Profile

The original Ebus came equipped with Ni-Cd batteries that were packaged in two parallel strings. The chargers that came with this bus from Emory University were programmed to charge the two strings in parallel. The new batteries were packaged in a single string, which made it impossible to use these chargers. Before purchasing a new charger for these batteries, the ABC-150, shown in Figure 2-14, was used to develop and test a charging profile that could be used to specify a purpose-built charger for these batteries.

Figure 2-14

ABC-150 Used to Develop Charge Profile for LiFePO₄ Batteries



The battery manufacturer provided a recommended charge profile for individual cells that allowed charging to be done at 0.5C until cell voltage reached 4.0 volts. For a string of 100 cells, this would have allowed the battery pack to be charged at 54.5 kW until the pack voltage reached 400 volts. To provide a margin of safety, the ABC-150 was programmed to charge at 50 amps with a maximum power output of 20 kW, at which point the ABC-150 would automatically switch to a voltage source type charger, holding voltage constant at 400 volts while letting the current drop in response to the change in impedance that would occur as the battery approached a full SOC. This rate is less than half the maximum allowable rate but fast enough to fully recharge the battery pack in five hours, which is within the time allowed between 11:30 PM and 6:30 AM for overnight charging.

Current and voltage during a typical charging operation are shown in Figures 2-15 and 2-16.

Figure 2-15

Current during Charging

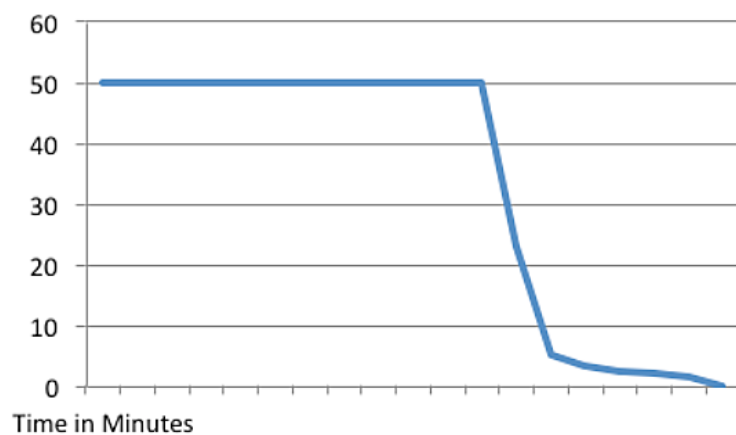
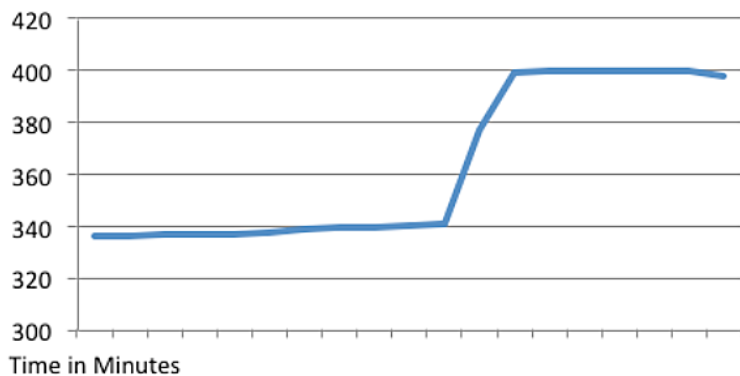
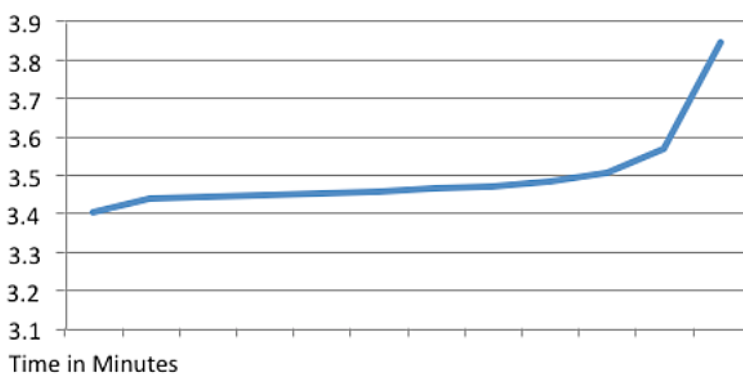
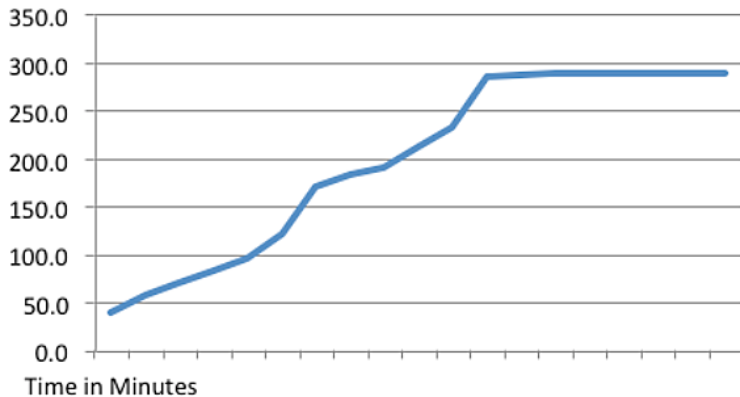


Figure 2-16*Voltage during Charging*

Individual cell voltages were monitored during the charging process to make sure that no single cell was overcharged. The highest individual cell voltage is shown in Figure 2-17.

Figure 2-17*Highest Cell Voltage during Charging at 100 Amps*

It should be noted that the rate of increase in cell voltage accelerated as the battery pack approached a full SOC. To establish a cut-off point for the design of a purpose-built charger, it was noted that very little energy was restored to the battery during the final stage when the rate of voltage increase began to accelerate. Figure 2-18 shows the cumulative amp hours restored to the battery.

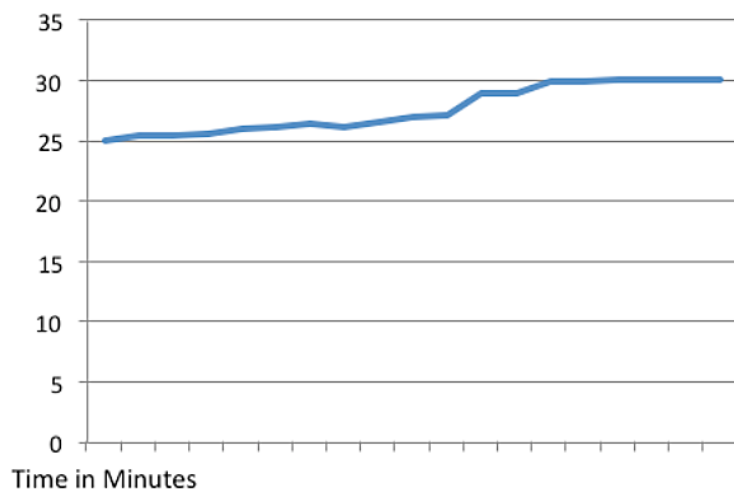
Figure 2-18*Cumulative Amp Hours during Charging*

Since so little energy is restored to the battery after the pack voltage reaches 400 volts, the recommended profile for a purpose-built charger would be to charge at 100 amps until voltage reaches 400 volts and then cut off charging immediately rather than risk cell damage after that point while attempting to add an insignificant amount of charge to the battery pack.

As safety precaution, individual cell temperatures were also monitored during charging. The results are shown in Figure 2-19 for the cell with the highest temperature. It can be seen that the batteries do not experience a significant increase in temperature, mirroring the behavior observed earlier during discharging.

Figure 2-19

Cell Temperature
(Highest)
during Charging



Lessons Learned about LiFePO₄ Batteries

For same space and less weight, LiFePO₄ batteries have been demonstrated to increase range by a factor of 2.3 (from 44 miles to more than 100 miles). These batteries also have a faster charge rate (0.5 C vs. 0.3), which reduces the recharge time by 40%. These batteries run cooler, which means that an on-board chiller is not needed, saving weight and energy. The batteries do not overheat when being charged, which means they can be safely charged without removing them from the bus, again saving time.

The combination of increased range and recharging time has the potential to reduce significantly the number of shuttle buses that must be maintained in order to meet the daily demand for service. For CARTA, this could mean a reduction in the number of shuttle buses needed to operate the downtown route from 13 to 5 or 6, depending on reliability and maintainability of all bus components.

Overall grid-to-motor efficiency will be the product of efficiency for charging and efficiency during discharging which can be estimated as follows:

$$\text{Grid-to-motor efficiency} \sim 0.85 \times 0.9 = 76.5\%$$

Auxiliary Power Unit (APU) Considerations

To comply with the Clean Air Act, any engine used for traction on public roadways must be certified by EPA and can be issued only to a vehicle manufacturer. At present, the only hydrogen-fueled engines that have EPA certification are large diesel conversions that are too big for this project. To proceed without violating the Clean Air Act, the generator can be used only for the auxiliary services and not for traction.

These auxiliary services (“hotel loads”) include air conditioning, power steering, lighting, air compressor (power brakes), and the cooling system for the batteries, if required. For the Ebus, the maximum power required for all auxiliary services is approximately 10 kW. However, CARTA does not intend to use the air conditioner, and new batteries do not require a separate cooling system. This would leave an auxiliary load of approximately 5 kW. However, a slightly larger unit was chosen because the power rating of the engine will be somewhat lower when running on hydrogen because of the higher air-fuel ratio required for complete combustion. For these reasons, a relatively small 10 kW generator, shown in Figure 2-20, was chosen to serve as an APU for this project.

Figure 2-20

10 kW Polar Power APU



This generator was selected based on the following features:

- Maximum continuous output of 10 kW at 2600 rpm
- Available in all voltages from 24 to 500 Volts dc
- Variable speed with a typical 500 rpm span from no load to full load
- Lower speed option available
- 3-cylinder water-cooled engine originally designed for diesel operation
 - Water-cooled
 - Outstanding durability: 20,000 to 30,000 hour life expectancy
- Easy to maintain
 - Oil change at 200 hours
- Temperature-compensated battery charging
- Alternator efficiency in excess of 85%
- Military specifications met without extra cost

Engine Modifications

Shown in Figure 2-21 is the APU installed in the rear compartment of the bus. It has been converted to run on hydrogen and compressed natural gas (CNG).

Figure 2-21
*H₂/CNG APU Installed
in Modified Bus*



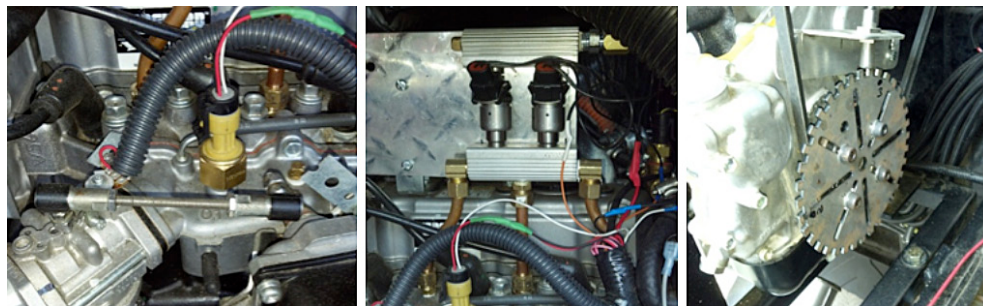
Major modifications to the APU for hydrogen operation were the additions of a separate, independent fuel and ignition system, a turbocharger, and a series of relays to switch inputs from the Daihatsu ignition module (IM) to the AEM® EMS-4 stand-alone engine control unit (ECU) to the ignition coils. This design allows the engine to be switched between CNG and hydrogen electronically.

without making any major mechanical changes to the engine or affecting the engine performance with respect to each fuel. The switchability of the unit also allows for the customer to use whichever fuel is the most economically viable at the time. Modifications made for CNG operation were the exchange of the propane regulators for CNG/methane regulators. The stock Daihatsu carburetor/mixer was designed to handle either fuel.

Other modifications to the engine include the installation of various sensors for the EMS-4 and the fabrication and installation of a fuel manifold. Figure 2-22 shows pictures of the modifications made to the APU for hydrogen operation.

Figure 2-22

Various Hydrogen Fuel and Ignition System Components and Sensors



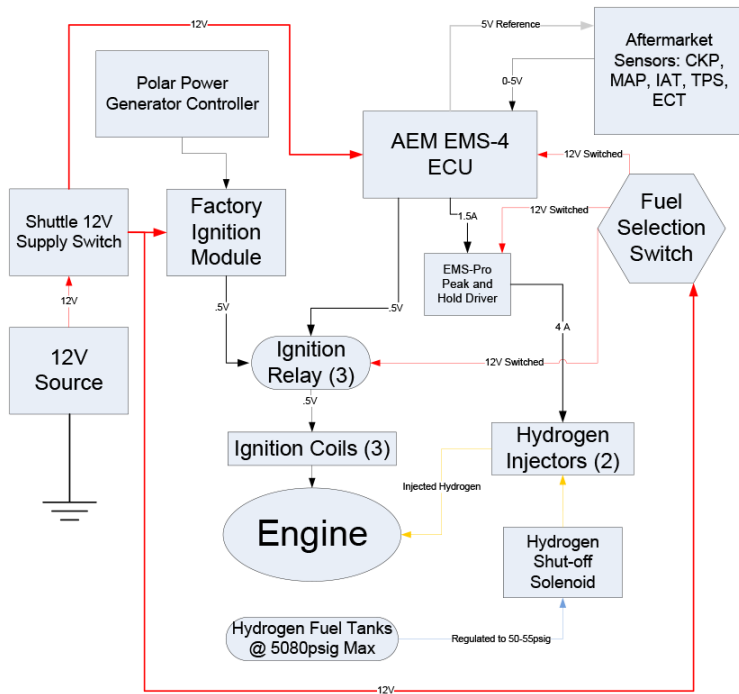
Fuel and Ignition

In designing an engine that is capable of operating on CNG and hydrogen independent of one another, two separate fuel systems must be in place to deliver each fuel efficiently. This operation is executed using a series of switchable relays to discern which ignition signal will be delivered to the ignition coils. When the selection is switched ON to use hydrogen, the EMS-4 and relays are energized and the ignition signals are switched to the EMS-4 rather than the Daihatsu ECM. The fuel selection switch is left in the OFF position for CNG operation as the Daihatsu IM and Polar Power engine controller controls the engine.

Figure 2-23 is a simplified schematic of the aftermarket and factory systems.

Figure 2-23

Dual Engine Management Diagram

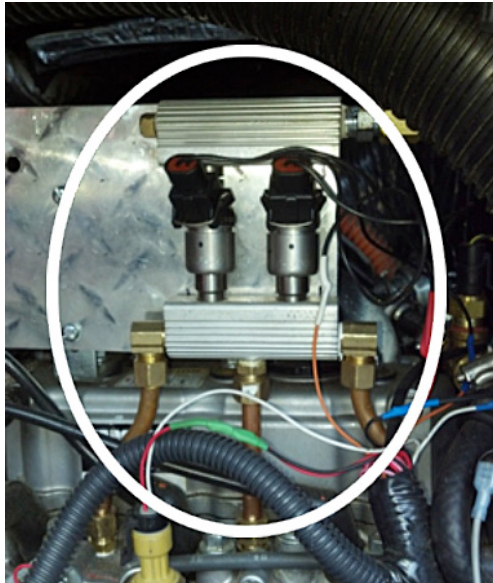


Fuel Delivery Apparatus

The hydrogen is injected into the engine for combustion by two injectors through three points in the slightly modified cylinder head using copper tubes, as shown in Figures 2-24.

Figure 2-24

Hydrogen Delivery Manifold



Dual Fuel Feature

Since hydrogen-fueling infrastructure has not been fully developed, the APU conversion was done in such a way that the engine could be switched from CNG to hydrogen, as previously mentioned. Shown in Figure 2-25 is a view of the engine management panel, which contains the fuel selection switch, EMS-4, and ignition control relays.

Figure 2-25

Engine Management Panel

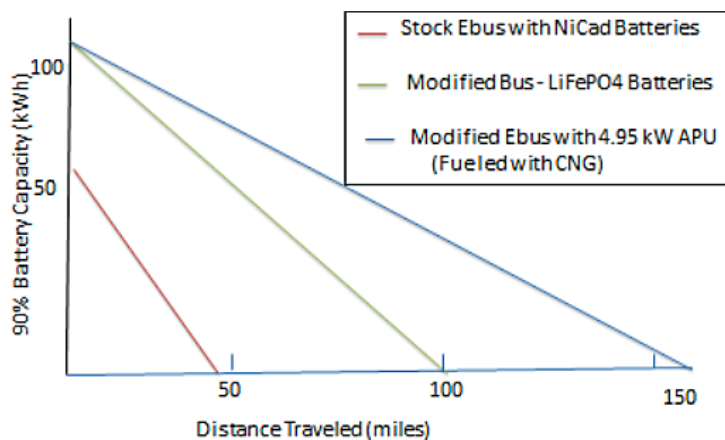


Test Results with CNG

The Ni-Cd batteries on the original Ebus shuttle were cooled with a 2.5 kW unit that was removed when the new batteries were installed. Likewise, the 2.5 kW air conditioning unit was also removed, thereby reducing the auxiliary load from a maximum of 10 kW to 5 kW. For this reason, the capacity of the APU had to be limited to no more than 5 kW to provide power for the auxiliary services only. Results for an empty bus with the APU set to deliver 4.95 kW are shown in Figure 2-26.

Figure 2-26

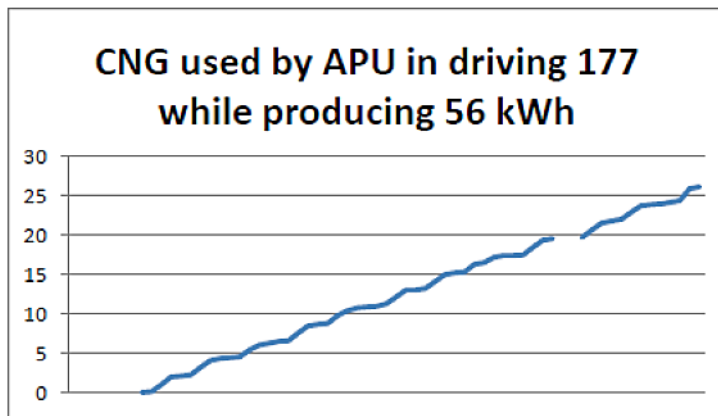
Improvement in Range with 4.95 kW APU Fueled by CNG



Fuel consumed during this test is shown in Figure 2-27. Note that the APU was not started until the SOC was reduced to 95% to protect the batteries from overcharging.

Figure 2-27

CNG Used by APU in Driving 177 miles



The overall efficiency of the APU can be estimated as follows:

$$Q_{in} = \text{mass of CNG consumed} \times \text{lower heating value}$$

$$Q_{in} = 26.1 \text{ kg} \times 12.8 \text{ kWh/kg} = 334 \text{ kWh}$$

$$Q_{out} = \text{APU Output} = 56 \text{ kWh}$$

$$\text{Efficiency APU} = Q_{out} / Q_{in} = 56 / 334 = 16.8\%$$

During this range test, the batteries provided 103 kWh of additional energy, so the total energy used for traction and auxiliary power can be estimated as follows:

$$\text{Total energy} = E_{\text{BATTERIES}} + Q_{\text{APU}} = 103 \text{ kWh} + 56 \text{ kWh} = 159 \text{ kWh}$$

The measured efficiency for charging the batteries has been found to be 85%. Assuming the efficiency during discharge is 90%, the overall grid to motor efficiency for this modified bus can be estimated as follows:

$$\text{Overall grid-to-motor efficiency} \sim ((0.85 \times 0.9 \times 103) + 0.168 \times 56) / 159 = 55.5\%$$

Test Results with Hydrogen

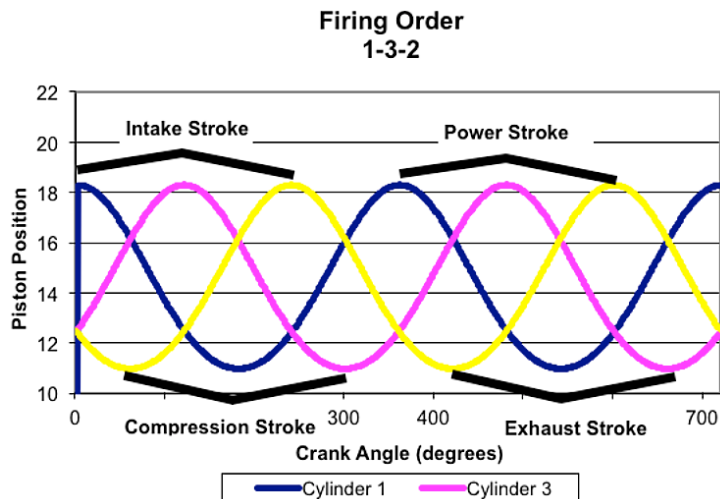
In theory, the thermodynamic efficiency of an internal combustion engine should be higher when fueled with hydrogen because of the higher flame temperature. However, the cooling system for this engine was not adequate to handle the higher flame temperatures without overheating.

This engine management system (EMS) was originally designed for a four-cylinder vehicle, but it can be reprogrammed and adapted to engines as large as ten cylinders using an ignition scheme called “wasted spark.” This scheme

fires multiple spark plugs simultaneously. In designing the ignition system, a wasted spark ignition scheme was used in which only three of the four available ignition channels were used on the EMS-4. When operating using a wasted spark ignition, it is important to know which stroke each cylinder is on at any given time to prevent pre-ignition and detonation. This would inhibit engine operation and could cause severe engine damage. The desired wasted spark operation had one cylinder fire on the power stroke while the wasted spark fires on the exhaust stroke where there is no combustible fuel available. To prevent this, a graphical representation of the cylinder motion for all six cylinders was created using the equations of motion for a slider crank mechanism with an arbitrary connecting rod length. This is shown graphically in Figure 2-28.

Figure 2-28

Firing Diagram



In practice, the wasted spark design of the ignition system limited operation to speeds below 2500 rpm to avoid pre-ignition caused when the wasted spark ignited hydrogen left in the combustion chamber from the previous power stroke of the engine. This problem was compounded by the relatively high air fuel ratio required for stoichiometric combustion of hydrogen. This prevented operation of the engine at rated capacity because it was impossible to get enough air into the cylinder, even with turbocharging, for complete combustion of the hydrogen charge that was needed to supply enough chemical energy to operate at rated capacity. This rich combustion also caused unacceptable levels of hydrocarbons to be emitted from the engine, thereby effectively erasing any gains in tailpipe emissions from burning hydrogen, and perhaps creating a fire hazard should the exhaust gases pass near an open flame. For all of these reasons, the maximum sustainable output of the APU running on hydrogen was limited to 2.5 kW, which was well below the average auxiliary load of approximately 7 kW. Results for operating the APU with hydrogen are shown in Figure 2-29. The hydrogen consumed during this test is plotted in Figure 2-30.

Figure 2-29
Range Improvement with
2.5 kW APU
Fueled by Hydrogen

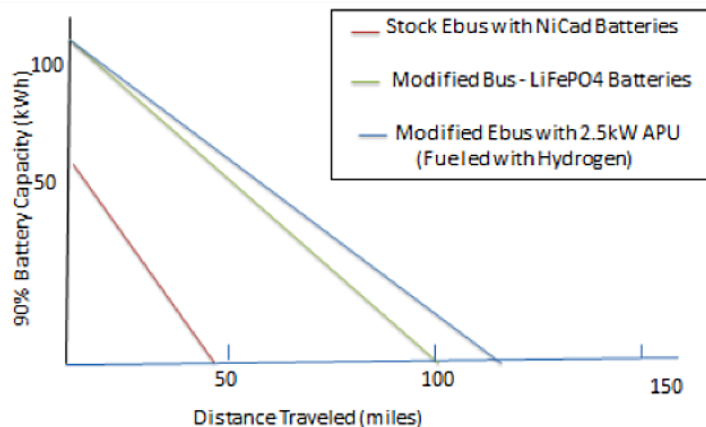
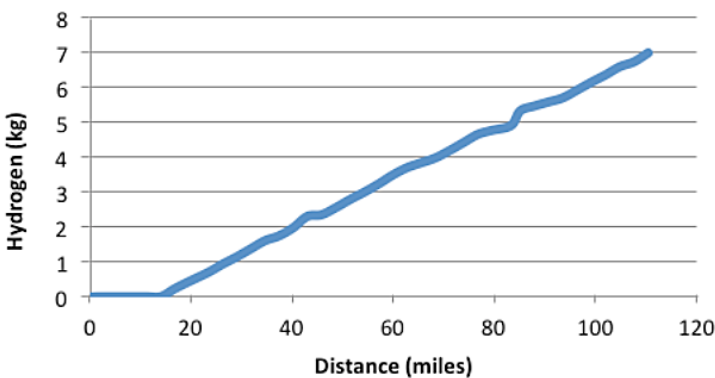


Figure 2-30
Hydrogen Used by APU
While Driving 117 Miles



It can be seen that 7.0 kg of hydrogen were consumed to increase the range by 20 miles. The overall efficiency of the APU can be estimated as follows:

$$\begin{aligned} Q &= 7 \text{ kg} \times 39 \text{ kWh/kg} = 273 \text{ kWh} \\ \text{APU output} &= 18.8 \text{ kWh} \\ \text{Efficiency} &= 18.8/273 = 7\% \end{aligned}$$

The fuel cost for this extra 20 miles would be approximately \$49.00 at an average commercial price of \$7.00 per kg, for an average of \$2.45 per extra mile. This can be compared with approximately \$0.10 per mile for fuel when running on batteries alone and approximately \$0.40 per mile for fuel for an equivalent diesel bus. Clearly, the cost for this modest gain in range is prohibitively expensive.

During this test, the batteries also supplied 86 kWh of energy with charging efficiency of approximately 85% and discharge efficiency of 90%. This would result in an overall grid-to-motor efficiency given by the following calculation:

$$\text{Overall grid-to-motor efficiency} = ((0.85 \times 0.9 \times 86) + 0.07 \times 18.8)/104.8 = 64\%$$

Lessons Learned about Use of an APU to Improve Range

It has also been shown that the range can be increased to a distance of more than 170 miles when the APU was operated at 4.95 kW with CNG. In theory, the range could have been extended to more than 200 miles if the APU had operated at its rated capacity of 10 kW, but this would have exceeded the power required by the auxiliary loads, which would have resulted in some of the energy being used for traction which would require certification by the EPA for roadway use. It was beyond the scope of this project to seek EPA certification, but the information may be of interest for future development of a true battery-centric hybrid bus.

Results were less promising when the APU was fueled with hydrogen, which increased the range by a modest 15 miles. This failure was due primarily to inability to tune the ICE for an output greater than 2.5 kW because the relatively high air-fuel ratio required for complete combustion limited the amount of hydrogen that could be injected into the combustion chamber for each power stroke. Even with turbocharging, it was impossible to tune the engine to run at speeds higher than 2500 rpm without experiencing pre-ignition that could have been caused by either hot spots from the higher flame temperature of hydrogen or hydrogen left in the combustion chamber that could be ignited by the wasted spark ignition system. It is possible that these tuning problems could have been overcome by implementation of an alternative ignition system, but that was beyond the scope of this project.

SECTION
3

Technical Support

The first technical support task was to provide technical assistance for a fleet of electric shuttle buses being operated by the City of Sevierville, Tennessee. After extensive analysis of the problems being encountered, it was determined that a dedicated technician was needed to keep the fleet of buses running smoothly. This task was accomplished by transferring funds to enable Sevierville to hire a technician.

The second support task was to assist Emory University with selecting and procuring new chargers for its fleet of electric shuttle buses. CETE had previously determined a number of issues with Emory's existing chargers and its general maintenance operation; however, task was rendered unnecessary when the university decided to replace its fleet of electric shuttle buses with diesel buses running on biodiesel to be manufactured from used cooking oil used in the campus food services. When that decision was made, Emory also agreed to transfer its fleet of electric shuttle buses to CARTA with assistance from FTA under Cooperative Agreement TN-26-7035. The lessons learned in supporting Emory University were applied to the current research project, which provided the information that CARTA needed to procure a proper charger for the buses transferred to it. CETE transferred funds originally intended for Emory to CARTA to purchase an appropriate charger for the Ni-Cd batteries used on the buses transferred to CARTA. One of these buses is now in regular service. One was used for the wireless charging project, and another was used for the hydrogen hybrid bus project described previously; a third was used for the battery-centric hydrogen hybrid bus project. The other two shuttle buses are being evaluated for possible future deployment as replacements for CARTA's aging fleet of electric shuttle buses.

Lessons Learned about Technical Support

It has been shown that the success of electric shuttle operation is highly dependent upon technical support in the maintenance operation. At Sevierville, the problem was solved by employment of a dedicated electric bus technician. Emory University decided to go another direction rather than dedicate technical support resources to its fleet of electric shuttles. During the course of this program, CETE had many opportunities to observe and interact with the maintenance personnel at CARTA. Its success in operating a fleet of electric shuttles continuously for more than 20 years can be attributed in part to the skill and level of dedication exhibited by its maintenance organization. Similar observations were made with regard to the successful operation of electric

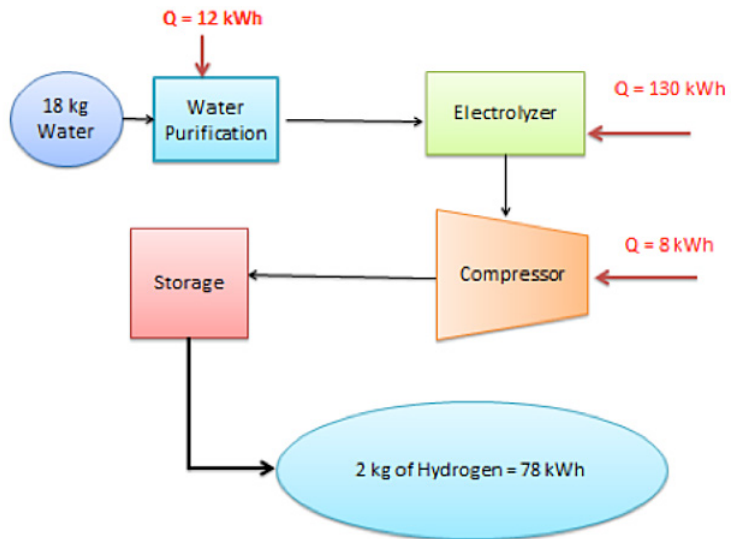
shuttles at Santa Barbara, California. The lesson here is that even the best technology will fail if not supported in the field.

SECTION
4

Acquire and Install Hydrogen Electrolyzer

The hydrogen fuelling station that was started under FTA Cooperative Agreement TN-26-7032, East Tennessee Hydrogen Initiative, was completed and commissioned in December 2009. The basic components of the fueling station are shown in Figure 4-1, which also shows the daily inputs and outputs for the as-built system.

Figure 4-1
Components of Hydrogen Fueling Station



The deionizer used for water purification is shown in Figure 4-2. The Proton Exchange Membrane (PEM) Fuel Cell shown in Figure 4-3 uses electrolysis to generate hydrogen from deionized water. The compressor shown in Figure 4-4 was used to compress the hydrogen from to 6,000 psi.

Figure 4-2
Water Deionizer



Figure 4-3

PEM Fuel Cell Electrolyzer
supplied by
Proton Energy Systems

**Figure 4-4**

Hydrogen Compressor



The hydrogen flows from the compressor through the wall and underground to the storage tanks and dispensing system shown in Figure 4-5. The tanks and dispensing system were set back 20 feet from the building and enclosed by a chain-link fence with a locking gate to comply with recommended standards for hydrogen storage and local fire codes. The dispensing system was also used

for filling the bus with CNG, which was supplied from tanks that were installed behind the red hydrogen tanks. The fueling station is capable of producing 2 kg of hydrogen per day and storing 10 kg at 6,000 psi. This system was completed and commissioned in December 2009.

Figure 4-5
Hydrogen Storage Tanks
(red) and Dispensing
System (in blue cabinet)



The energy required to produce 2 kg of hydrogen was found to be 140 kWh. The useful chemical energy in 1kg of hydrogen is equal to the lower heating value of 78 kWh. Thus, the overall efficiency of the system can be calculated as follows:

$$\text{Efficiency} = \text{Output/input} = 78 \text{ kWh}/140 \text{ kWh} = 56\%$$

At the present retail cost of electricity at the AVTF of \$0.0757 per kWh, the energy cost to produce one kg of hydrogen can be estimated as follows:

$$\text{Energy cost/kg of hydrogen} = 39 \text{ kWh/kg} \times \$0.0757/\text{kWh} = \$2.95 \text{ per kg}$$

Lessons Learned about the Hydrogen Electrolyzer

The system has the advantage of being able to produce fuel for transportation from water and electricity. In an ideal environment, the electricity to run the system could be provided by solar panels, so an electric vehicle could be said to run on sunlight and water. However, the capital cost of the equipment without solar panels is in excess of \$220,000. If these capital expenses were amortized over 20 years, the fully-burdened cost of producing hydrogen with this system would be more than \$17 per kg compared with delivered commercial price of approximately \$7 per kg or the current price of \$4 per gallon of diesel fuel, which has approximately the same energy as 1 kg of hydrogen.

It should be noted that the compressor failed three times during the first two years of operation. In each instance, the failure was traced to the O-rings used to seal the diaphragm. The first repair was done under warranty so original equipment type O-rings were installed. The second failure occurred after the warranty had expired. Repairs were made locally this time, with the same type of O-ring. When the compressor failed a third time, the material used for the O-rings was examined and found to be incompatible with hydrogen. Hydrogen-rated silicone O-rings were substituted for the original equipment type of O-rings. No further problems have been encountered with the compressor. The vendor of the compressor has been advised of the problem.

Safety was paramount throughout the design and build stages of the project, which was conducted in strict compliance with standards for the safe handling of hydrogen. For example, care was taken to avoid electrostatic discharge by grounding everything near the dispenser. A photograph of fuel being dispensed into the bus is shown in Figure 4-6. Note the green ground wire, which is required to eliminate the possibility that a spark from electrostatic discharge could ignite the fuel tank.

Figure 4-6

*Fueling the Bus
with Hydrogen*



An attractive alternative to on-site electrolysis is to deliver hydrogen from commercial producers by tube trailers like the one shown in Figure 4-7. Depending on distance between the production site and the delivery point, these trailers can deliver hydrogen at very competitive prices

Figure 4-7*Hydrogen Tube Trailer*

In anticipation that greater volumes of hydrogen would be required if CARTA decided to deploy the hydrogen hybrid bus, an arrangement was made with United Hydrogen Group of Tennessee to provide commercial hydrogen with a tube trailer similar to the one shown in Figure 4-6. Since CARTA decided that the range provided by the new batteries alone was sufficient for use of the modified bus on its downtown shuttle route, this capability was not needed; but it does offer a more cost-effective way to deliver hydrogen as a motor fuel. The cost of hydrogen delivered by this method depends upon the distance between the source and delivery point.

SECTION
5

Outreach

The goal of this task was to share lessons learned with the transit industry through an outreach program that would include publication of technical reports and participation in industry-sponsored events that promote advanced transportation.

CETE has participated in a number of regional, national, and international conferences that focus on advanced transportation. These include making presentations and publishing papers in the proceedings of Electric Vehicle Symposium (EVS) conferences in California, Norway, and China. These publications are listed in the References section of this document. CETE also accepted responsibility for publishing the second edition of the World Electric Vehicle Journal, with Dr. Bailey serving as editor-in chief. Dr. Bailey is also a member of an international task force charged by the Society of Automotive Engineers (SAE) with writing a standard for wireless charging. He is currently co-chair of the subcommittee for buses and trucks.

Over the course of this investigation, it became obvious that a better method was needed to specify the performance of vehicles used for public transit. Whether the task was to determine the suitability of a particular bus for a given route or to design a bus for service over a given route, few tools were available to assist the decision makers. What began as a rather tedious mathematical modeling exercise using formulas and spreadsheets eventually evolved into a sophisticated, easy-to-use simulator that can be used to match the physical demands of deployment with the particular attributes of vehicles to reduce risk of failure.

Description of EViSim

The Electric Vehicle Visualization and Simulator (EViSim) incorporates topographical and curvature of the planned route, vehicle weight, requirements for acceleration and instantaneous speed, aerodynamic drag, rolling resistance, and overall energy efficiencies to predict performance over selected routes. A screen shot of EViSim is provided in Figure 5-1.

Figure 5-1

Screen Shot of EViSim



Functionality

Three primary functions of EViSim have been identified: range prediction, EV comparisons, and charging infrastructure planning.

- *Range Prediction* – By calculating the power use of specific electric vehicles along custom user-entered routes, EViSim provides the very important functionality of range prediction. The simulator predicts the energy use of the vehicle along a designated route, taking into account vehicle characteristics, terrain information, charging and loading stops, traffic, and driving behavior. This allows the end-user to answer questions such as how many times a bus can run a route prior to requiring a full charge or how far along an interstate an electric vehicle can travel before needing to recharge.
- *EV Comparison* – By allowing for vehicle input from the end-user, the simulator can effectively compare the performance and energy-use characteristics of different vehicles. This functionality is highly useful to individuals such as transportation officials who must select a particular bus for a planned electric shuttle route or as a tool for consumers to determine which electric vehicle most ideally suits their driving habits and geographic location.
- *Charging Infrastructure Planning* – The EViSim application, when used to simulate a large number of electric vehicles along a wide range of common routes, can assist infrastructure planners to determine the most desirable and cost-effective locations for charging stations. By identifying points along

each simulated route where each vehicle is in need of a recharge and then applying a clustering algorithm, candidate locations for high-speed charging stations can be identified. These candidate station areas can then be analyzed by infrastructure planners using other variables such as power grid layout and real estate availability to intelligently place charging stations.

Promising Applications

Four applications of EViSim have been identified that could lead to increased adoption of electric vehicles: manufacturer sales tool, mass-transit implementation analysis tool, infrastructure planning tool, and end-user trip planning tool.

- *Manufacturer Sales Tool* – EViSim can be used to demonstrate to potential electric vehicle buyers how well an electric vehicle would suit their daily lives. Potential buyers would be able to see how far their electric vehicle would be able to take them on a single charge and how far they would be able to drive using the area's existing charging infrastructure. Custom simulations could be run that demonstrate the vehicle's performance on routes from the potential buyer's home to their place of work, recreational destinations, and other common driving points. This would make an unsure customer feel much more comfortable in their decision to purchase an EV.
- *Mass-Transit Implementation Analysis* – EViSim can assist government (or private) planners to decide the most efficient routes for EV transit solutions, aid in vehicle selection, determine running times between charges, and determine the number of EVs required to provide uninterrupted service.
- *Infrastructure Planning Tool* – The performance of EVs along an area's commonly-traveled routes can help in deciding where to place charging stations and where to encourage the early adoption of EVs.
- *Trip-Planning Tool* – EViSim can help EV owners feel more comfortable with driving to areas where charging stations may not be available. By accurately calculating the range of the vehicle, owners will know if they can safely complete a trip along a previously untested route.

Implementation

EViSim relies on vehicle data including weight, battery and charging properties, frontal surface area and drag coefficient, rolling resistance, and acceleration characteristics provided by vehicle manufacturers. It uses this information in conjunction with road information, traffic patterns, speed limits, individual driving behavior, dynamic driving route calculations, and elevation data. To calculate the energy use of EVs, the following formulas are used:

$$P_{Inertia} = m * \frac{\Delta v^2}{2\Delta t}$$

$$P_{Hill} = v * m * g * \frac{\Delta e}{\Delta d}$$

$$P_{Roll} = \mu * v * m * g * \frac{\Delta h}{\Delta t}$$

$$P_{Drag} = \frac{p}{2} * v^3 * C_d * A_f$$

Where:

- P power consumption
- v current speed
- m vehicle mass
- g gravity
- e elevation
- d distance over land
- h distance horizontal
- μ rolling resistance
- p air density
- C_d coefficient of drag
- A_f vehicle frontal area
- t time

The simulator refines calculation results by taking into account varying acceleration behaviors, peak power output limits, road conditions, and terrain conditions such as steepness of ascent or descent. Elevation and driving route information are obtained using the public application programming interfaces (APIs) provided by Google.

Design and Features

One shortcoming of many vehicle simulation programs is the end-user's detachment from the route being driven. By combining EViSim with visualization components, the user can see the energy-use and performance of a vehicle while watching it traverse the route virtually. EViSim is presented using both 2D overhead maps (Figure 5-2) and 3D fly-behind views (Figure 5-3). The 2D overview map provides for quick location reference, and the 3D visualization

provides the user with a sense of immersion and locality reference along the simulated route(s).

Figure 5-2
Two-Dimensional (2d)
Overhead Map

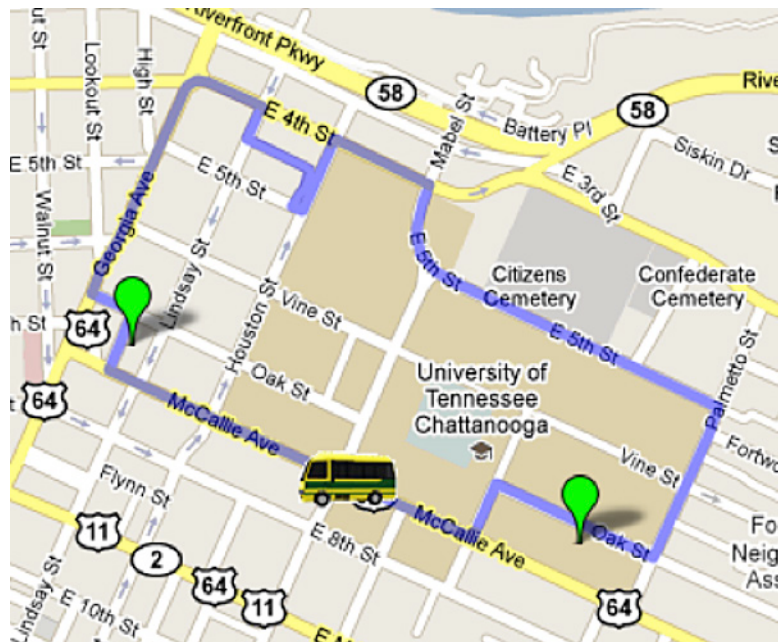


Figure 5-3
Three-Dimensional (3-d)
Fly-behind View



Charts and gauges visualize otherwise difficult to interpret numerical data. The vehicle's energy level, energy level history, current speed, and elevation information are all displayed in easy-to-understand formats. Other vital statistics are shown in a simple, centrally-located display. The charts are able to be expanded to view more detail, and raw numerical data can be accessed if necessary. The current location of the vehicle is also represented on the

elevation graph, so current elevation gradient can quickly be seen. These features are shown in Figures 5-4, 5-5, 5-6, and 5-7.

Figure 5-4

Energy Level and Speed Gauges

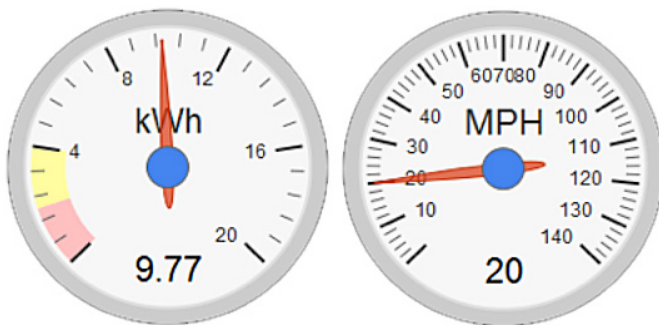


Figure 5-5

*Energy Level History
(Time vs. Energy Level)*

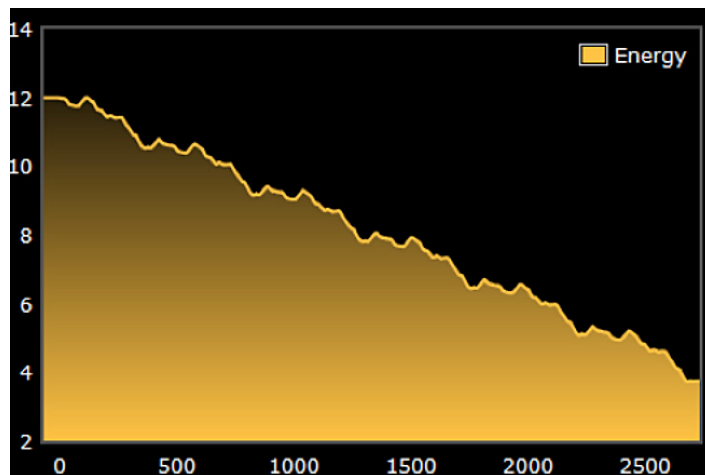


Figure 5-6

*Elevation Profile of Route
(Distance vs. Elevation)*

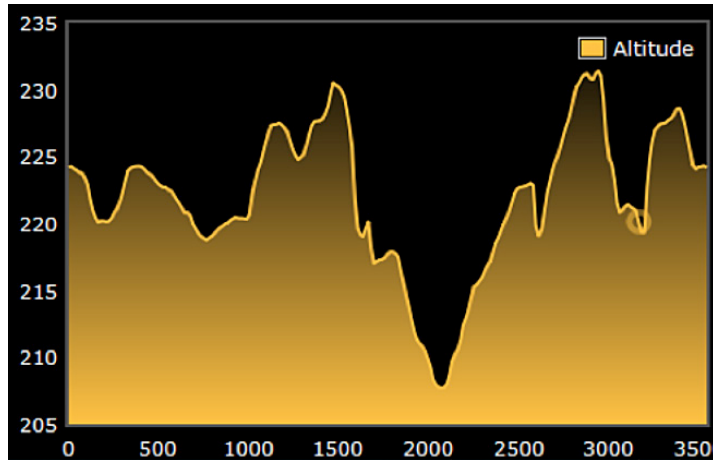
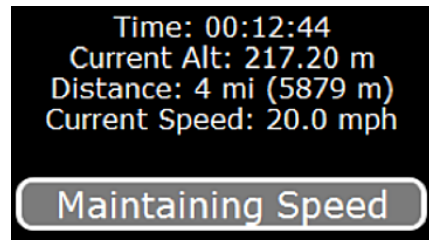


Figure 5-7
Central Status Display



Route Creation

The simulator is designed for dynamic input. Routes are specified by the end-user selecting starting and ending locations, and optionally, several waypoints in between. Points along the route can be added to represent charging stations, stopping points, and simulated traffic, and, in the case of mass transit vehicles, passenger loading. Figure 5-8 shows a customized route.

Figure 5-8
Customized Driving
Route Creation



Analysis

To provide real-world data for comparison with the simulation, an electric shuttle bus was driven over the above route on the UTC campus. Instantaneous readings of power required for the bus to navigate up the steep grades on campus were compared with predicted values from the simulator. Likewise, actual total energy consumption over this route was compared with predicted values. The bus was then driven around the downtown shuttle route. Data from extensive testing at the AVTF test track were also available for comparison with predictions from the simulator. Through a process of iteration, correction factors were built into the simulator to account for unknown efficiencies of the various subsystems to align predicted outcomes with actual data from these experiments. Our analysis shows that EViSim provides a viable method to predict the energy use of vehicles to a high-enough degree of accuracy to be a valuable tool in the types of EV-related decisions. Our goal was to provide a tool that encourages the adoption of electric vehicles. The inventors of this technology have filed a patent disclosure with the University of Tennessee Research Foundation. Going forward, the intent is to make this tool available to assist public transit stakeholders understand the full potential for electric and hybrid vehicles.

References

- Bailey, J. Ronald, Justin McBath, and Mark E. Hairr. 2012. "Increasing the Range of Electric Shuttle Buses with Wireless Charging." Paper presented at EVS 26 International Battery, Hybrid and Fuel Cell Electric Vehicle Symposium, Los Angeles, California, May 6–9.
- Bailey, J. Ronald, Mark E. Hairr, Thomas Dugan, Albert E. Curtis III, and Dick Boothe, 2012. "Wireless Charging of Electric Shuttle Buses." Paper presented at Conference on Electric Roads and Vehicles, Park City, Utah, February 3–6.
- Bailey, J. Ronald, Wayne Davis, and Cliff Ricketts. 2010. "East Tennessee Hydrogen Initiative." Paper presented at the NHA Hydrogen Conference & Expo, Long Beach, California, May 3–6.
- Gasior, Wade, Li Yang, Ignatius Fomunung, Mark Hairr, and Ronald Bailey. 2010. "So You Want to Drive an Electric Vehicle." Paper presented at EVS 25, the 25th World Battery, Hybrid and Fuel Cell Vehicle Symposium and Exhibition, Shenzhen, China, November 5–9.
- Hairr, Mark E., Paul Griffith, J. Ronald Bailey, and Woodlyn Madden. 2009. "Data Acquisition System for Electric and Hybrid-Electric Buses." Paper presented at EVS 24 International Battery, Hybrid and Fuel Cell Electric Vehicle Symposium, Stavanger, Norway, May 13–16.
- Hairr, Mark E., Paul Griffith, Tom Dugan, and J. Ronald Bailey. 2010. "Development of a Hydrogen Hybrid Internal Combustion Engine Bus." Paper presented at APTA Conference, Washington, DC, May 4.
- Hairr, Mark E., Ron D. Sweeney, J. Ronald Bailey, and Ignatius Fomunung. 2010. "Developing Hydrogen Hybrid ICE and Inductive Power Transfer Technologies for Buses: Chattanooga, Tennessee, USA Continues to Lead in Advanced Transit Technologies After Twenty Years." Paper presented at EVS 25, the 25th World Battery, Hybrid and Fuel Cell Vehicle Symposium and Exhibition, Shenzhen, China, November 5–9.
- Madden, Woodlyn, J. Ronald Bailey, and Mark Hairr. 2009. "Topographical Inertial Energy Simulator for Hybrid Electric Vehicle." Paper presented at EVS 24 International Battery, Hybrid and Fuel Cell Electric Vehicle Symposium, Stavanger, Norway, May 13–16.
- McBath, Justin, Roger LeMond, Mark Hairr, and J. Ronald Bailey. 2011. "ICE Conversions as a Bridge to the Hydrogen Economy." Paper presented at NHA Fuel Cell & Hydrogen Conference, Washington, DC, February 13–16.
- Thomas, Tricia, Mark Hairr, Paul Griffith, Woodlyn Madden, and J. Ronald Bailey. 2009. "Using Topographical and State of Charge Information to Predict the Actual Range of Electric Vehicles." Paper presented at EVS 24 International Battery, Hybrid and Fuel Cell Electric Vehicle Symposium, Stavanger, Norway, May 13–16.



**U.S. Department of Transportation
Federal Transit Administration**

U.S. Department of Transportation
Federal Transit Administration
East Building
1200 New Jersey Avenue, SE
Washington, DC 20590
<http://www.fta.dot.gov/research>